



# POLITECNICO DI TORINO

Master's Degree in Civil Engineering

MASTER'S DEGREE THESIS

# A Simplified 2D Modelling Approach for Soil-Structure Interaction in the Dynamic Analysis of End-Shield Bridges

SIMONE CALABRESE

# A Simplified 2D Modelling Approach for Soil-Structure Interaction in the Dynamic Analysis of End-Shield Bridges

# Simone Calabrese



Master of Science Thesis TRITA-ITM-EX 2025:2025 KTH Structural Engineering and Bridges SE-100 44 STOCKHOLM

#### **Author:**

Simone Calabrese

simoneca@kth.se

# **Supervisors:**

Jean-Marc Battini

Cecilia Surace

# **Co-supervisors:**

Seyed Amin Hosseini Therani

Abbas Zanganeh

#### **Abstract**

This thesis investigates the dynamic response of end-shield railway bridges subjected to high-speed train loading, with a particular focus on the role of soil—structure interaction (SSI). The objective is to assess the performance of a simplified 2D modelling approach that can reliably estimate bridge accelerations under resonance conditions, while significantly reducing computational effort compared to full 3D finite element models.

Eighteen existing railway bridges with varying span numbers, geometries, and foundation types were analysed. A reference 2D model incorporating impedance functions, validated against experimental data, served as the benchmark. The proposed simplified 2D model introduces the effect of surrounding soil with concentrated springs and dashpots at the abutments and columns foundations, and distributed springs and dashpots at the end-shields. Sensitivity analyses were conducted to evaluate the effects of soil stiffness, damping, and boundary conditions on the response of the bridge.

The results show that the simplified model generally produces slightly higher accelerations and lower natural frequencies, yielding conservative but acceptable predictions. While shallow foundations at the abutments show minimal influence on the bridge response, the contribution of pile foundation becomes significant, especially in single-span bridges. The flexibility of column foundations gives a substantial contribution to the dynamic response of the bridge. Moreover, the sensitivity analysis confirms that the stiffness and damping properties of the backfill soil at the end-shields influence the modal damping and may affect the acceleration response, especially for single span bridges. The findings confirm that the simplified approach offers a practical and conservative tool for early-stage design and evaluation of end-shield bridges under dynamic loading.

This Master's thesis was carried out at the Division of Structural Engineering and Bridges at KTH Royal Institute of Technology as part of the final requirements for the Master of Science in Civil Engineering at Politecnico di Torino.

I would like to express my sincere gratitude to my supervisors, Amin, Jean-Marc, and Abbas, for their invaluable guidance, feedback, and encouragement throughout the project.

I would also like to extend a special thank you to my girlfriend Emily for her constant support and encouragement during this unforgettable experience in Stockholm.

Lastly, I would like to thank my family for their continuous support, patience, and motivation during this experience.

Simone Calabrese

Stockholm, July 2025

# **TABLE OF CONTENTS**

AB	STRA	ACT		1
FOI	RWA]	RD		3
TAI	BLE (	OF CON	NTENTS	6
1	INT	RODU	CTION	7
	1.1	Backg	round	7
	1.2	Purpos	se and Aim	8
	1.3	Limita	ations	8
2	TH	EORET	ICAL BACKGROUND	9
	2.1	Previo	ous studies on SSI in railway bridges	9
	2.2	Imped	ance Function	11
	2.3	HSLM	1 Train Passage	12
3	ME	THODO	DLOGY	15
	3.1	Case s	tudy bridges	15
	3.2	Nume	rical models	16
	3.3	Found	ations	17
		3.3.1	Shallow Foundation	. 17
		3.3.2	Pile Foundation	. 19
	3.4	End Sl	hield	20
	3.5	Materi	ial Properties	23
	3.6	Dynan	nic Loading and Response Evaluation	24
4	RES	SULTS/	ANALYSIS	25
	4.1	Single	Span Bridges	27
		4.1.1	Aspan	. 28
		412	Bodavågen	31

	4.1.3	Brustjärnsbäcken
	4.1.4	Bubäcken
	4.1.5	Degernäsbäcken
	4.1.6	Norrmjöleån
	4.1.7	Ångerån
	4.2 Two S	Span Bridges
	4.2.1	Leduån
	4.2.2	Leån
	4.2.3	Stridbäcken
	4.3 Three	Span Bridges
	4.3.1	Hinnsjöbäcken
	4.3.2	Husån
	4.3.3	Nordmaling
	4.3.4	Sidensjövägen
	4.3.5	Styrnäs
	4.3.6	Sörmjöleån
	4.3.7	Vasavägen
	4.3.8	Åhedaån
5	DISCUSSI	ON
6	REFEREN	CES

#### 1.1 Background

The end-shield bridge, a common type of railway bridge used in Sweden, is characterized by one or more spans and a deck that extends beyond the end supports, embedding into the surrounding soil through end frames, as illustrated in Figure 1.

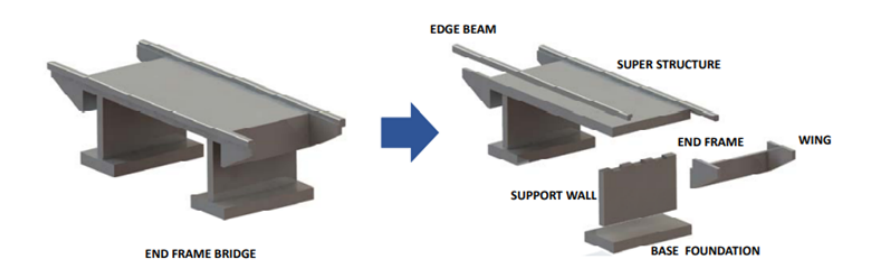


Figure 1. Schematic representation of the end shield bridge.(adopted from Sandberg et al.[1])

The continuous implementation of high-speed railways necessitates a thorough analysis of the dynamic behavior of such bridges. Vibrations induced by high-speed trains are significantly greater than those caused by commuter trains. These bridges usually have natural vibration frequencies that cannot be reached with the passage of typical trains. As train speeds increase, the natural vibration modes of the bridge may be excited, potentially reaching resonance conditions. This phenomenon can cause passenger discomfort, rail instability, and damage to the track embankment.

The analyses conducted in this project consist of simulating train passages at different speeds. The train is modelled as a series of moving point loads traveling along the bridge deck, and the focus is placed on identifying resonance conditions by measuring the resulting accelerations throughout the structure. According to Eurocode (EN 1990) [2], maximum allowable accelerations are limited to  $3.5 \ m/s^2$  for ballasted tracks and  $5 \ m/s^2$  for slab tracks. Exceeding these limits compromises safety and passenger comfort, making dynamic analysis crucial to confirm or reject the suitability of existing infrastructure for high-speed operations.

As previously described, the bridge's end shields are in contact with the soil. Numerous studies have been conducted to understand the influence of Soil-Structure Interaction (SSI) on the dynamic response of bridges. These studies

demonstrate that the additional damping provided by the soil significantly reduces bridge accelerations [3]. Most of this research has relied on 3D finite element models (FEM) that incorporate soil in the analysis. While this approach has yielded accurate results, it demands substantial computational resources and time due to the complexity of modeling soil behavior and defining its properties.

To address this challenge, researchers have explored simplified approaches by replacing detailed soil models with spring-dashpot systems that approximate the soil's effects. These simplified models reduce computational costs while maintaining reasonable accuracy.

Building on this body of work, the current project seeks to further evaluate and refine simplified 2D models for different end-shield bridges. Hosseini Tehrani [3] developed initial simplified models, and this project will extend that research by introducing additional simplifications and validating their performance.

#### 1.2 Purpose and Aim

The purpose of this thesis is to investigate the suitability of simplified 2D beam models for assessing the maximum resonance response of end shield bridges. This objective is pursued by testing the proposed simplifications on a series of existing bridges, using both their as-built and design geometry. The results are compared to those from a reference model, which has been validated against experimental results and can be considered reliable.

The aim is to develop a simple model that provides a good and conservative approximation of the real dynamic response of these bridges, and to propose its adoption by companies involved in such assessments.

#### 1.3 Limitations

The use of existing bridges allows us to obtain realistic results, that would have been different with a parametric study on the geometric characteristics. Despite that, every bridge has his own cross section, span length, and cantilever part length, which means that the response is singular and difficult to predict.

Moreover, the geometry is well defined, but the material properties are usually unknown. Especially for the soil, there are several uncertainties regarding the elastic modulus and the damping ratio. A sensitivity analysis on these properties is addressed in the following chapters.

#### 2 THEORETICAL BACKGROUND

The first section of this chapter reviews previous studies on the dynamic analysis of end-shield bridges and SSI, highlighting key findings and identifying gaps in the existing literature. This review is essential to understand the current state of knowledge in the field and demonstrate the need for further investigation, particularly in developing a practical and simplified model to assess the dynamic behaviour of end-shield bridges efficiently.

#### 2.1 Previous studies on SSI in railway bridges

In the past, the dynamic analysis of railway bridges was simplified using Dynamic Amplification Factors (DAF) for the estimation of the response to moving loads. These solutions were conservative and the interaction between the structure and the surrounding soil was disregarded. With the growing demands for higher performance of these bridges, the subject has been thoroughly investigated in various studies. In particular, the role of SSI in the dynamic behavior of bridges has been analysed. Ülker-Kaustell et al. [4] have analysed a portal frame bridge with a traditionally clamped model and two other models with static and dynamic SSI incorporated in the supports. They showed that the original model largely overestimates the vertical acceleration of the bridge; the soil contributes significantly the modal damping ratio, especially for soil with a low elastic modulus.

Several studies on the interpretation of SSI for embedded bridges have been conducted by Zangeneh. In [5], Zangeneh analyzed the dynamic response of a short-span portal frame bridge considering the effect of the backfill and the subsoil supporting the bearings. He created a 3D Finite Element Model (FEM) of the concrete bridge, and he modelled the interaction with the soil by using distributed spring-dashpots over the walls. The model was calibrated using the experimental results from field tests with applied harmonic load. The results showed an increase in the natural frequencies and the damping ratios due to the contribution of the surrounding soil. In [6] another portal frame bridge was analysed. This time, a full 3D model of the bridge-soil system was used, and the experiments included monitoring of train passages. He found that the damping ratio of the fundamental mode of the bridge is about five times higher than the recommended values. Moreover, a simplified model with spring-dashpot system for the backfill soil was proposed, similar to [5], but with tangential directions included. The results have shown an overestimation of the dissipative

effect with respect to the calibrated model.

Also, Hosseini Therani has thoroughly investigated the SSI in railway bridges, focusing particularly on end-shield bridges with one or more spans. The findings of his studies are presented in the following three papers:

- I.Dynamic soil-structure interaction of a continuous railway bridge [7].
- II.Dynamic soil-structure interaction of a three-span bridge subject to high-speed train passage [8].
- III. Simplified soil-structure interaction modeling techniques for the dynamic assessment of end shield bridges [9].

In the first paper, the subject of study is a continuous three-span railway bridge. A 2D model was proposed to assess the effect of SSI on the bridge's response. In this model, the SSI was incorporated using springs and for each degree of freedom. A 3D model of the surrounding soil was created, and the values for the dynamic stiffness of these springs were derived from the impedance function of this model. Dashpots were ignored in this model and the damping for the entire structure was assigned using the modal damping obtained from experimental results. The train passage was conducted using moving point loads along the bridge deck. Four different scenarios were analysed: the model with soil and the contribution of the first three modes of vibration; the model with soil but only the first mode; the model without soil; and the model with removal of the cantilever part, including the end shield.

The results showed that the presence of soil contributes significantly to the reduction of the bridge's accelerations. The first bending mode was dominant; the contribution of the higher modes was negligible. Removing the end shield reduced the overall stiffness, with a consequent shift of the resonance speed and a slight increase in accelerations.

In the second paper, the same bridge was analysed using a 3D model of the structure and the surrounding soil, which was calibrated against the experimental results obtained from dynamic tests on the bridge. The calibrated model was used to evaluate the dynamic response under different loading scenarios. Consistent with the first paper, the results indicated that the presence of soil reduces the accelerations of the bridge. In contrast, the absence of soil results in an impact effect when the train reaches the end shield, with consequent high accelerations.

A parametric study was conducted on the calibrated 3D model to investigate uncertainties related to soil properties. The properties of the backfill soil were

shown to influence both the stiffness of the system and the amplitude of the accelerations. A similar trend was obtained for the soil under the columns. However, the properties of the soil under the end supports did not affect the response of the bridge.

The third paper investigates various scenarios aimed at simplifying the 3D model developed in the second paper. In this analysis, three additional bridges were examined, resulting in a total of two single-span and two three-spans end-shield bridges. First, a calibrated 3D model was created for each bridge and calibrated to the experimental data. The simplified models proposed in the study are:

- A 3D model of the bridge incorporating spring-dashpot systems to replace the soil.
- A 2D model with springs-dashpots placed at the location of the end-shield, supports, and columns.

In the simplified 3D model, the spring and dashpot values were derived from empirical expressions that account for the geometry and properties of the surrounding soil. These springs and dashpots were applied across the entire surface of the shield.

For the 2D model, the spring and dashpot values at the end shield, were obtained using the impedance function, as in the first paper. This time, the dashpot coefficients were explicitly derived from the impedance function and applied in the numerical model. For the soil under the supports and columns, values were taken from formulas found in existing literature.

The results showed that the simplified models provided a good approximation of the bridge response and yielded conservative results. However, the level of accuracy was found to be higher for three-span bridges compared to the single-span ones.

#### 2.2 Impedance Function

The most accurate method to capture the interaction between a structure and the surrounding soil is to develop a full numerical 3D model that includes both the structure and the soil. While this approach yields accurate results, both in static and dynamic analysis, it is computationally expensive due to the large amount of data involved. To reduce the complexity, impedance functions are the most suitable solution to represent the soil's contribution.

The impedance function, for a single- or multiple-degree-of-freedom system, is defined as the ratio between the applied force and the resulting displacement at

a given frequency:

$$Z(\omega) = \frac{Applied force at \omega}{Displacement at \omega}$$
 (1)

In structural dynamics, it is typically expressed as a complex-valued function:

$$Z(\omega) = K(\omega) + i\omega C(\omega) \tag{2}$$

Here,  $K(\omega)$  is the frequency-dependent stiffness, and  $C(\omega)$  is the frequency-dependent damping coefficient. The dynamic stiffness can be decomposed as:

$$K(\omega) = k - \omega^2 m \tag{3}$$

Eq. 2 highlights the two components of the impedance function. The real part,  $K(\omega)$ , represents the dynamic stiffness of the system composed of the static stiffness k and the mass contribution  $\omega^2 m$ . The imaginary part,  $C(\omega)$ , accounts for the dynamic damping of the system, including the material and the radiation damping.

Using the impedance function, the contribution of the soil can be represented through equivalent spring-dashpot systems for each degree of freedom, where the spring stiffness is given by  $K(\omega)$  and the dashpot coefficient corresponds to  $C(\omega)$ .

# 2.3 HSLM Train Passage

The dynamic analysis of structures is essential for evaluating their response to dynamic loads. In the case of railway bridges, dynamic loads induced by passing trains play a critical role in assessing the bridge's suitability for accommodating specific train types and speeds.

The Eurocode [10] provides a standard procedure for the dynamic analysis of railway bridges. For international railway lines that satisfy the European high-speed standards, Eurocode recommends the use of a series of load models, referred to as High-Speed Load Models (HSLM). These models are designed to represent the range of trains that may operate on these lines.

Based on the characteristics of the end-shield bridges, the analysis is carried out using the HSLM-A models, which range from HSLM-A1 to HSLM-A10, as shown in the table extracted from the codes in Table 1.

The bridges analysed in this thesis were tested under all the HSLM-A models, and the most critical was identified and used for all other analyses. The procedure to apply these load models to the FE models will be explained in Section 3.6.

Table 1. HSLM-A models provided by Eurocode [10]

Universal Train	Number of intermediate coaches N	Coach length D [m]	Bogie axle spacing d [m]	Point force P [kN]
A1	18	18	2.0	170
A2	17	19	3.5	200
A3	16	20	2.0	180
A4	15	21	3.0	190
A5	14	22	2.0	170
A6	13	23	2.0	180
A7	13	24	2.0	190
A8	12	25	2.5	190
A9	11	26	2.0	210
A10	11	27	2.0	210

This chapter presents the methodology adopted to assess the dynamic response of end-shield bridges using simplified modeling approaches. The objective is to develop 2D beam models and evaluate their effectiveness and accuracy by comparing them to more detailed reference models.

The methodology includes the selection of case study bridges, the development of numerical models, the definition of loading conditions, and the comparison of dynamic responses under resonance conditions. The simplified models are validated against 2D models that incorporate impedance functions.

Each step is presented in detail in the following sections.

#### 3.1 Case study bridges

To validate the simplified models, the most reliable approach is to test them on real bridges. This ensures that key parameters affecting the dynamic response, such as the cross-sectional area, second moment of inertia, span length, and dimensions of the end shields, reflect realistic structural characteristics.

In contrast, a purely parametric study may involve variations that lead to unrealistic bridge configurations, which may not satisfy basic static verifications or design standards.

Hence, the drawings of several real, built bridges among the Swedish railway lines were collected. The selected bridges are part of single-line railway infrastructures with ballasted track. They vary in configuration, from single-spans to three-spans, from fixed to pinned connections between the deck and the columns. However, they all have in common the cantilever end-shield frame.

For a clear exposition of the results, these bridges are classified into three categories:

- Single span bridges.
- Two span bridges.
- Three span bridges.

The design drawings were used to model the geometry of the bridge and the surrounding soil.

#### 3.2 Numerical models

As discussed in Chapter 2, simplified 3D and 2D models have been previously developed and validated. The starting point of this project is the 2D model that incorporates impedance functions, as proposed and validated by Hosseini Therani [9]. Consequently, all models in this study have been developed in a two-dimensional environment, where the deck and the columns are modelled using beam elements.

The real cross sections of the bridges are geometrically complex. However, since only the cross-sectional area and the second moment of inertia significantly influence the dynamic behaviour, each section has been simplified to an equivalent rectangular section. This equivalent section has the same area and moment of inertia, and its dimensions are derived as follows:

$$h = \sqrt{\frac{12 \cdot I}{A}} \tag{4}$$

$$b = \frac{A}{h} \tag{5}$$

These railway bridges have a ballasted track system, where a thick layer of ballast supports the rails. While the ballast does not provide structural stiffness, its mass, along with that of the rails and sleepers, significantly affects the dynamic characteristics of the structure. This effect has been incorporated by assigning a non-structural distributed mass along the deck. The total added mass was estimated using the embankment geometry provided in the technical drawings and supplemented by standard values for rail and sleeper weights.

With these simplifications, the 2D models maintain the same key structural properties as the more detailed 3D models: total mass, cross-sectional area, and moment of inertia.

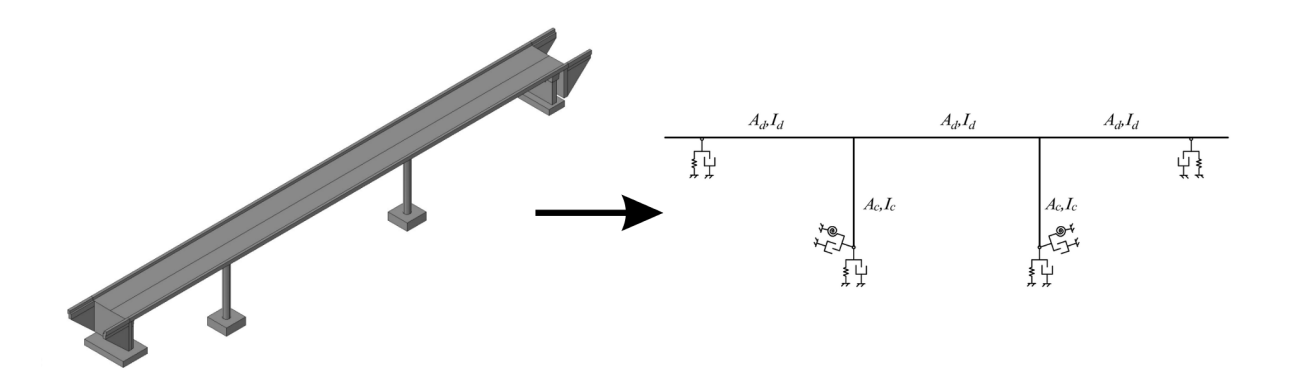


Figure 2. Transition from 3D to 2D of a three-span bridge. The effect of backfill soil is not considered in this stage.

Regarding boundary conditions, different approaches were used depending on the type of bridge. For single-span bridges, the deck is supported at both ends by abutments, which are connected to the deck via roller constraints. In addition, the end-shield is embedded in the soil, contributing to load transfer. In the 2D models, neither the abutments nor the surrounding soil are explicitly modelled. Instead, the abutments are replaced by spring-dashpot systems in the vertical direction. The total stiffness of each of these systems is calculated as the series combination of the stiffness of the concrete abutment and the supporting soil. The concrete stiffness is obtained using simple static formulas, while the soil contribution is described in detail in Section 3.3. The interaction between the end shield and the surrounding soil is treated using different modelling strategies, which are explained in the following sections.

In two- and three-span bridges, the deck is supported not only by the abutments and end shields, but also by one or two intermediate columns. These columns can be both rigidly connected or pinned to the deck and are explicitly modelled in the 2D environment as beam elements. Their interaction with the ground is represented by spring-dashpot systems placed at their base, as described in Section 3.3.

#### 3.3 Foundations

In the studied bridges, two types of foundation are present: shallow foundations and pile groups. The former consists of a concrete plate resting on a thin layer of compacted materials. It's depth ranges from 0.5 m to a few metres, depending on the bedrock's topography. The latter -pile foundations- are used where a deep layer of soft soil overlays the bedrock. In these cases, the pile groups are driven through the soil layer and anchored to the bedrock. The depth of the piles ranges from 9 to 22 meters.

For both types of foundation, the effect on the dynamic response cannot be neglected. Their influence is taken into account using springs and dashpots at the location of supports and columns.

#### 3.3.1 Shallow Foundation

The stiffness and damping coefficient for shallow foundations were adopted from Hosseini Therani [9]. Given the limited thickness of the compacted fill layers and their low elastic modulus, the natural frequency of the soil is significantly higher than that of the bridge. As a result, dynamic soil behaviour can be neglected, and the spring stiffness is defined only by its static component. For

a rectangular foundation, the vertical component is given by:

$$k_{\rm v} = \frac{2GL}{1 - v} \cdot \left(0.73 + 1.54 \left(\frac{B}{L}\right)^{0.75}\right) \cdot \left[1 + \frac{2.5 \frac{B}{H}}{0.5 + \frac{B}{L}}\right] \tag{6}$$

Here, H is the thickness of the soil layer, B and L are the semi-width and the semi-length of the foundation base (see Figure 3), and G and V are the are the soil's shear modulus and Poisson's ratio, respectively.

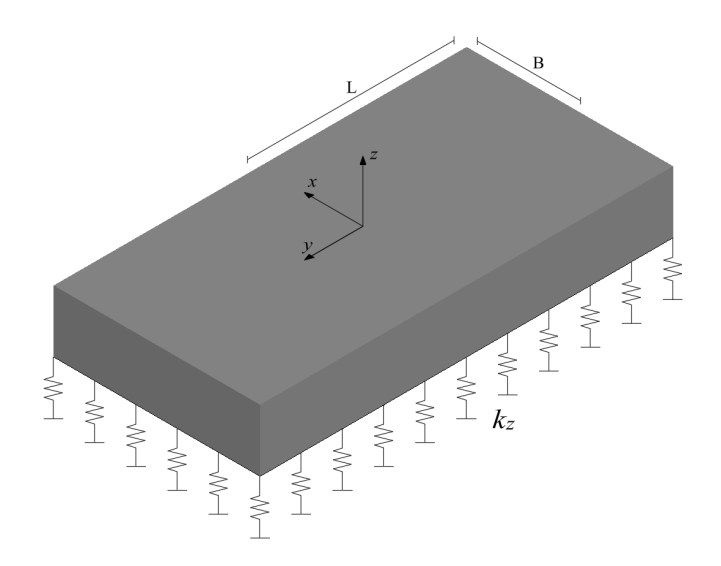


Figure 3. Rectangular shallow foundation resting on a spring bed, showing semi-width B and semi-length L

The end supports are connected to the bridge only in the vertical direction; thus, the rotational stiffness of the foundation does not influence the structural response. In contrast, the columns on two- and three-span bridges are rigidly connected to the deck, and the rotational contribution makes an important contribution to the dynamic response of the bridge.

Considering the first bending mode as the dominant one, only the rotation in the axis of the deck is relevant. The rotational stiffness of the soil foundation can be determined as a function of the vertical stiffness  $k_v$ .

$$k_{\rm r} = \frac{k_{\rm v} \cdot B^2}{3} \tag{7}$$

The dashpot coefficients include only hysteretic damping, as radiational damping is disregarded for this type of foundation. These dashpots are frequency-dependent. Given the first natural frequency  $\omega$  of the bridge and the soil damping ratio  $\xi_s$ , the dashpot coefficient is calculated as:

$$c_{\rm r} = \left(\frac{2k_{\rm r}}{\omega}\right)\xi_{\rm s} \tag{8}$$

This general formula can be used for both vertical and rotational dashpots by using the corresponding stiffness values.

#### 3.3.2 Pile Foundation

Pile foundations are more complex than shallow foundations. This type of foundation is used for thick layers of soft soil with low elastic modulus. The piles are rigidly connected to the base of the abutment or column and extend through the soil layer until they reach the bedrock. The complexity of this system makes it difficult to determine the dynamic stiffness using analytical formulas.

Therefore, the dynamic stiffness and the dashpot coefficient of the pile foundation are obtained using impedance functions. For this purpose, 3D numerical models were created in COMSOL Multiphysics using the geometrical data provided in the technical drawings. Since the geometry is different for each foundation, due to differences in pile inclination, orientation, and length, separate models were developed for each case.

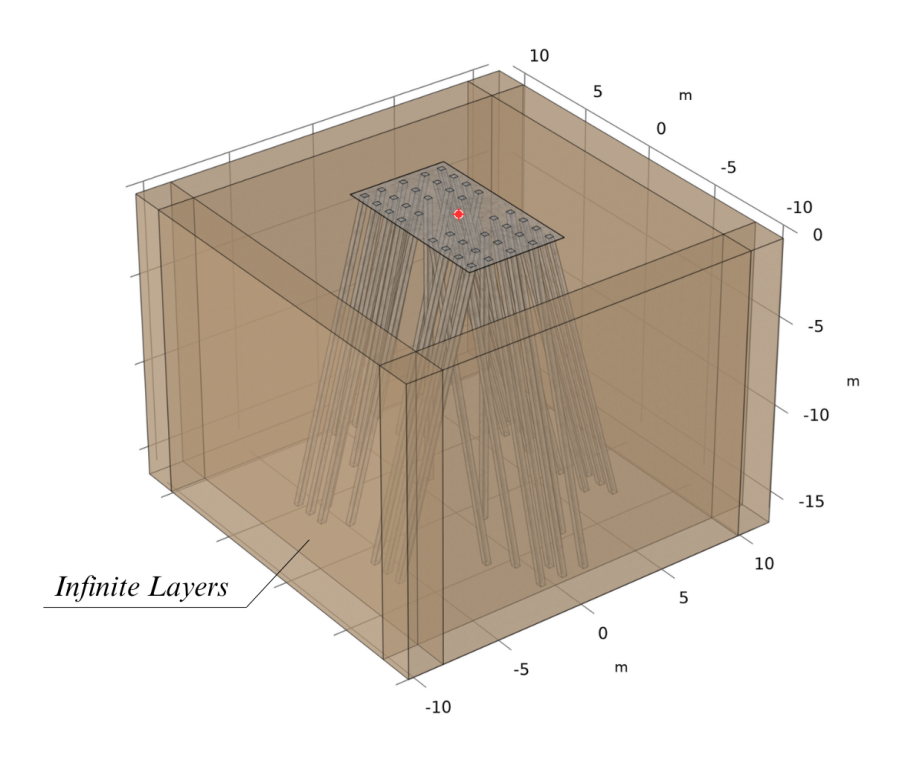


Figure 4. 3D Model of a pile group foundation created in COMSOL Multiphysics.

Figure 4 shows an example of the 3D model, which includes the piles, the surrounding soil, and the PMLs (Perfectly Matched Layers). The PMLs act as a

boundary condition, simulating an infinite domain to prevent wave reflection at the model's edges, which could otherwise distort the foundation's dynamic properties.

The piles are rigidly connected to the pile cap, forming a single rigid surface. The impedance function is then evaluated at a defined reference point within this rigid connection.

#### 3.4 End Shield

The modelling of the end shield is a crucial aspect of this project. It consists of a retaining wall and two wing walls embedded in the surrounding soil. In a 3D model, both the concrete elements and the surrounding soil are explicitly modelled and included in the dynamic analysis. However, since the purpose of this work is to create a simplified 2D model, these parts are not directly modelled. This section presents two approaches for accounting for the interaction of the end-shield with the backfill soil: impedance functions, and empirical springs and dashpots on the retaining wall.

The most accurate approach is to use impedance functions to represent the SSI via vertical and rotational springs and dashpots. This method, already consolidated in [9], was used to create a reference model to compare the results obtained with the proposed simplified model. For this purpose, 3D models of the backfill soil were created in COMSOL Multiphysics to evaluate the impedance functions. The 3D model, shown in Figure 5, includes the soil, the retaining wall, and the two wings. As in the pile group model, PML elements were used to avoid wave reflection. On the bottom, due to the presence of a stiffer layer, usually the bedrock, the model is constrained with fixed boundaries. The geometry of the model follows the specifications provided in the technical drawings and was adapted to the specific parameters of each bridge. In many cases, the two ends of the same bridges have different configurations, and separate models were created accordingly.

In Figure 5, a rigid surface is visible on the retaining wall. This surface represents the cross section of the deck and was used as the reference surface to evaluate the impedance function. The red point indicates the centroid of this rigid surface, which served as the reference point for computing the vertical and rotational components of the impedance.

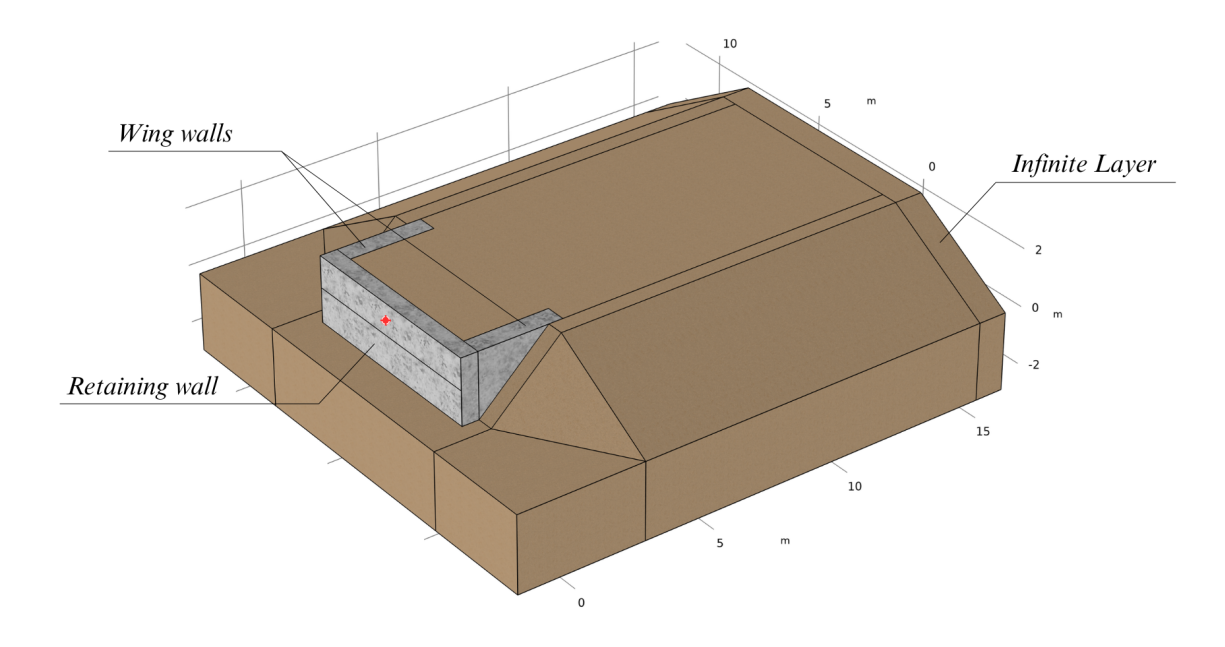


Figure 5. 3D Model of the backfill created in COMSOL Multiphysics.

With the values obtained from the impedance function, the 2D model in Figure 6 was obtained. The depicted model represents a three-span bridge; the same considerations are valid for single-span and two-span bridges.



Figure 6. 2D Model of a three-span bridge with Impedance Functions at the end-shields

The second approach concerns the use of empirical springs and dashpots. In this method, the retaining wall is included in the 2D beam model, while the wing walls are not considered. The spring-dashpot formulations presented here were originally used in a simplified 3D model in [9]. In that model, the soil was replaced by distributed springs and dashpots acting on the surfaces of the retaining wall and the wings, in the normal direction and two tangential directions.

In this project, the same formulas were applied to the 2D model. Specifically, the normal springs and the tangential springs in the vertical direction were retained. The horizontal tangential direction does not exist in a two-dimensional environment and was therefore omitted. Moreover, the same expression from Section 3.3 was used to apply a concentrated spring at the base of the wall.

For the normal springs on the wall, the following formulas were used:

$$k_{\rm s,n} = \frac{2\pi}{\sqrt{2(1-\nu_{\rm s})}} \frac{\rho_{\rm s} V_{\rm s}^2}{H_{\rm w}}$$
 (9)

$$c_{s,n}(\omega) = \begin{cases} \frac{2\xi_{s}k_{s,n}}{\omega} & \text{for } \phi \leq 1\\ \frac{2\xi_{s}k_{s,n}}{\omega} + \rho_{s}V_{La,s}\sqrt{1 - \left(\frac{1}{\phi}\right)^{2}} & \text{for } \phi > 1 \end{cases}$$
(10)

Here,  $\rho_s$ ,  $v_s$ ,  $\xi_s$ ,  $V_s$ , and  $V_{La,s}$  refer to the density, Poisson's ratio, hysteretic damping ratio, shear wave velocity, and Lysmer's analog wave velocity of the backfill soil, respectively.  $H_w$  is the height of the retaining wall,  $\omega$  is the bridge's first natural frequency, and  $\phi$  is a dimensionless frequency parameter representing the ratio between the natural frequency of the bridge and that of the backfill soil. It is expressed as:

$$\phi = \frac{\omega}{(\pi V_{\rm s}/2H_{\rm s})}\tag{11}$$

where  $H_s$  is the height of the backfill soil, measured from the top of the retaining wall to the bedrock.

Unlike the impedance-based approach, the stiffness calculated in Eq. 9 is not frequency dependent. Eq. 10 defines the dashpot coefficient associated with the normal spring as a function of the relative frequency parameter  $\phi$ . When the natural frequency of the bridge is lower than that of the backfill soil ( $\phi \leq 1$ ), only material damping is considered. When the bridge's natural frequency exceeds that of the soil ( $\phi > 1$ ), both the material and the radiational damping are included.

The springs and the dashpots in the tangential direction, which account for the frictional effect, are assumed to be proportional to the normal ones:

$$k_{\mathrm{s,t}} = \left(\frac{V_{\mathrm{s}}}{V_{\mathrm{La,s}}}\right)^2 k_{\mathrm{s,n}} \tag{12}$$

$$c_{s,t} = \left(\frac{V_s}{V_{La.s}}\right) c_{s,n} \tag{13}$$

In the 2D model, these springs are applied along the vertical beam that represents the retaining wall. To ensure uniform distribution, the wall is divided into

segments and a spring is assigned to each. The spring values are scaled by the effective area that each segment represents.

In this new approach, concentrated spring and dashpot are also applied on the bottom surface of the wall, using Eq. 6 and 8.

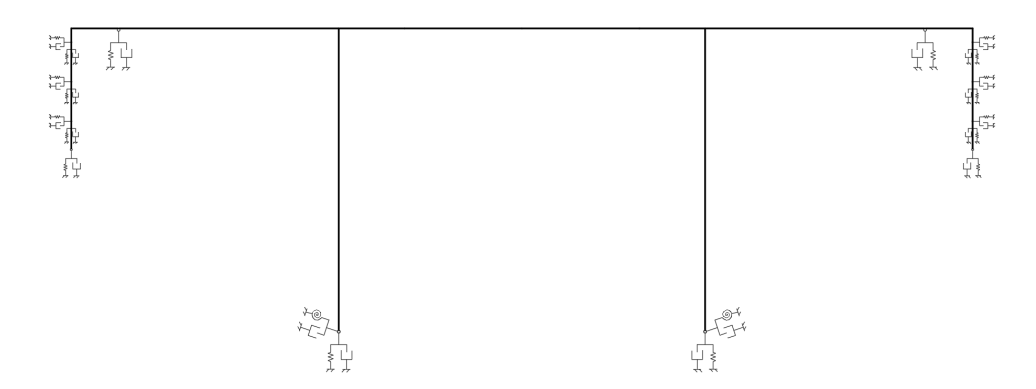


Figure 7. Simplified 2D Model of a three-span bridge with the new springs and dashpots distributed on the vertical retaining wall.

#### 3.5 Material Properties

The bridges analysed in this thesis have been designed by Swedish companies and have already been built in the existing railway lines. However, the actual properties of the materials are difficult to evaluate.

This evaluation would require in situ tests on the soil and concrete and accurate dynamic experiments to obtain calibrated values for the elastic modulus and material damping ratio. This procedure was performed on the four bridges adopted from [9]. For the other bridges, the same properties were assumed for the first analysis and their effect on the response of the bridge during the train passage was investigated in the next analyses. Table 2 shows the material properties for the concrete, the backfill soil, and the underpinning soil which are used for the first analysis.

Table 2. Material properties used for the comparison between different models.

	Density	Elastic Modulus	Damping Ratio
Concrete	$\rho_{\rm c}=2400~{\rm kg/m^3}$	$E_{\rm c}=40~{ m GPa}$	$\xi_{\rm c}=1\%$
Backfill Soil	$\rho_{\rm s}=1800~{\rm kg/m^3}$	$E_{s,b} = 100 \text{ MPa}$	$\xi_{s,b}=6\%$
Underpinning Soil	$\rho_{\rm s}=1800~{\rm kg/m^3}$	$E_{\rm s,c} = 100  \mathrm{MPa}$	$\xi_{\rm s,c}=6\%$

Consequently, the results of the first analysis, in which the different models are compared, do not always represent the most unfavorable response of the bridge.

# 3.6 Dynamic Loading and Response Evaluation

To evaluate the dynamic response of the bridge models under high-speed train loading, a frequency-domain approach was employed. The Frequency Response Function (FRF) was extracted from Abaqus using a steady-state dynamic analysis and subsequently post-processed in MATLAB.

The FRF was computed over a frequency range of 0 to 20 Hz with a resolution of 0.01 Hz. To simulate the train loading, the FRF was multiplied by the Fast Fourier Transform (FFT) of the selected load model (HSLM-A), allowing for the efficient calculation of the system's response. The maximum acceleration was then obtained by transforming the result back into the time domain and evaluating the peak response for each train speed of interest.

This chapter presents the results of the dynamic analyses performed on the selected bridges. The chapter is structured into three sections, based on the number of spans of the bridges:

- 7 single-span bridges
- 3 two-span bridges
- 8 three-span bridges

Each bridge is briefly described, and an overview of its configuration is provided using technical drawings. A series of analyses were carried out to evaluate the influence of key parameters on the maximum acceleration response of the bridge during the train passage. For each bridge, the following graphs are presented:

• **Model Comparison Analysis**: The analysis tests the accuracy of the proposed simplified model. The 2D model with impedance functions at the end shield is used as a reference.

For single-span bridges, the supports are initially modelled using springs and dashpots. An additional curve is included in the results to show the effect of replacing these with fixed supports, enabling a direct comparison between the two boundary conditions.

For two- and three-span bridges, both the supports and intermediate columns are modelled with springs and dashpots. To evaluate their individual influence, the replacement with fixed constraints is performed in two stages: first, only the supports are fixed, and then both supports and columns are fixed. This results in two additional curves per graph, each representing a different level of constraint, allowing a step-by-step assessment of boundary condition effects. For more clarity, these models are presented at the beginning of each section.

- **Backfill soil sensitivity analysis**: This graph explores the influence of backfill soil properties, which are often uncertain in practice. The upper and lower bound values are assumed to reflect a realistic range of bridge response. Specifically, the elastic modulus is varied between 100 MPa and 500 MPa, while the damping ratio is varied between 2% and 6%.
- Column foundation sensitivity analysis (two- and three-span bridges only): This graph examines the influence of the soil beneath the columns.

Two values of the elastic modulus are considered: 100 MPa and 500 MPa. In addition, a model with fully fixed column bases is included for comparison.

The purpose of these analyses is to validate the proposed simplified model and to assess how SSI influences the dynamic response of the bridge. The model incorporates springs and dashpots to simulate the effects of SSI. By testing various soil properties and boundary condition configurations, the most conservative modelling approach can be identified.

# 4.1 Single Span Bridges

The single-span bridges presented in this section share the same key characteristics: end shields on both sides and roller-type connection at the abutments. Figures 8 and 9 show the two models used to analyse these bridges. Regarding the boundary conditions, the abutments are initially modelled using spring and dashpot in the vertical direction (Figure 9). Then, fixed constrains are applied at the supports to assess the influence of the supports flexibility on the dynamic response (Figure 10).



Figure 8. 2D Model of single span bridges with the impedance functions at the end-shields.



Figure 9. Simplified 2D Model of single span bridges with the retaining wall and distributed springs and dashpots.



Figure 10. Simplified 2D Model with fixed supports.

#### 4.1.1 **Aspan**

The Aspan bridge has a span length of 24 m and extends with a cantilever length of 1 m on each side. The deck has a constant cross section throughout its length. The abutments are supported by a shallow foundation placed on compacted crushed rock material.

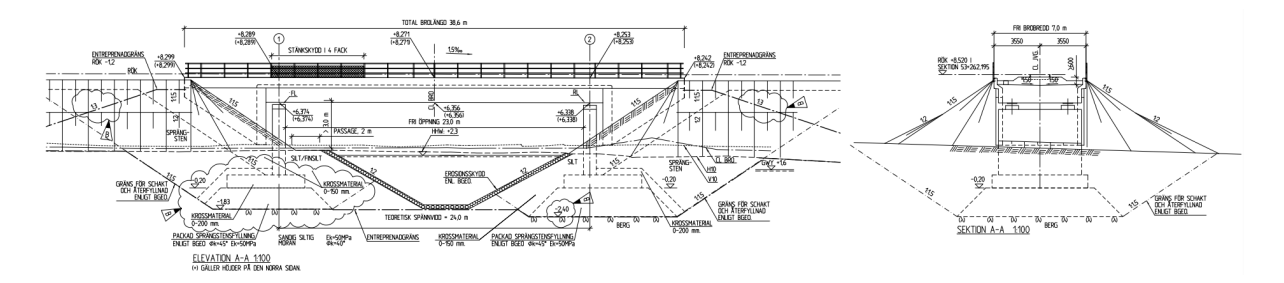


Figure 11. Technical drawings of Aspan bridge.

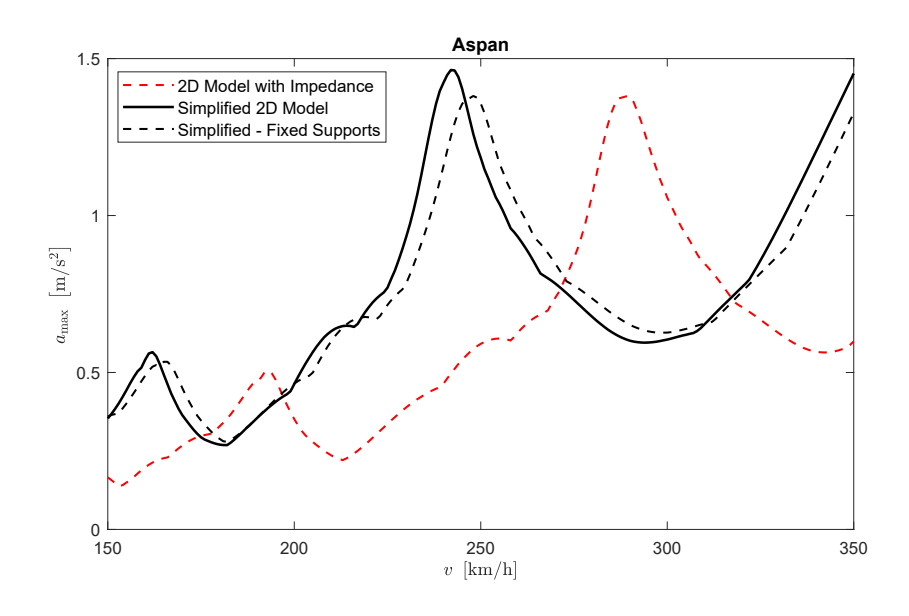


Figure 12. Maximum acceleration of the bridge during HSLM-A9 train passage: comparison between the 2D model with Impedance, the Simplified 2D Model and the Simplified 2D Model with Fixed Support.

Figure 12 shows the maximum acceleration of the bridge for the three different models. The simplified model produces a slightly higher acceleration peak compared to the model with impedance, indicating that this simplification remains on the conservative side. However, a noticeable shift in critical speed is observed, corresponding to a reduction in the first natural frequency of the bridge, as reported in Table 3.

Table 3. First natural frequency and damping ratio of the models in Figure 12.

	$f_1$ (Hz)	<i>ξ</i> <sub>1</sub> (%)
2D Model with Impedance	6.07	2.07
Simplified 2D Model	5.18	3.23
Simplified – Fixed Supports	5.30	3.58

When the spring and dashpot at the supports are replaced by fixed boundary conditions, the results show an increase in natural frequency and a decrease in peak acceleration. This is also reflected in the data in Table 3. Interestingly, even though the dashpot at the supports are removed, the overall damping ratio of the structure increases. This behaviour is driven by a change in the mode shape: the displacement and the velocity at the end-shield increase; therefore, also the effect of the dampers increases.

Based on these observations, the most conservative model in this case is the one that includes spring-dashpot systems at the supports.

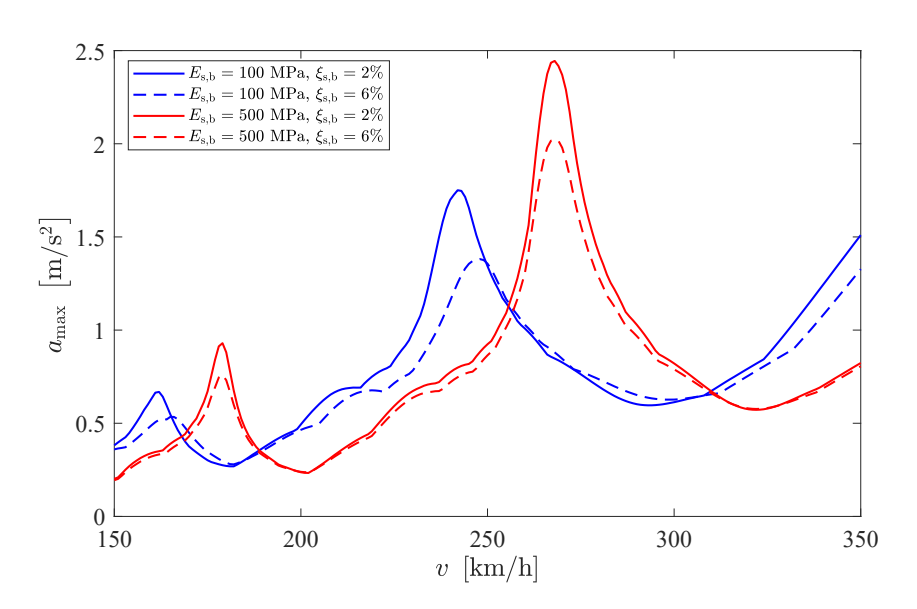


Figure 13. Bridge response for different properties of the backfill soil:  $E_{s,b} = 100 \,\text{MPa}$ ,  $\xi_{s,b} = 6\%$ ;  $E_{s,b} = 100 \,\text{MPa}$ ,  $\xi_{s,b} = 2\%$ ;  $E_{s,b} = 500 \,\text{MPa}$ ,  $\xi_{s,b} = 500 \,\text{MPa}$ ,  $\xi_{s,b} = 500 \,\text{MPa}$ ,  $\xi_{s,b} = 2\%$ .

Table 4. Damping ratio of the first mode for the four scenarios in Figure 13.

Model with:	<i>ξ</i> <sub>1</sub> (%)
$E_{s,b} = 100$ MPa and $\xi_{s,b} = 2\%$	2.60
$E_{s,b} = 100$ MPa and $\xi_{s,b} = 6\%$	3.23
$E_{s,b} = 500$ MPa and $\xi_{s,b} = 2\%$	1.41
$E_{\rm s,b} = 500$ MPa and $\xi_{\rm s,b} = 6\%$	1.85

The sensitivity analysis for the properties of the backfill soil in Figure 13 shows a noticeable increase in maximum acceleration when the elastic modulus increases to 500 MPa. The key parameter influencing this behaviour is the frequency parameter  $\phi$ , defined in Eq. 11. The dashpots distributed along the retaining wall are evaluated using Eq. 10, which includes both hysteretic and radiational damping when  $\phi > 1$ , and only hysteretic damping when  $\phi < 1$ .

The transition from 100 MPa to 500 MPa results in a significant increase in the natural frequency of the backfill soil. As a consequence, the value of  $\phi$  decreases from 1.31 to 0.65, shifting the system from a regime where radiational damping is present to one where it is no longer included. This loss of radiational damping has an impact on modal damping (Table 4), leading to the observed increase in maximum acceleration.

# 4.1.2 Bodavågen

The Bodavågen bridge has a span length of 22 m and extends with a cantilever length of 2.4 m on each side. The deck features a constant cross section throughout its length. The abutments are supported by a shallow foundation placed on compacted crushed rock material.

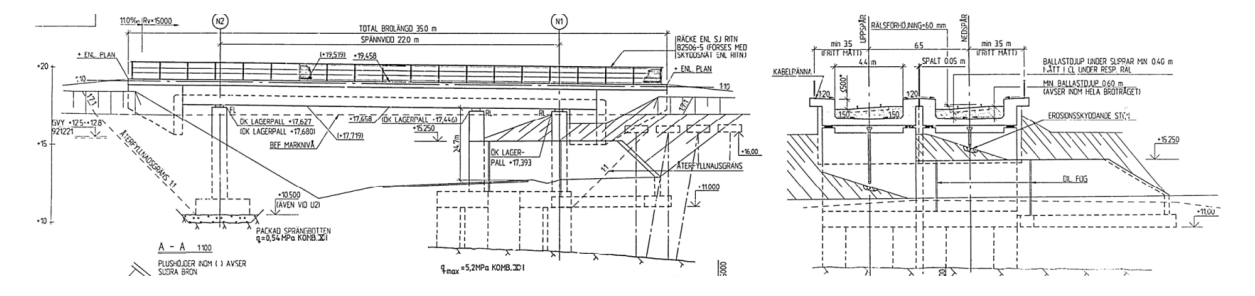


Figure 14. Technical drawings of Bodavågen bridge.

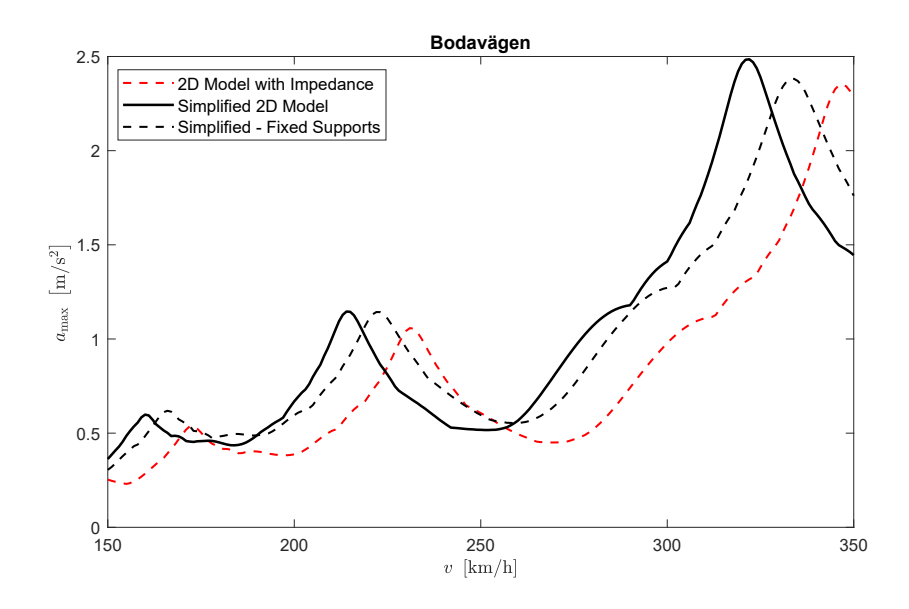


Figure 15. Maximum acceleration of the bridge during HSLM-A7 train passage: comparison between the 2D model with Impedance, the Simplified 2D Model and the Simplified 2D Model with Fixed Support.

The comparison in Figure 15 reveals the same differences as for the previous bridge: the maximum acceleration of the simplified model is higher and the first natural frequency is reduced. The model with fixed supports presents a lower acceleration, due to an higher effect of the dampers at the end-shield and a consequent increase in modal damping ratio (Table 5).

Table 5. First natural frequency and damping ratio of the models in Figure 15.

	$f_1$ (Hz)	<i>ξ</i> <sub>1</sub> (%)
2D Model with Impedance	8.02	3.09
Simplified 2D Model	7.45	3.42
Simplified – Fixed Supports	7.72	4.08

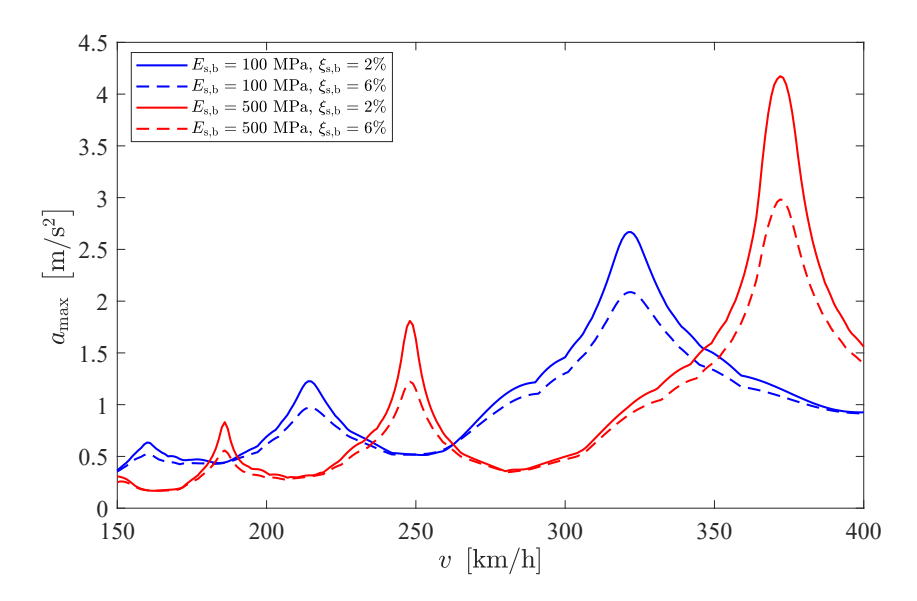


Figure 16. Bridge response for different properties of the backfill soil:  $E_{s,b} = 100 \,\text{MPa}$ ,  $\xi_{s,b} = 6\%$ ;  $E_{s,b} = 100 \,\text{MPa}$ ,  $\xi_{s,b} = 500 \,\text{MPa}$ ,  $\xi_{s,b} = 2\%$ .

Table 6. Damping ratio of the first mode for the four scenarios in Figure 16.

Model with:	<i>ξ</i> <sub>1</sub> (%)
$E_{\mathrm{s,b}} = 100 \mathrm{MPa}$ and $\xi_{\mathrm{s,b}} = 2\%$	3.14
$E_{s,b} = 100$ MPa and $\xi_{s,b} = 6\%$	4.20
$E_{s,b} = 500$ MPa and $\xi_{s,b} = 2\%$	1.02
$E_{\mathrm{s,b}} = 500 \mathrm{MPa}$ and $\xi_{\mathrm{s,b}} = 6\%$	1.72

The sensitivity analysis on the backfill soil properties in Figure 16 shows a substantial difference between the two limit cases. When using a stiff soil, the acceleration exceeds the 3.5 m/s<sup>2</sup> limit. However, the critical speed also increases, causing resonance to occur at speeds outside the range of interest. The frequency parameter  $\phi$  is 1.60 for 100 MPa and 0.83 for 500 MPa, indicating that the increase is due to the loss of radiational damping as the elastic modulus increases.

# 4.1.3 Brustjärnsbäcken

The Brustjärnsbäcken bridge has a span length of 30 m and extends with a cantilever length of 1 m on each side. The deck is post-tensioned and features a constant cross section in the internal span, which increases near the ends above the supports. The abutments are supported by shallow foundations placed on compacted crushed rock material.

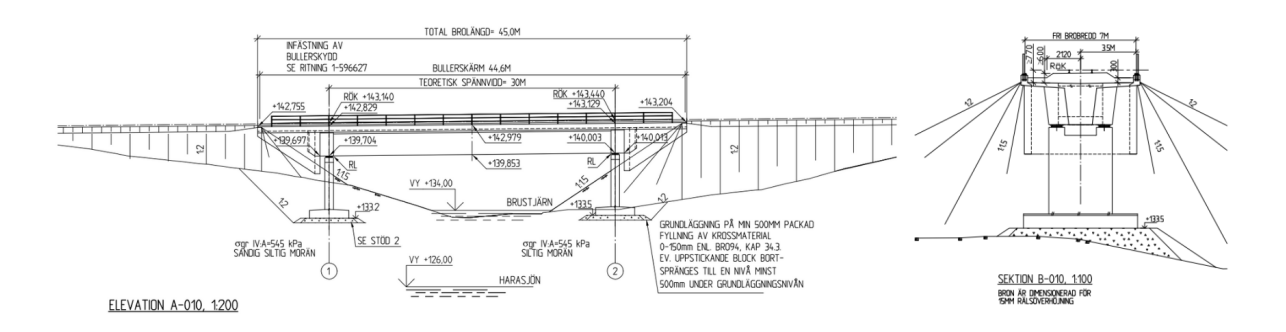


Figure 17. Technical drawings of Brustjärnsbäcken bridge.

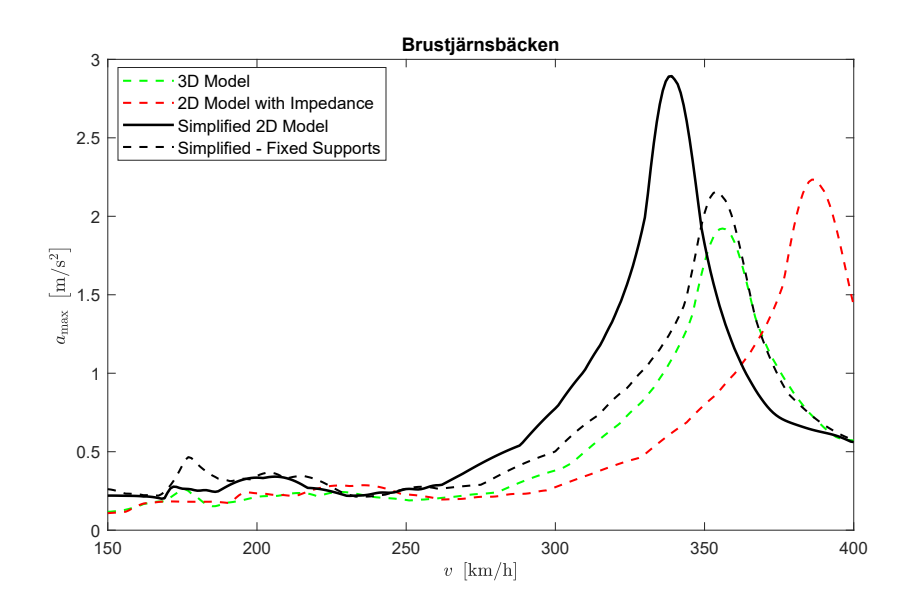


Figure 18. Maximum acceleration of the bridge during HSLM-A1 train passage: comparison between the 3D Model, the 2D Model with Impedance, the Simplified 2D Model and the Simplified 2D Model with Fixed Support.

The previous bridges featured slab-type deck cross sections connected to the top of the retaining wall. In contrast, this bridge has a deep trapezoidal cross section that interacts with the retaining wall over approximately half its depth, as illustrated in Figure 17. Due to this configuration, a 3D model of the bridge and backfill soil was developed in Abaqus and used as a reference for comparison, as shown in Figure 19. The results indicate that the 2D model with impedance functions slightly overestimates the natural frequency compared to

the 3D model, while the difference in peak acceleration remains minimal. Conversely, the simplified 2D model underestimates the natural frequency and yields higher acceleration, confirming that it provides conservative estimates.

The removal of the spring-dashpot system at the supports has a more significant impact on this bridge, resulting in a decrease in peak acceleration of approximately  $0.5 \text{ m/s}^2$ .

Table 7. First natural frequency and damping ratio of the models in Figure 18.

	$f_1$ (Hz)	<i>ξ</i> <sub>1</sub> (%)
3D Model	5.49	2.45
2D Model with Impedance	5.97	2.15
Simplified 2D Model	5.24	1.80
Simplified – Fixed Supports	5.50	2.23

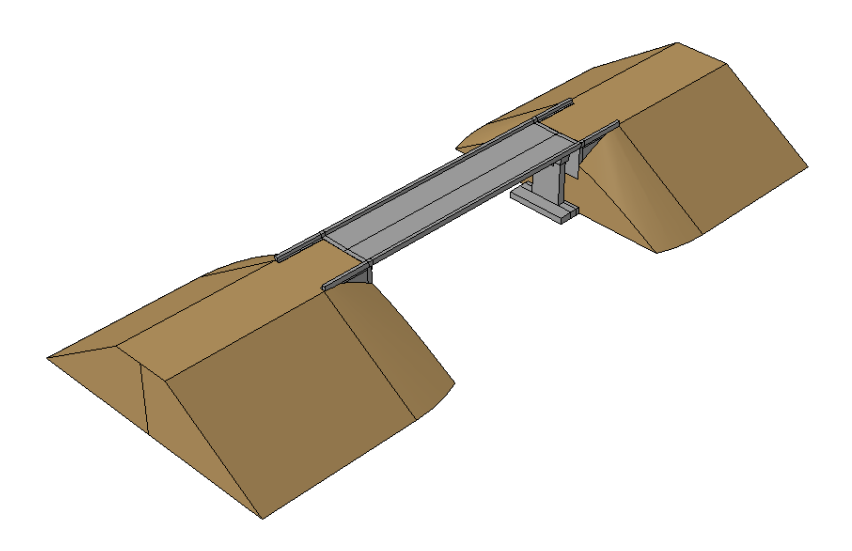


Figure 19. 3D Model of the Brustjärnsbäcken bridge created with Abaqus.

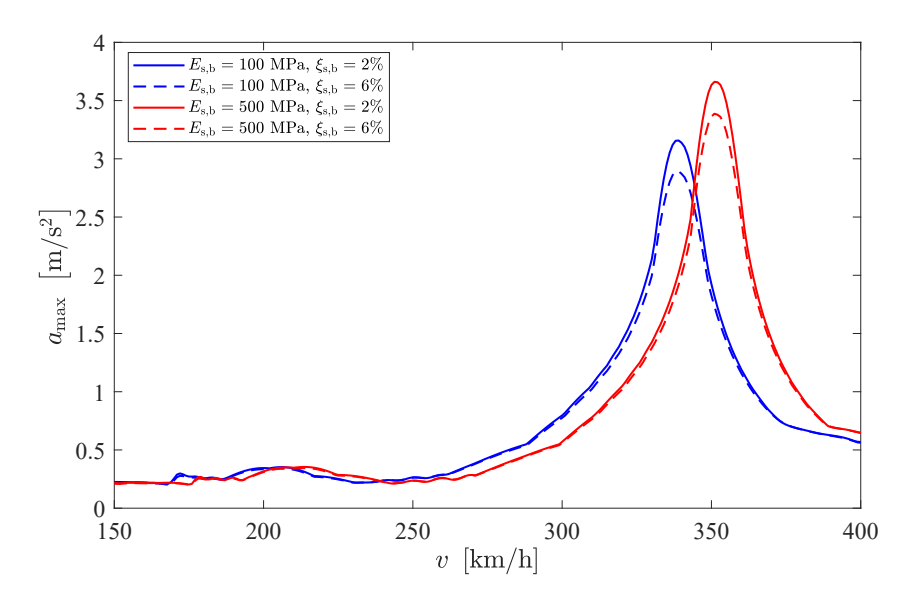


Figure 20. Bridge response for different properties of the backfill soil:  $E_{s,b} = 100 \,\mathrm{MPa}$ ,  $\xi_{s,b} = 6\%$ ;  $E_{s,b} = 100 \,\mathrm{MPa}$ ,  $\xi_{s,b} = 2\%$ ;  $E_{s,b} = 500 \,\mathrm{MPa}$ ,  $\xi_{s,b} = 500 \,\mathrm{MPa}$ ,  $\xi_{s,b} = 500 \,\mathrm{MPa}$ ,  $\xi_{s,b} = 2\%$ .

Table 8. Damping ratio of the first mode for the four scenarios in Figure 20.

Model with:	<i>ξ</i> <sub>1</sub> (%)
$E_{\mathrm{s,b}} = 100 \mathrm{MPa}$ and $\xi_{\mathrm{s,b}} = 2\%$	1.60
$E_{s,b} = 100$ MPa and $\xi_{s,b} = 6\%$	1.80
$E_{s,b} = 500$ MPa and $\xi_{s,b} = 2\%$	1.25
$E_{\mathrm{s,b}} = 500 \mathrm{MPa}$ and $\xi_{\mathrm{s,b}} = 6\%$	1.41

The sensitivity analysis on the backfill soil in Figure 20 shows a trend similar to that observed for the previous bridges. The computed values of the frequency parameter  $\phi$  are 1.31 for an elastic modulus of 100 MPa and 0.58 for 500 MPa, indicating the same transition from a regime with radiational damping to one without.

#### 4.1.4 Bubäcken

The Bubäcken bridge has a span length of 17 m and extends with a cantilever length of 1 m on each side. The deck features a constant cross section in the internal span, which gradually increases near the ends above the supports. The abutments are supported by pile foundations reaching a depth of 15 m, anchored in the bedrock.

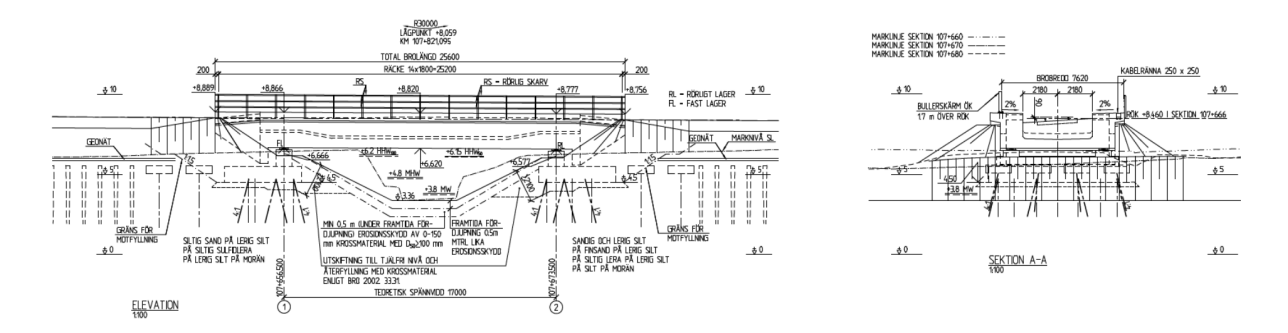


Figure 21. Technical drawings of Bubäcken bridge.

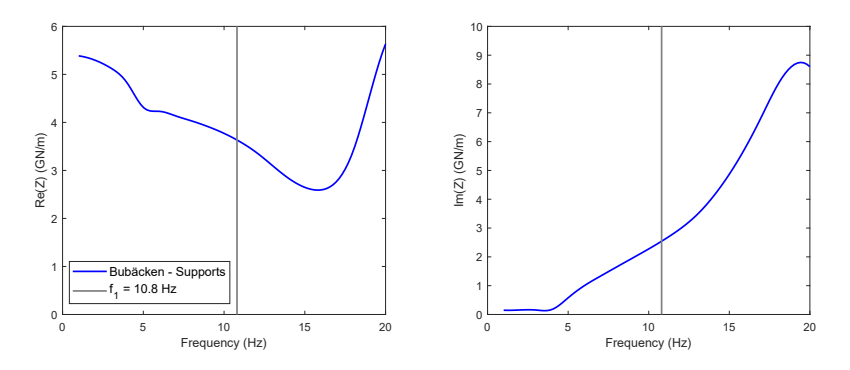


Figure 22. Vertical impedance function of the pile group for the Bubäcken bridge: real part (left) and imaginary part (right), corresponding to the response at the supports.

Figure 22 presents the vertical impedance function of the pile group, computed using COMSOL Multiphysics. The imaginary part of the impedance function clearly illustrates the combined effect of hysteretic and radiational damping. The curve remains nearly constant up to approximately 4 Hz, indicating the dominance of hysteretic damping in that frequency range. Beyond this threshold—corresponding to the natural frequency of the pile group—radiation damping becomes significant, resulting in a sharp increase in the damping coefficient. Given that the natural frequency of the bridge is 10.8 Hz, which lies well beyond this transition point, the resulting damping coefficient is relatively high.

This effect carries over into the bridge's response, resulting in a higher damping ratio, as illustrated in Table 9. Figure 23 illustrates this difference through the

comparison between the simplified model with spring and dashpot at the supports and the same model with fixed supports. This significant variation in peak acceleration is primarly due to the high dashpot coefficient at the supports, as well as the lower stiffness of the pile foundation compared to that of a shallow foundation.

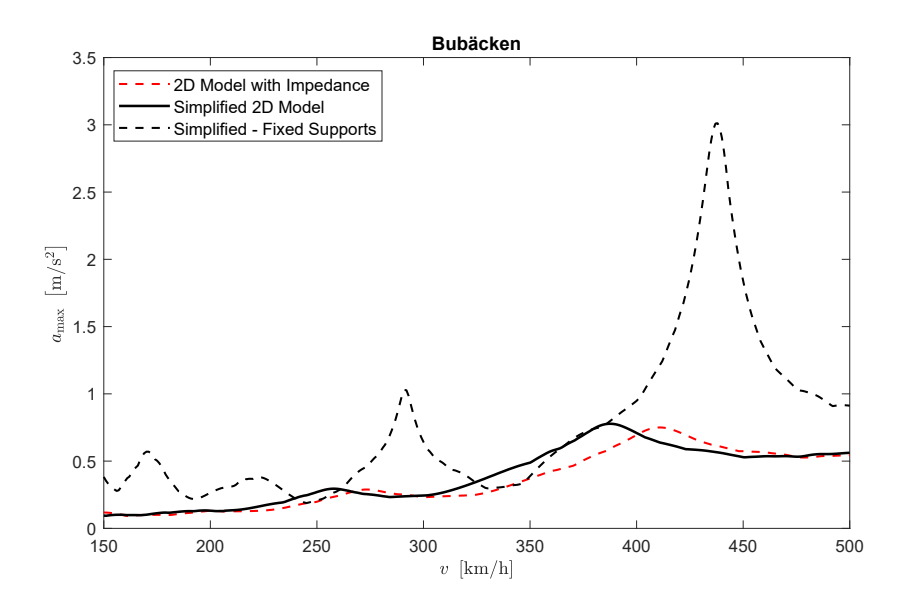


Figure 23. Maximum acceleration of the bridge during HSLM-A1 train passage: comparison between the 2D model with Impedance, the Simplified 2D Model and the Simplified 2D Model with Fixed Support.

Table 9. First natural frequency and damping ratio of the models in Figure 23.

	$f_1$ (Hz)	<i>ξ</i> <sub>1</sub> (%)
2D Model with Impedance	11.35	6.03
Simplified 2D Model	10.80	6.00
Simplified – Fixed Supports	13.50	1.53

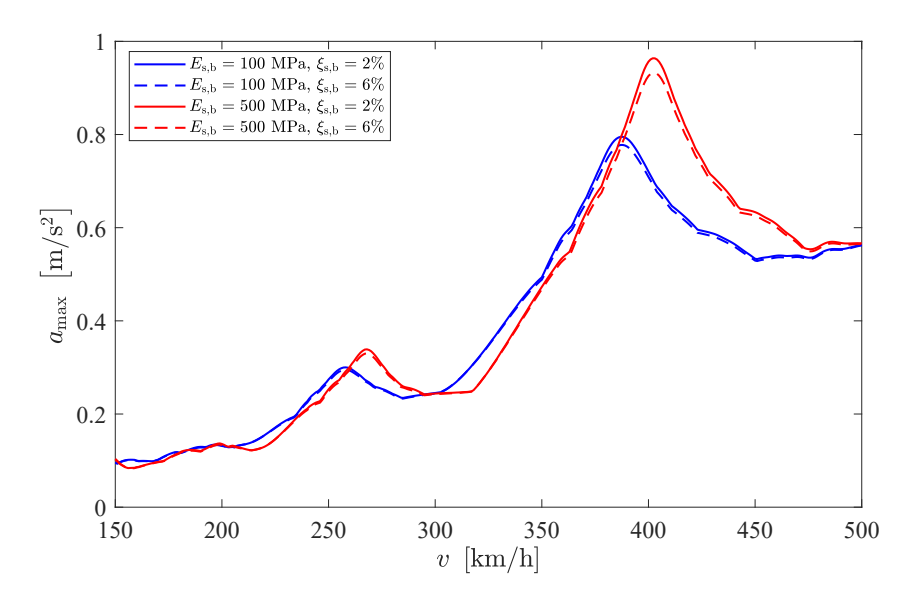


Figure 24. Bridge response for different properties of the backfill soil:  $E_{s,b} = 100 \,\text{MPa}$ ,  $\xi_{s,b} = 6\%$ ;  $E_{s,b} = 100 \,\text{MPa}$ ,  $\xi_{s,b} = 2\%$ ;  $E_{s,b} = 500 \,\text{MPa}$ ,  $\xi_{s,b} = 500 \,\text{MPa}$ ,  $\xi_{s,b} = 500 \,\text{MPa}$ ,  $\xi_{s,b} = 2\%$ .

The sensitivity analysis in Figure 24 shows only a relatively small difference between the models with varying elastic modulus. However, the computed frequency parameter  $\phi$  is 0.57 for 100 MPa and 0.26 for 500 MPa. Based on these values, radiational damping is not involved in either model, and therefore, the acceleration for the 500 MPa model would be expected to be lower. As previously mentioned, this bridge is strongly influenced by the spring and dashpot at the supports, which alters the contribution of the end shield compared to the other bridges.

Table 10. Damping ratio of the first mode for the four scenarios in Figure 24.

Model with:	$\xi_1$ (%)
$E_{\rm s,b} = 100$ MPa and $\xi_{\rm s,b} = 2\%$	5.90
$E_{s,b} = 100$ MPa and $\xi_{s,b} = 6\%$	6.00
$E_{s,b} = 500$ MPa and $\xi_{s,b} = 2\%$	4.70
$E_{\mathrm{s,b}} = 500 \mathrm{\ MPa}$ and $\xi_{\mathrm{s,b}} = 6\%$	4.90

# 4.1.5 Degernäsbäcken

The Degernäsbäcken bridge has a span length of 20.5 m and extends with a cantilever length of 1 m on each side. The deck features a constant cross section in the internal span, which gradually increases near the ends above the supports. The abutments are supported by pile foundations reaching a depth of 9 m, anchored in the bedrock.

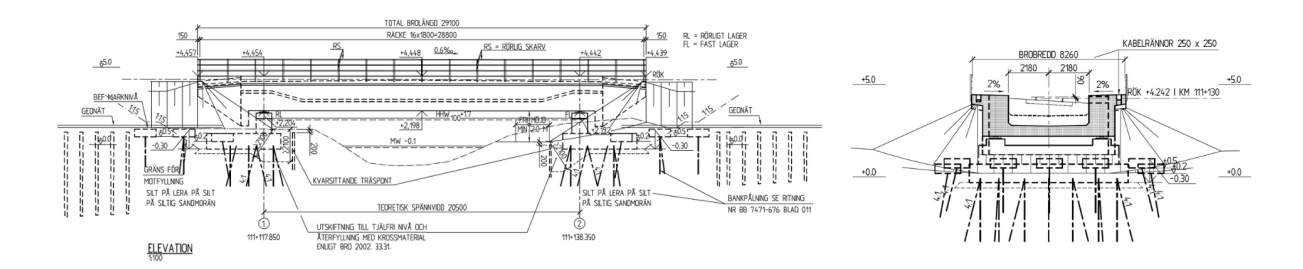


Figure 25. Technical drawings of Degernäsbäcken bridge.

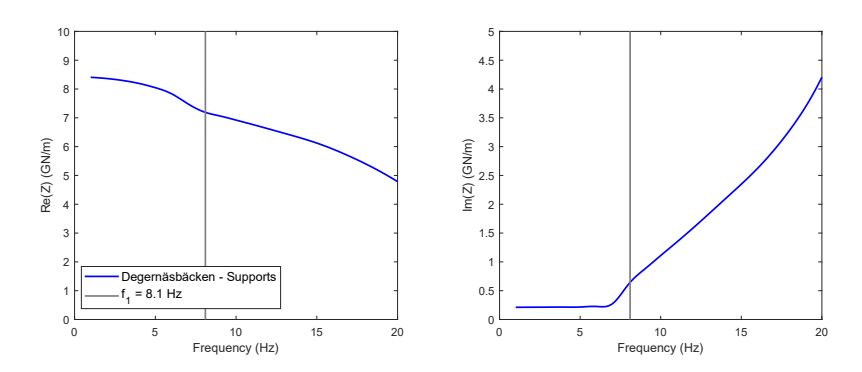


Figure 26. Vertical impedance function of the pile group for the Degernäsbäcken bridge: real part (left) and imaginary part (right), corresponding to the response at the supports.

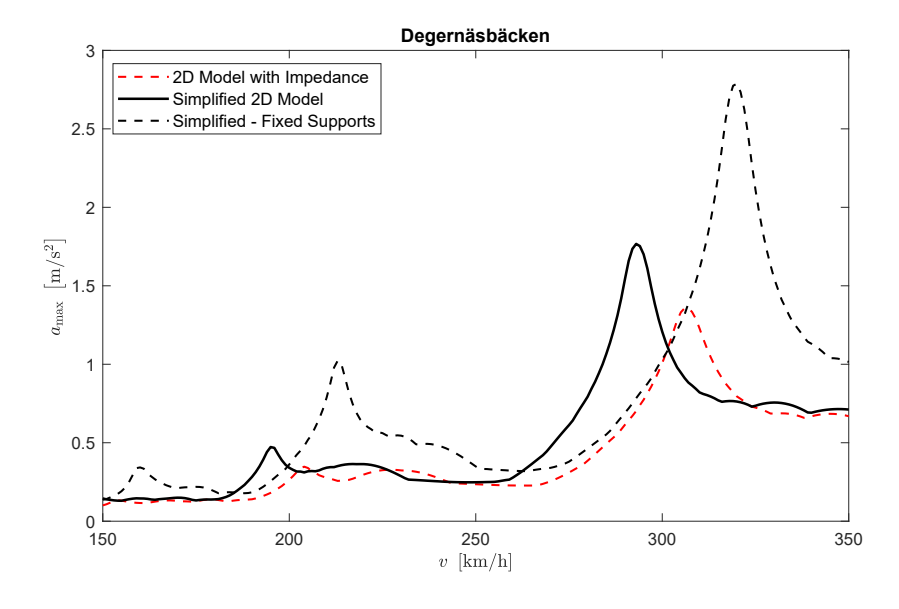


Figure 27. Maximum acceleration of the bridge during HSLM-A3 train passage: comparison between the 2D model with Impedance, the Simplified 2D Model and the Simplified 2D Model with Fixed Support.

A comparison between Figure 22 and Figure 26 clearly shows that the damping coefficient—represented by the imaginary part of the impedance function—is lower in the latter case. This difference is due to the reduced depth of the pile foundation and the lower first natural frequency of the bridge. As a result, a lower influence of the supports on the dynamic response of the bridge can be anticipated.

This assumption is confirmed by the results in Figure 27 and Table 11. While the simplified model with fixed supports still shows higher acceleration and resonance speed, the differences are limited, further confirming the reduced sensitivity to boundary conditions in this case.

Table 11	First natural	fraguancy	and	damnina	ratio c	of tha	modale	in Ei	oura 2	7
Table 11.	riist naturai	nequency	anu	uamping	ratio (	n me	moders	шгі	guie 2	٠/.

	$f_1$ (Hz)	<i>ξ</i> <sub>1</sub> (%)
2D Model with Impedance	8.51	1.80
Simplified 2D Model	8.15	1.38
Simplified – Fixed Supports	8.88	1.33

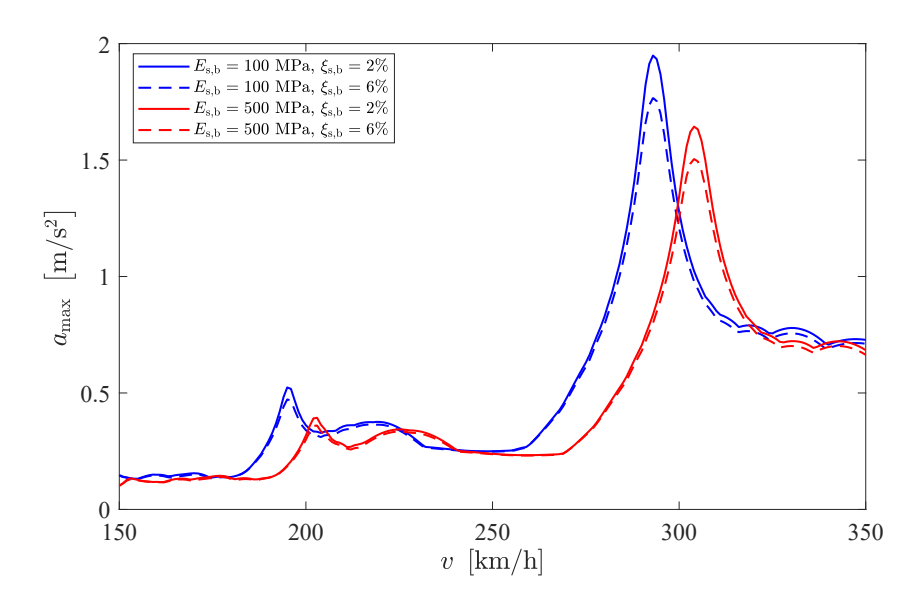


Figure 28. Bridge response for different properties of the backfill soil:  $E_{s,b} = 100 \,\text{MPa}$ ,  $\xi_{s,b} = 6\%$ ;  $E_{s,b} = 100 \,\text{MPa}$ ,  $\xi_{s,b} = 2\%$ ;  $E_{s,b} = 500 \,\text{MPa}$ ,  $\xi_{s,b} = 500 \,\text{MPa}$ ,  $\xi_{s,b} = 500 \,\text{MPa}$ ,  $\xi_{s,b} = 2\%$ .

Table 12. Damping ratio of the first mode for the four scenarios in Figure 28.

Model with:	<i>ξ</i> <sub>1</sub> (%)
$E_{\mathrm{s,b}} = 100$ MPa and $\xi_{\mathrm{s,b}} = 2\%$	1.21
$E_{\mathrm{s,b}} = 100 \mathrm{MPa}$ and $\xi_{\mathrm{s,b}} = 6\%$	1.38
$E_{s,b} = 500$ MPa and $\xi_{s,b} = 2\%$	1.33
$E_{\mathrm{s,b}} = 500 \mathrm{MPa}$ and $\xi_{\mathrm{s,b}} = 6\%$	1.50

Unlike the previous bridges, the sensitivity analysis of the backfill soil shows a reduction in peak acceleration when the elastic modulus is increased to 500 MPa. This occurs because, in this case, the frequency parameter  $\phi$  is below 1 for both soil stiffness values: 0.56 for 100 MPa and 0.26 for 500 MPa. As  $\phi < 1$  in all cases, radiational damping is not activated, and only material damping is used. Since material damping increases proportionally with stiffness, the model with  $E_{\rm s,b} = 500$  MPa exhibits higher damping and consequently lower peak accelerations.

# 4.1.6 Norrmjöleån

The Norrmjöleån bridge has a span length of 29 m and extends with a cantilever length of 1.4 m on each side. The deck features a constant cross section throughout its length. The abutments are supported by a shallow foundation placed on compacted crushed rock material.

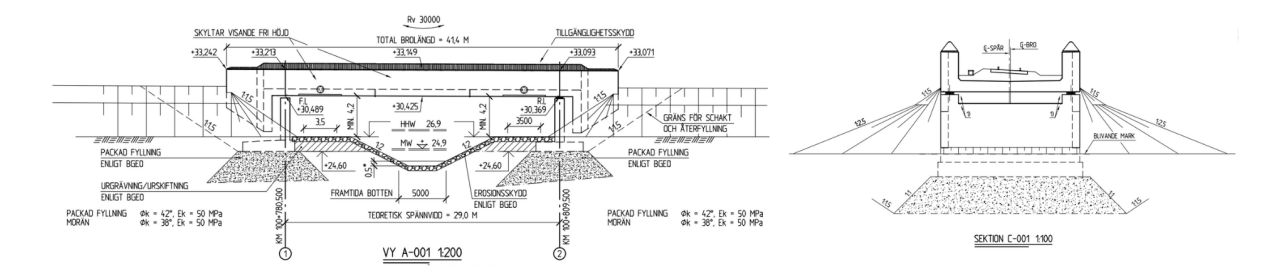


Figure 29. Technical drawings of Norrmjöleån bridge

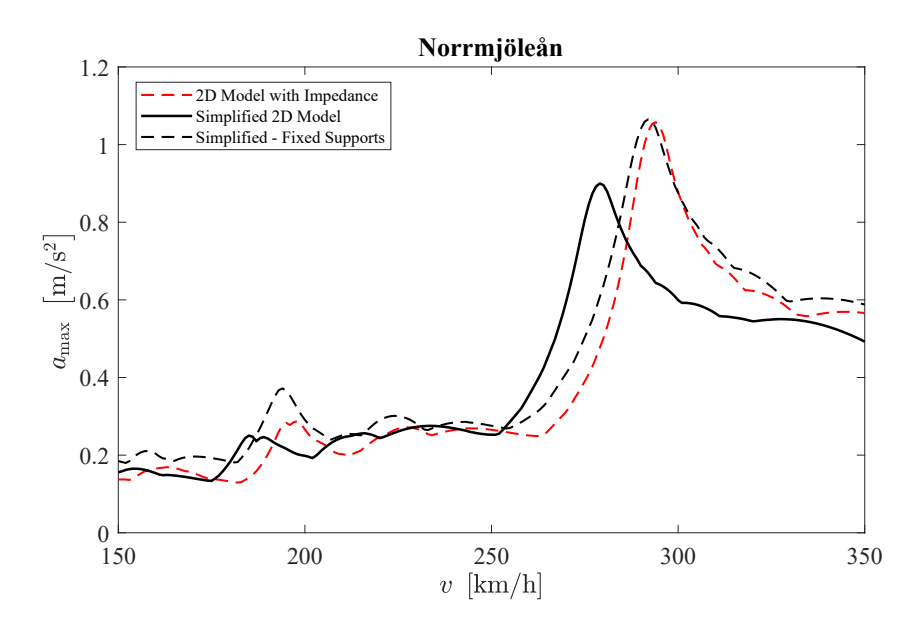


Figure 30. Maximum acceleration of the bridge during HSLM-A10 train passage: comparison between the 2D model with Impedance, the Simplified 2D Model and the Simplified 2D Model with Fixed Support.

For this bridge, the simplified 2D model yields a lower maximum acceleration than the 2D model with impedance functions, as shown in Figure 30. Since each bridge has a different configuration, variations in behaviour are expected depending on their specific parameters. However, the difference in acceleration is approximately 0.2 m/s<sup>2</sup>, which is relatively small compared to the threshold of interest. Fixing the supports results in an increase in both the natural frequency and maximum acceleration, indicating that the spring and dashpot at the supports have a reductive effect on the resonance response. This behaviour contrasts with that observed in the other bridges with shallow foundations.

Table 13. First natural frequency and damping ratio of the models in Figure 30.

	$f_1$ (Hz)	<i>ξ</i> <sub>1</sub> (%)
2D Model with Impedance	6.03	1.89
Simplified 2D Model	5.74	2.36
Simplified – Fixed Supports	6.00	2.68

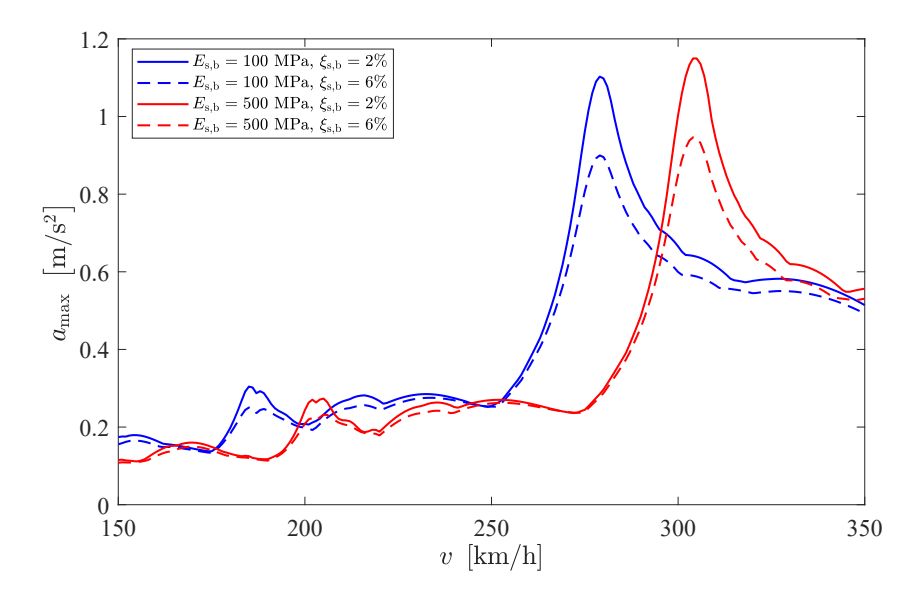


Figure 31. Bridge response for different properties of the backfill soil:  $E_{s,b} = 100 \,\text{MPa}$ ,  $\xi_{s,b} = 6\%$ ;  $E_{s,b} = 100 \,\text{MPa}$ ,  $\xi_{s,b} = 2\%$ ;  $E_{s,b} = 500 \,\text{MPa}$ ,  $\xi_{s,b} = 500 \,\text{MPa}$ ,  $\xi_{s,b} = 2\%$ .

In this case as well, the difference between the two limit scenarios for the backfill soil depends on the frequency parameter  $\phi$ , which is 1.04 for 100 MPa and 0.48 for 500 MPa. The amplitude increases with the stiffer soil due to the loss of radiational damping. However, since  $\phi = 1.04$  is close to the threshold value, the contribution of radiational damping is small. As a result, the difference in response between the two models is minimal, as shown in Figure 31.

Table 14. Damping ratio of the first mode for the four scenarios in Figure 31.

Model with:	<i>ξ</i> <sub>1</sub> (%)
$E_{\mathrm{s,b}} = 100 \mathrm{MPa}$ and $\xi_{\mathrm{s,b}} = 2\%$	1.81
$E_{s,b} = 100$ MPa and $\xi_{s,b} = 6\%$	2.36
$E_{s,b} = 500 \text{ MPa} \text{ and } \xi_{s,b} = 2\%$	1.42
$E_{\mathrm{s,b}} = 500 \mathrm{MPa}$ and $\xi_{\mathrm{s,b}} = 6\%$	1.87

# 4.1.7 Ångerån

The Ångerån bridge has a span length of 21 m and extends with a cantilever length of 1.4 m on each side. The deck features a constant cross section in the internal span, which gradually increases near the ends above the supports. The abutments are supported by a shallow foundation placed on compacted crushed rock material.

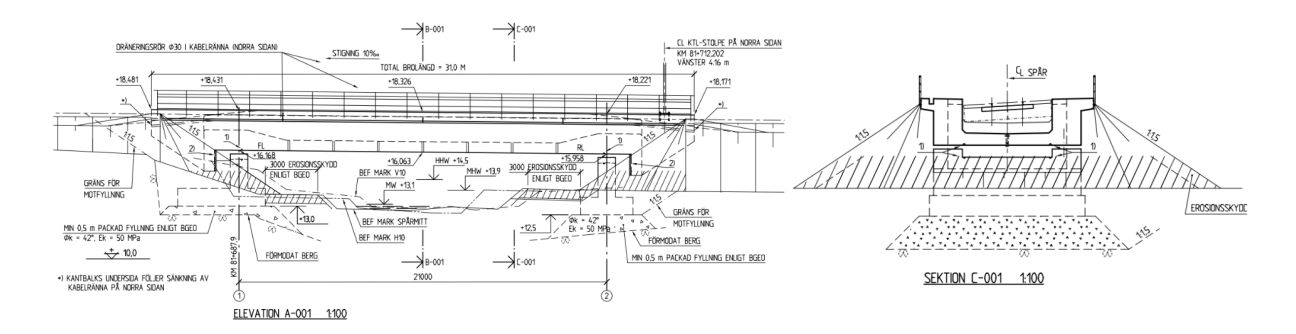


Figure 32. Technical drawings of Ångerån bridge.

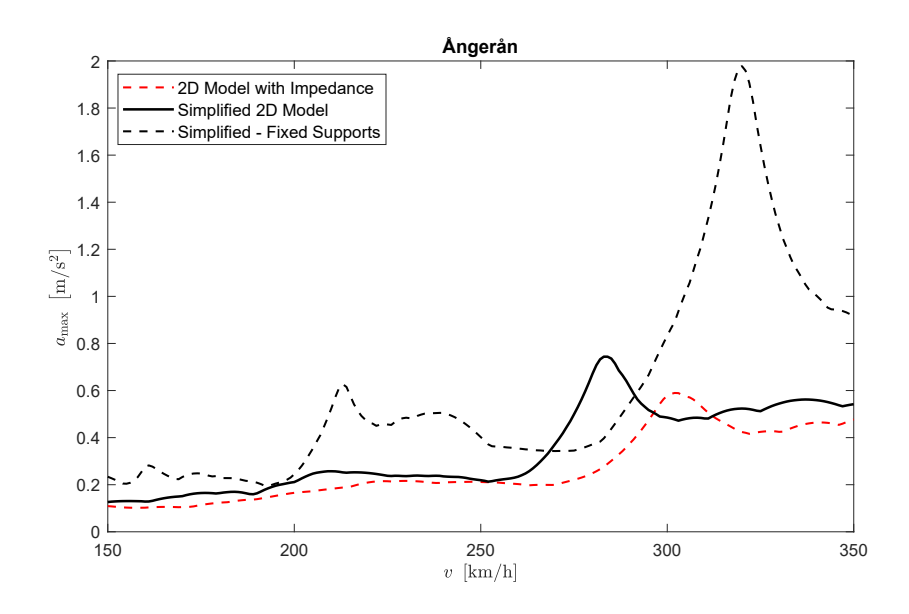


Figure 33. Maximum acceleration of the bridge during HSLM-A3 train passage: comparison between the 2D model with Impedance, the Simplified 2D Model and the Simplified 2D Model with Fixed Support.

Comparing the layout in Figure 32 with those of the previously analyzed bridges, it is evident that the retaining wall in this case has a significantly smaller depth. This geometric difference reduces the contribution of the backfill soil to the overall system stiffness, thereby increasing the influence of foundation flexibility on the dynamic response. As shown in Figure 33, fixing the supports leads to a notable increase in acceleration, with a difference of approximately 1.3 m/s<sup>2</sup> between the model incorporating springs and dashpots and the model with fixed supports.

Table 15. First natural frequency and damping ratio of the models in Figure 33.

	$f_1$ (Hz)	<i>ξ</i> <sub>1</sub> (%)
2D Model with Impedance	8.38	2.42
Simplified 2D Model	7.87	2.01
Simplified – Fixed Supports	8.88	1.92

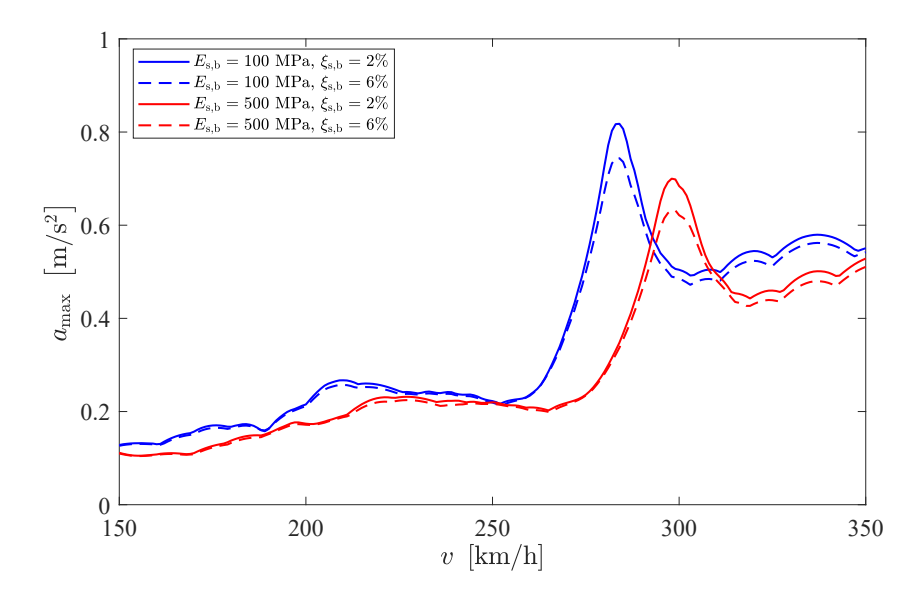


Figure 34. Bridge response for different properties of the backfill soil:  $E_{s,b} = 100 \,\text{MPa}$ ,  $\xi_{s,b} = 6\%$ ;  $E_{s,b} = 100 \,\text{MPa}$ ,  $\xi_{s,b} = 2\%$ ;  $E_{s,b} = 500 \,\text{MPa}$ ,  $\xi_{s,b} = 500 \,\text{MPa}$ ,  $\xi_{s,b} = 2\%$ .

Table 16. Damping ratio of the first mode for the four scenarios in Figure 34.

Model with:	<i>ξ</i> <sub>1</sub> (%)
$E_{\mathrm{s,b}} = 100 \mathrm{MPa}$ and $\xi_{\mathrm{s,b}} = 2\%$	1.80
$E_{s,b} = 100$ MPa and $\xi_{s,b} = 6\%$	2.01
$E_{\mathrm{s,b}} = 500 \mathrm{\ MPa}$ and $\xi_{\mathrm{s,b}} = 2\%$	1.89
$E_{s,b} = 500$ MPa and $\xi_{s,b} = 6\%$	2.13

The sensitivity analysis of the backfill soil shows a reduction in peak acceleration when the elastic modulus is increased to 500 MPa. This occurs because, in this case, the frequency parameter  $\phi$  is below 1 for both soil stiffness values: 0.68 (left) and 0.95 (right) for 100 MPa, and 0.32 (left) and 0.44 (right) for 500 MPa. As  $\phi$  < 1 in all cases, radiational damping is not activated, and only material damping is used. Since material damping increases proportionally with stiffness, the model with  $E_{\rm s,b} = 500$  MPa exhibits higher damping and consequently lower peak accelerations.

# 4.2 Two Span Bridges

Two-span bridges are supported by abutments at the ends and additionally by a central column. The connection between the column and the deck varies depending on the bridge, and can be either rigid or pinned. The end-shield exhibits the same characteristics as in the single-span bridges and is therefore modeled using the same approach. The two models in Figure 37 features different boundary conditions to evaluate their effect on the response of the bridge.

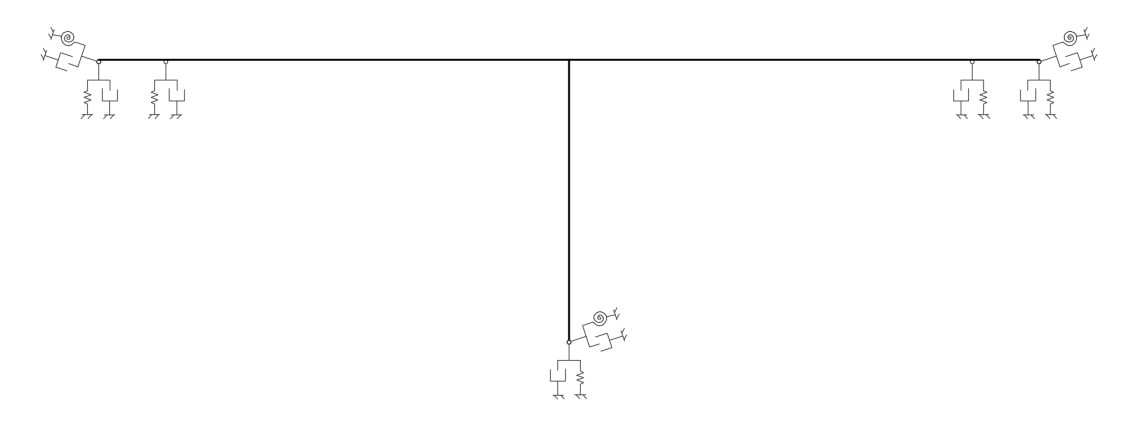


Figure 35. 2D Model of three-span bridges with the impedance functions at the end-shields

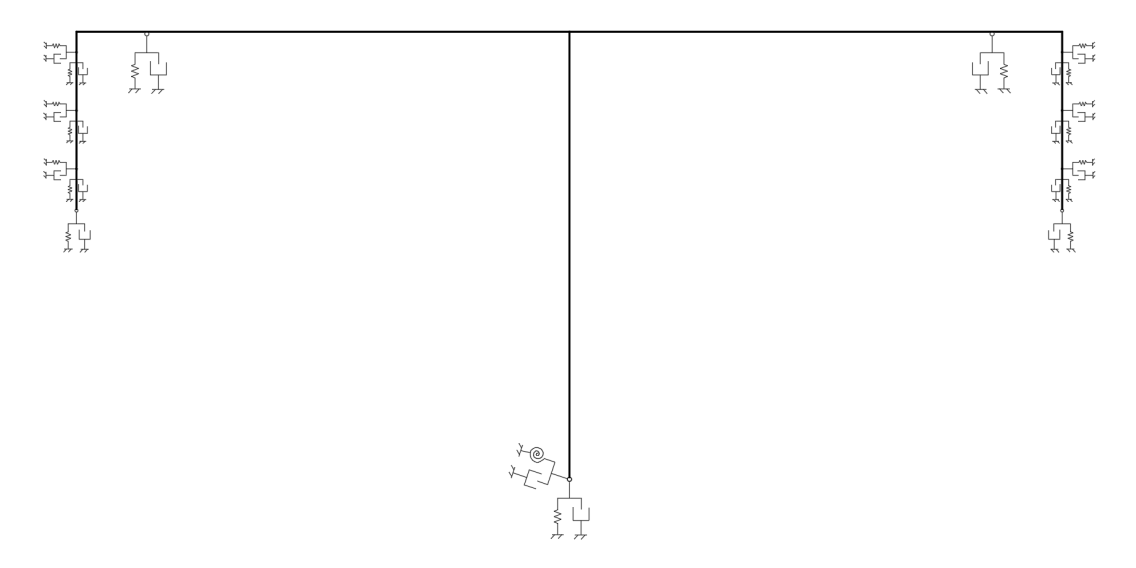


Figure 36. Simplified 2D Model of two-span bridges with the retaining wall and distributed springs and dashpots.

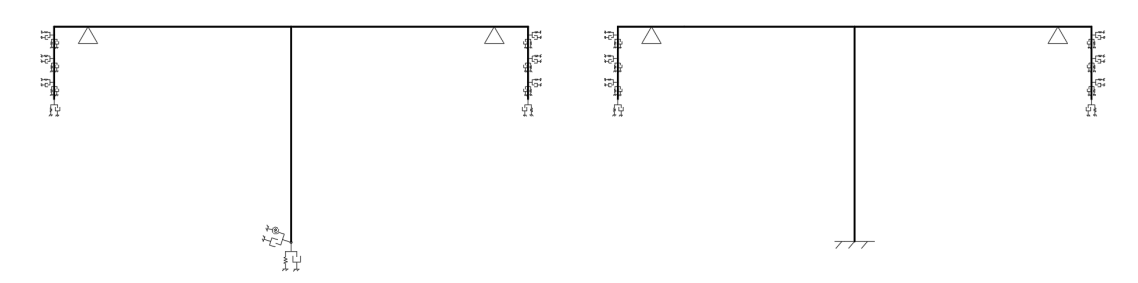


Figure 37. Simplified 2D Model with fixed supports (left) and with both supports and columns fixed (right).

### 4.2.1 Leduån

The Leduån bridge has a span length of 23 m and extends with a cantilever length of 1 m on each side. The deck has a constant cross section in the internal spans, which gradually increases near the central column. Both the abutments and the column are supported by pile foundations, with depths of 22 m and 16 m for the abutments and the column, respectively.

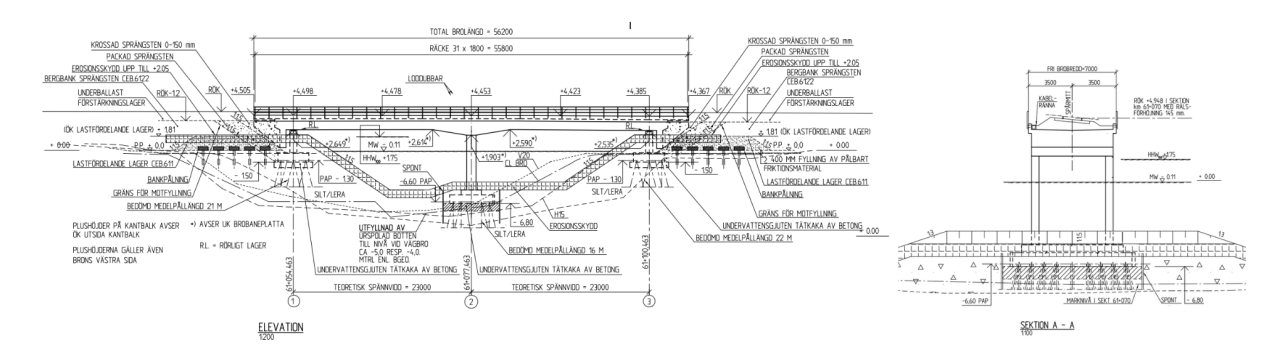


Figure 38. Technical drawings of Leduan bridge.

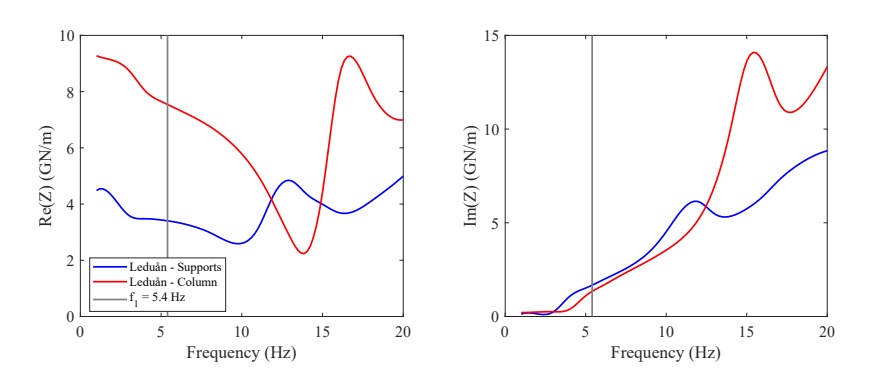


Figure 39. Vertical impedance function of the pile group for the Leduån bridge: real part (left) and imaginary part (right). Each plot shows two curves corresponding to the response at the supports and at the column.

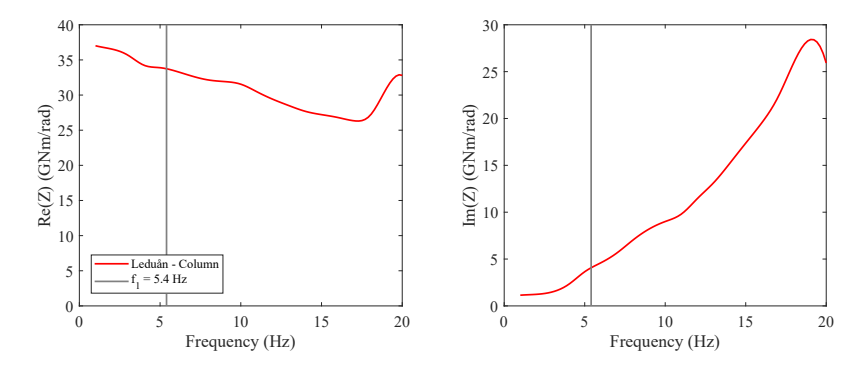


Figure 40. Rotational impedance function of the pile group for the Leduån bridge: real part (left) and imaginary part (right), corresponding to the response at the column.

Figure 39 shows the vertical impedance functions for both the supports and the column. The difference in foundation depth, 22 m for the supports and 16 m for

the column, has a clear impact on the dynamic stiffness (real part) of the system. However, the damping component (imaginary part) does not show significant variation near the frequency of interest.

The model comparison in Figure 41 reveals a significant shift in frequency between the model with impedance and the simplified model. Removal of the spring-dashpot systems at the supports leads to an increase in acceleration due to the resulting reduction in damping, as confirmed by the values in Table 17. In contrast, removing the spring-dashpot system at the column produces only a minimal variation in the response, indicating a limited influence of column rigidity on overall dynamic behavior.

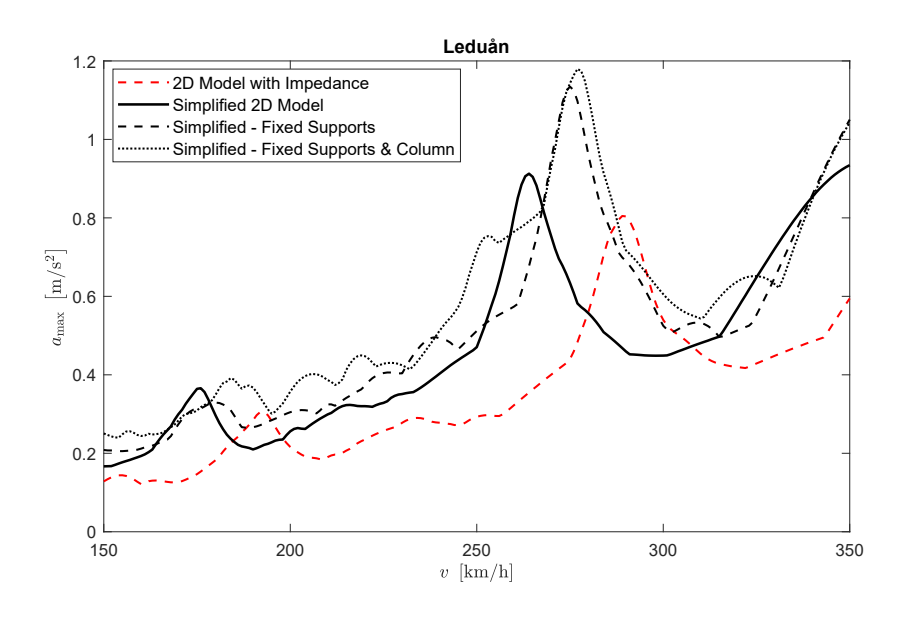


Figure 41. Maximum bridge acceleration during HSLM-A10 train passage: comparison between the 2D model with impedance and three simplified 2D models with varying boundary conditions.

Table 17. First natural frequency and damping ratio of the models in Figure 41.

	$f_1$ (Hz)	<i>ξ</i> <sub>1</sub> (%)
2D Model with Impedance	5.92	2.21
Simplified 2D Model	5.40	2.44
Simplified – Fixed Supports	5.63	2.10
Simplified – Fixed Supports and Columns	5.68	2.06

The sensitivity analysis of the backfill soil shows a reduction in maximum acceleration when the elastic modulus is increased to 500 MPa. This occurs because, in this case, the frequency parameter  $\phi$  is below 1 for both soil stiffness values: 0.64 for 100 MPa and 0.31 for 500 MPa. As  $\phi < 1$  in all cases, radiational damping is not activated and only material (hysteretic) damping is used. Since

material damping is lower than radiational damping, increase in soil stiffness is predominant in this case and the model with  $E_{s,b} = 500$  MPa exhibits higher damping and consequently lower peak accelerations.

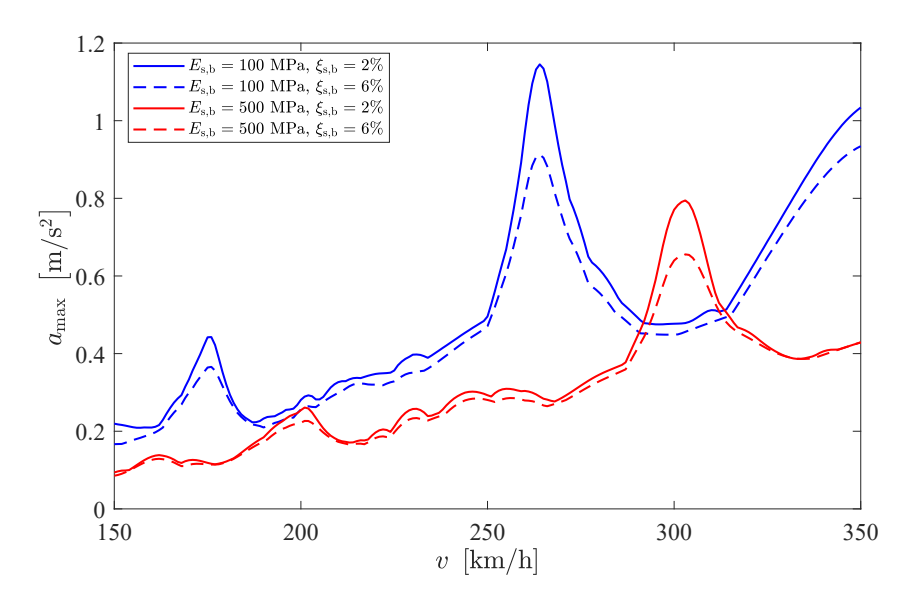


Figure 42. Bridge response for different properties of the backfill soil:  $E_{s,b}=100\,\mathrm{MPa}$ ,  $\xi_{s,b}=6\%$ ;  $E_{s,b}=100\,\mathrm{MPa}$ ,  $\xi_{s,b}=6\%$ ; and  $E_{s,b}=500\,\mathrm{MPa}$ ,  $\xi_{s,b}=2\%$ .

To evaluate the effect of the column foundation on the bridge's response, different boundary conditions were tested. Figure 43 presents the maximum acceleration for the simplified model, along with a model in which the column support is fixed. The results clearly indicate that the flexibility of the column foundation has a negligible impact on the bridge's dynamic response, resulting in only a minimal variation in maximum acceleration.

Table 18. Damping ratio of the first mode for the four scenarios in Figure 43.

Model with:	ξ <sub>1</sub> (%)
$E_{\mathrm{s,b}} = 100 \mathrm{MPa}$ and $\xi_{\mathrm{s,b}} = 2\%$	1.82
$E_{s,b} = 100$ MPa and $\xi_{s,b} = 6\%$	2.44
$E_{s,b} = 500$ MPa and $\xi_{s,b} = 2\%$	1.70
$E_{\mathrm{s,b}} = 500$ MPa and $\xi_{\mathrm{s,b}} = 6\%$	2.30

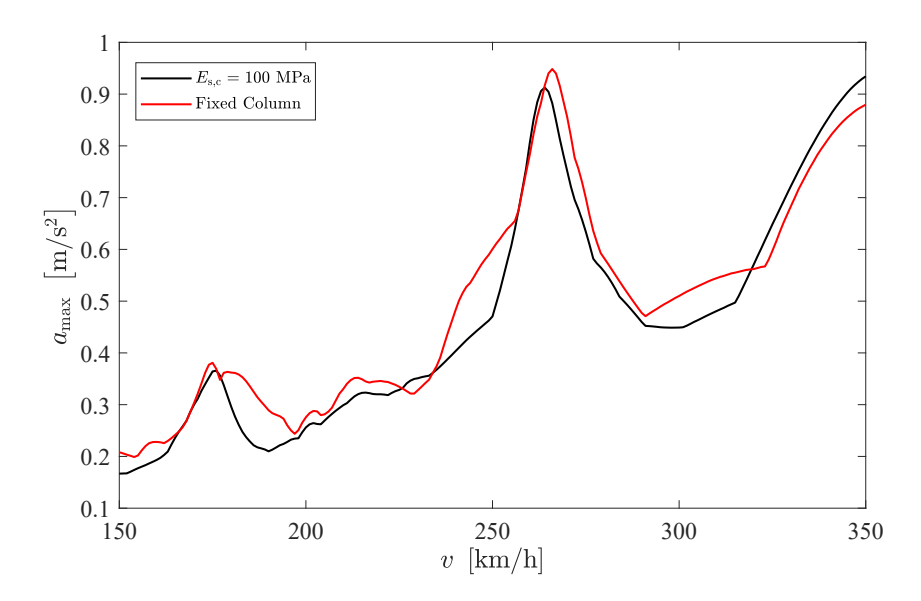


Figure 43. Bridge response for different values of the elastic modulus of the soil beneath the column foundations:  $E_{s,c} = 100 \,\mathrm{MPa}$  and Fixed, where the springs and dashpots are replaced with fixed constraints.

#### 4.2.2 Leån

The Leån bridge has a span length of 18 m and extends with a cantilever length of 0.9 m on each side. The deck is post-tensioned and features a constant cross section in the internal spans, which increases near the ends above the supports. The abutments are supported by shallow foundations placed on compacted crushed rock material, while the central column is supported by a sealing plate (*tätkaka*), which is used to stabilize the soil.

Unlike the other bridges, the column is not rigidly connected to the deck; instead, it is connected with a pinned joint.

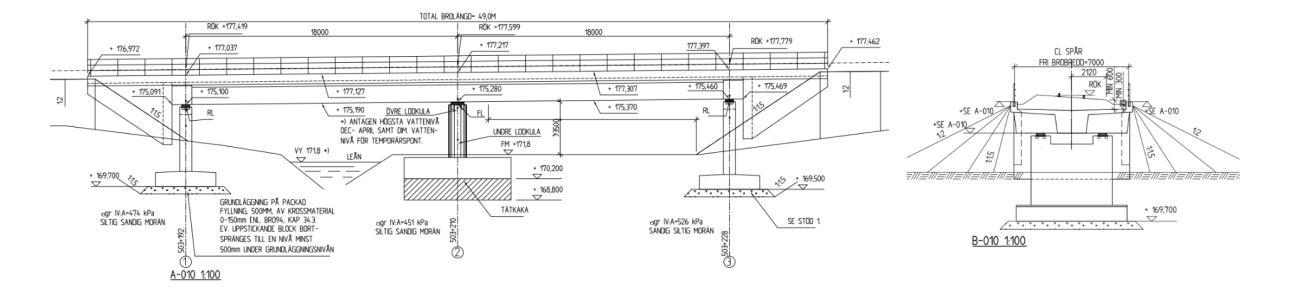


Figure 44. Technical drawings of Leån bridge.

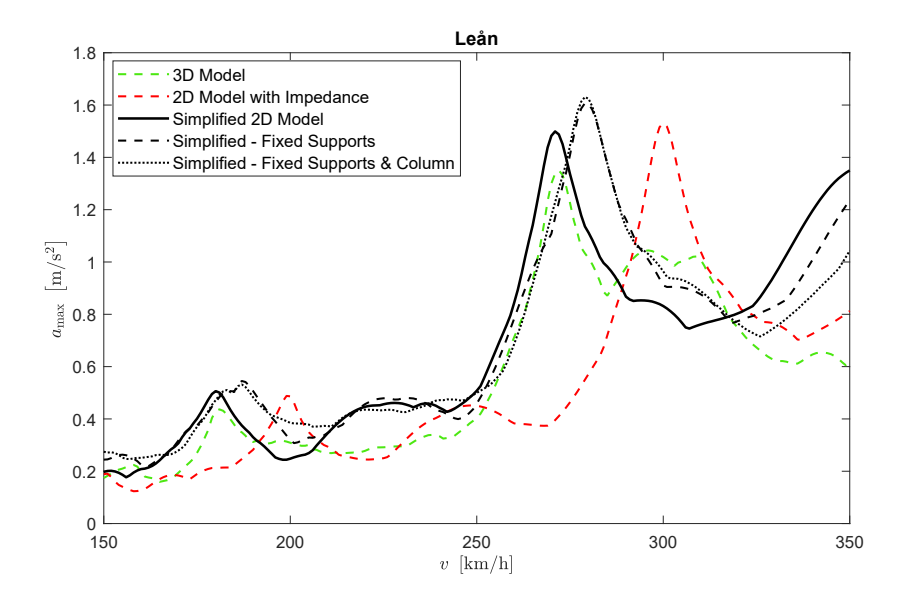


Figure 45. Maximum bridge acceleration during HSLM-A3 train passage: comparison between the 3D model, the 2D model with impedance and three simplified 2D models with varying boundary conditions.

Table 19. First natural frequency and damping ratio of the models in Figure 45.

	$f_1$ (Hz)	<i>ξ</i> <sub>1</sub> (%)
3D Model	7.54	1.74
2D Model with Impedance	8.32	1.35
Simplified 2D Model	7.51	2.30
Simplified – Fixed Supports	7.75	2.75
Simplified – Fixed Supports and Columns	7.75	2.75

For this bridge, a 3D model was developed (Figure 46) and compared to the two 2D models in Figure 45. Among the two, the simplified 2D model yields results that are closer to those of the 3D model. The influence of the spring-dashpot systems at the supports and the column is minimal; their replacement results in only a slight increase in both acceleration and stiffness. In particular, the column has no influence on the dynamic response due to its pinned connection with the deck.

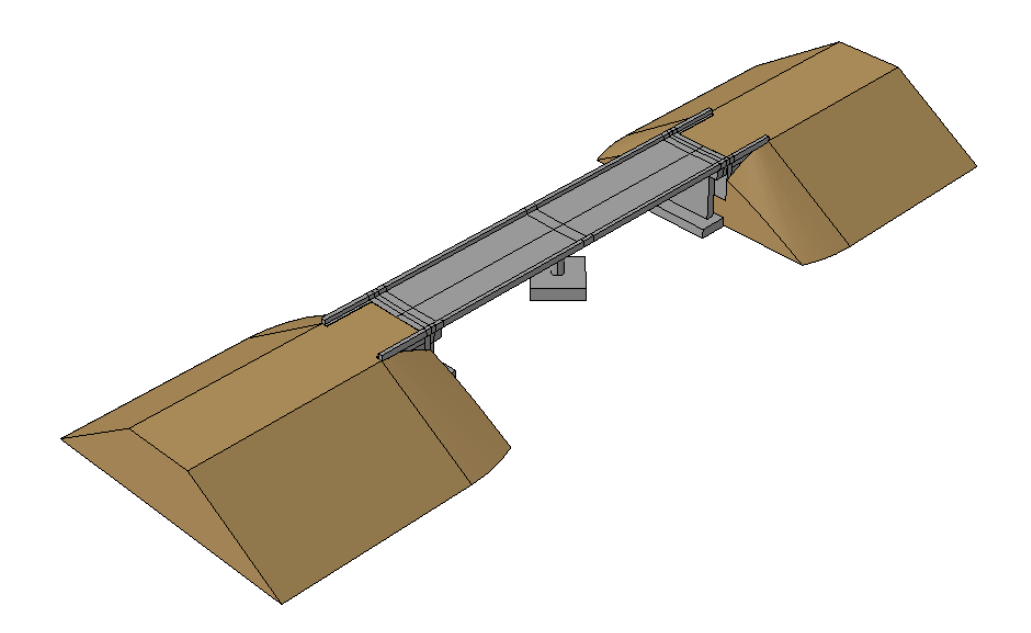


Figure 46. 3D Model of the Leån bridge created with Abaqus.

The sensitivity analysis of the backfill soil properties reveals a similar variation to that observed in the other bridges. The frequency parameter  $\phi$  is 1.43 for an elastic modulus of 100 MPa and 0.64 for 500 MPa. As a result, the acceleration increases due to the loss of radiational damping and the corresponding reduction in modal damping.

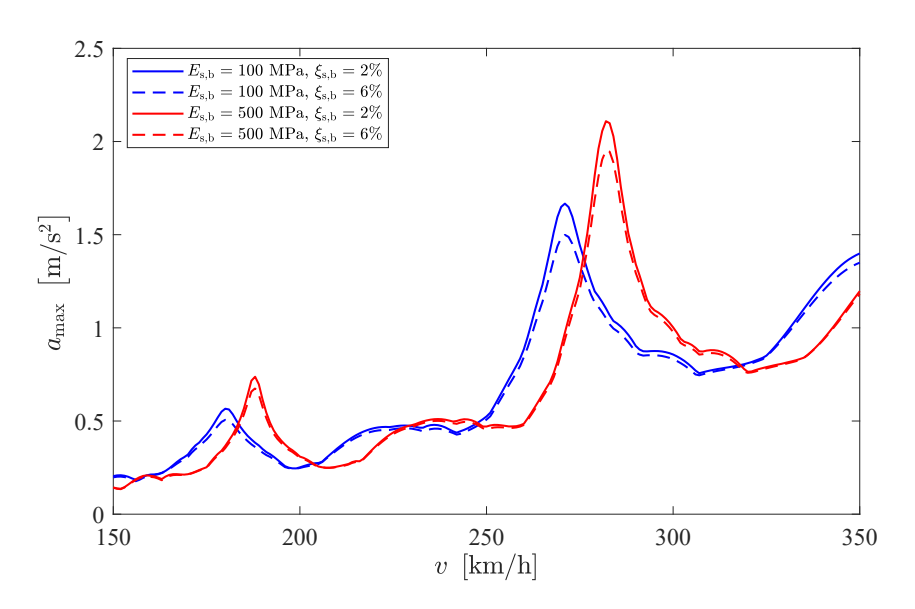


Figure 47. Bridge response for different properties of the backfill soil:  $E_{s,b}=100\,\mathrm{MPa}$ ,  $\xi_{s,b}=6\%$ ;  $E_{s,b}=100\,\mathrm{MPa}$ ,  $\xi_{s,b}=6\%$ ; and  $E_{s,b}=500\,\mathrm{MPa}$ ,  $\xi_{s,b}=2\%$ .

Table 20. Damping ratio of the first mode for the four scenarios in Figure 47.

Model with:	<i>ξ</i> <sub>1</sub> (%)
$E_{\mathrm{s,b}} = 100  \mathrm{MPa} \ \mathrm{and} \ \xi_{\mathrm{s,b}} = 2\%$	2.00
$E_{s,b} = 100$ MPa and $\xi_{s,b} = 6\%$	2.30
$E_{s,b} = 500$ MPa and $\xi_{s,b} = 2\%$	1.22
$E_{\mathrm{s,b}} = 500 \mathrm{MPa}$ and $\xi_{\mathrm{s,b}} = 6\%$	1.37

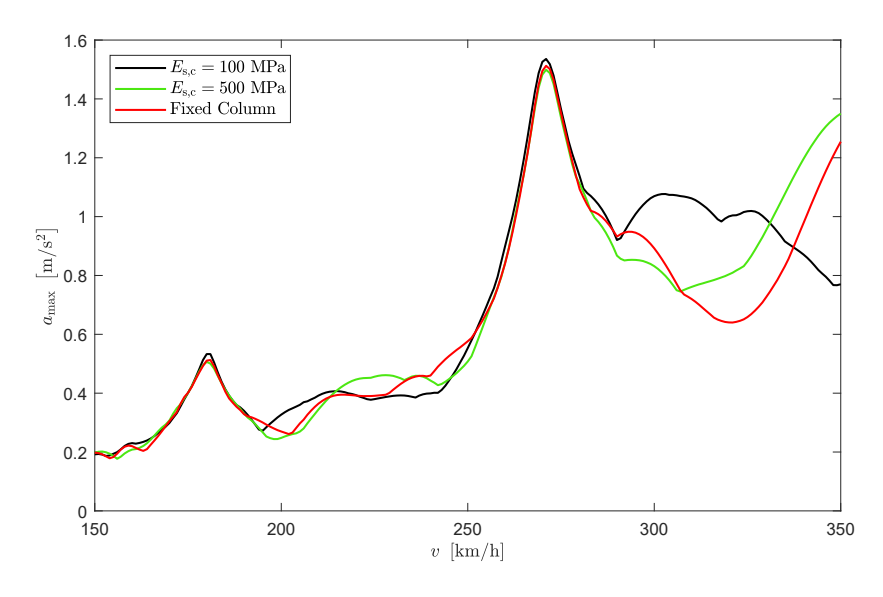


Figure 48. Bridge response for different values of the elastic modulus of the soil beneath the column foundations:  $E_{s,c} = 100 \,\text{MPa}$ ;  $E_{s,c} = 500 \,\text{MPa}$ ; and Fixed, where the springs and dashpots are replaced with fixed constraints.

The column foundation sensitivity analysis confirms the previous observations. The three curves, corresponding to two different elastic modulus and fixed con-

dition, show the same peak acceleration. For this bridge, the soil-structure interaction at the foundation can be considered negligible.

#### 4.2.3 Stridbäcken

The Stridbäcken bridge has an unsymmetrical configuration, with a span of 19.5 m and the other of 22 m. They both extend with a cantilever length of 1 m. The deck has a constant cross section in the internal spans, which gradually increases near the central column. The abutments and the column are supported by shallow foundations placed on compacted crushed rock material.

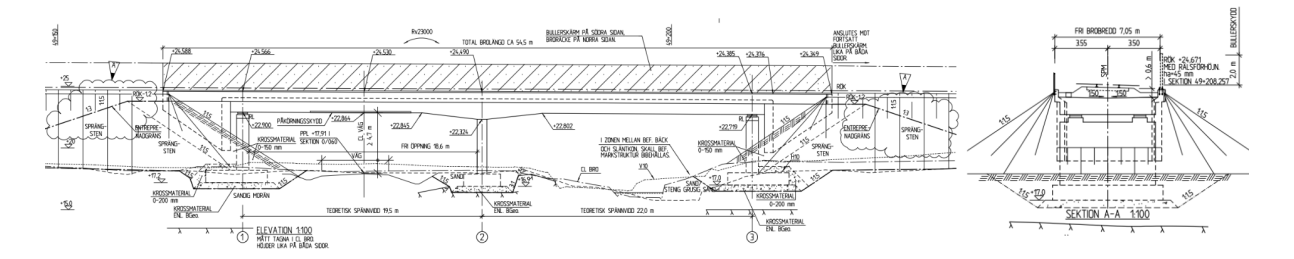


Figure 49. Technical drawings of Stridbäcken bridge.

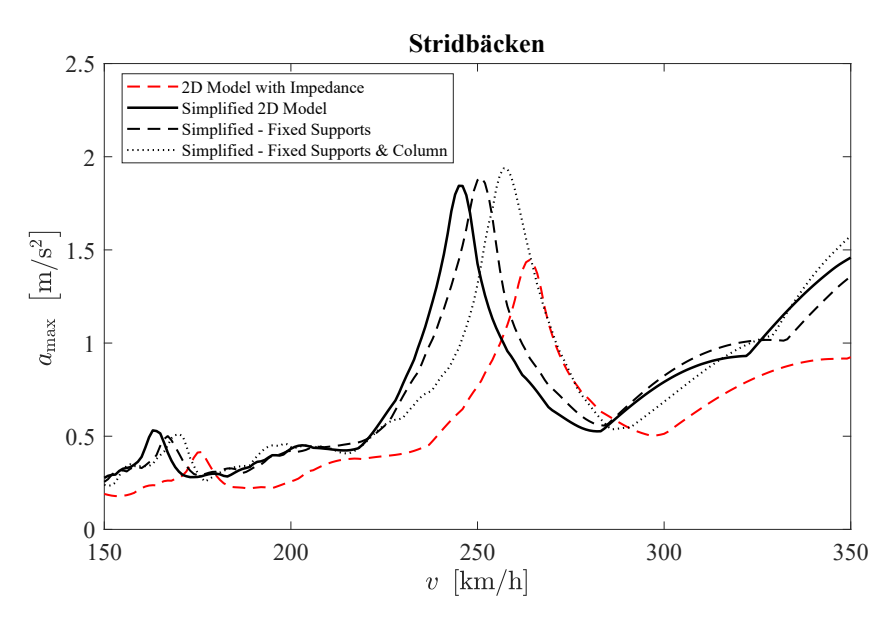


Figure 50. Maximum bridge acceleration during HSLM-A10 train passage: comparison between the 2D model with impedance and three simplified 2D models with varying boundary conditions.

The model comparison in Figure 50 shows that the simplified 2D model results in higher accelerations compared to the reference model. On the other hand, varying the boundary conditions does not lead to substantial differences in the bridge response, except for a slight increase in the first natural frequency. Consequently, SSI at the supports and the column does not play a predominant role in the dynamic response of the bridge.

Table 21. First natural frequency and damping ratio of the models in Figure 50.

	$f_1$ (Hz)	<i>ξ</i> <sub>1</sub> (%)
2D Model with Impedance	6.12	1.56
Simplified 2D Model	5.69	1.54
Simplified – Fixed Supports	5.82	1.65
Simplified – Fixed Supports and Columns	5.92	1.57

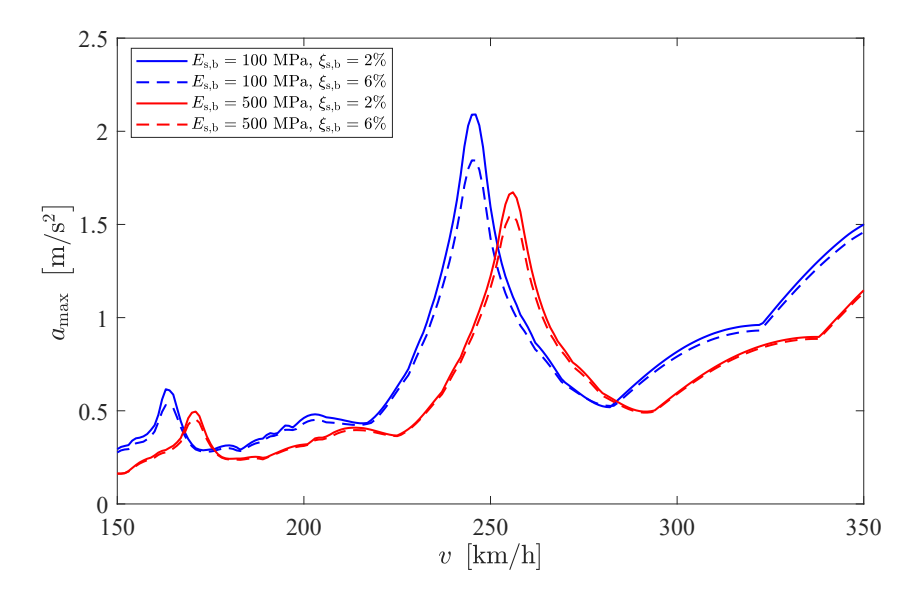


Figure 51. Bridge response for different properties of the backfill soil:  $E_{s,b} = 100 \,\text{MPa}$ ,  $\xi_{s,b} = 6\%$ ;  $E_{s,b} = 100 \,\text{MPa}$ ,  $\xi_{s,b} = 2\%$ ;  $E_{s,b} = 500 \,\text{MPa}$ ,  $\xi_{s,b} = 500 \,\text{MPa}$ ,  $\xi_{s,b} = 500 \,\text{MPa}$ ,  $\xi_{s,b} = 2\%$ .

The sensitivity analysis of the backfill soil shows a reduction in peak acceleration when the elastic modulus is increased to 500 MPa. This occurs because, in this case, the frequency parameter  $\phi$  is below 1 for both soil stiffness values: 0.68 (left) and 0.95 (right) for 100 MPa, and 0.32 (left) and 0.44 (right) for 500 MPa. As  $\phi$  < 1 in all cases, radiational damping is not activated, and only material damping is used. Since material damping increases proportionally with stiffness, the model with  $E_{\rm s,b} = 500$  MPa exhibits higher damping and consequently lower peak accelerations.

Table 22. Damping ratio of the first mode for the four scenarios in Figure 51.

Model with:	$\xi_1$ (%)
$E_{\rm s,b} = 100$ MPa and $\xi_{\rm s,b} = 2\%$	1.28
$E_{s,b} = 100$ MPa and $\xi_{s,b} = 6\%$	1.54
$E_{s,b} = 500$ MPa and $\xi_{s,b} = 2\%$	1.35
$E_{\mathrm{s,b}} = 500 \mathrm{\ MPa}$ and $\xi_{\mathrm{s,b}} = 6\%$	1.52

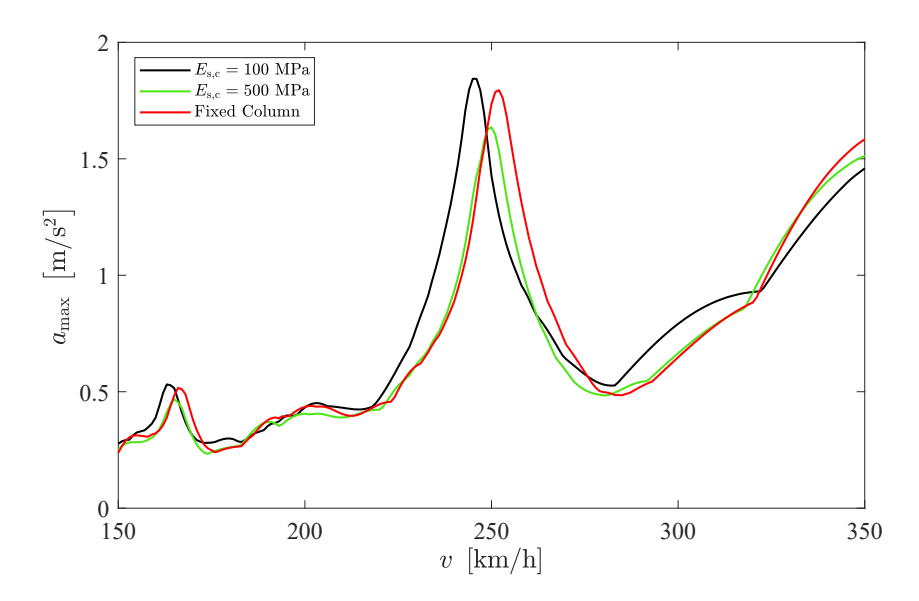


Figure 52. Bridge response for different values of the elastic modulus of the soil beneath the column foundations:  $E_{s,c} = 100 \,\text{MPa}$ ;  $E_{s,c} = 500 \,\text{MPa}$ ; and Fixed, where the springs and dashpots are replaced with fixed constraints.

The sensitivity analysis on the column foundation confirms the previous observations. The three response curves—corresponding to two different values of soil elastic modulus and the fixed-base condition—exhibit only minor differences in peak acceleration. For this bridge, the soil—structure interaction at the column foundations has a limited influence on the dynamic response during the train passage.

# 4.3 Three Span Bridges

Three-span bridges are supported by abutments at the ends and additionally by two central column. The connection between the column and the deck varies depending on the bridge, and can be either rigid or pinned. The end-shield exhibits the same characteristics as in the other categories of bridges and is therefore modeled using the same approach. The two models in Figure 55 features different boundary conditions to evaluate their effect on the response of the bridge.



Figure 53. 2D Model of three-span bridges with the impedance functions at the end-shields

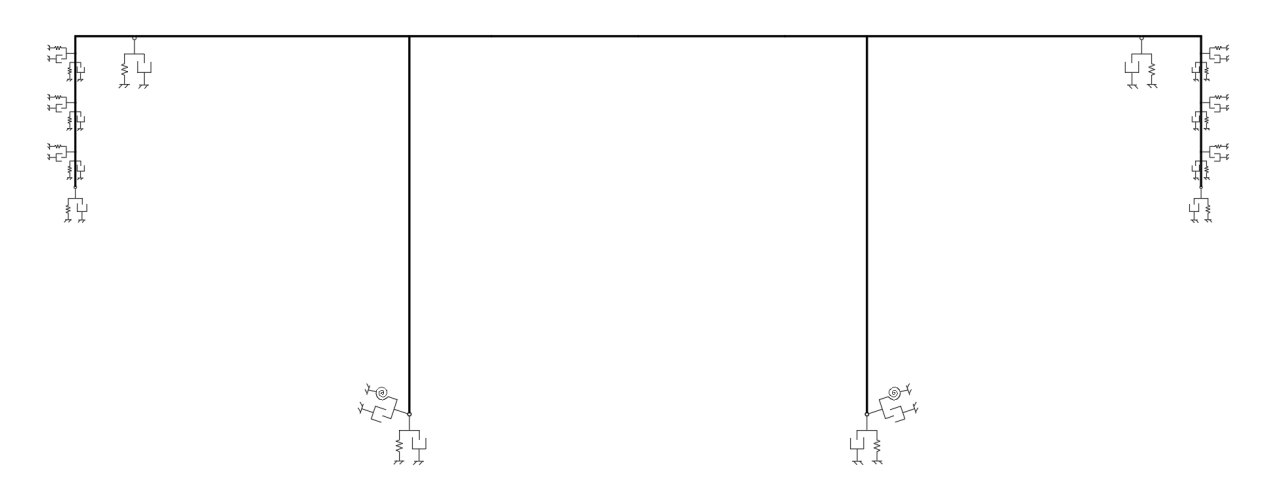


Figure 54. Simplified 2D Model of three-span bridges with the retaining wall and distributed springs and dashpots.

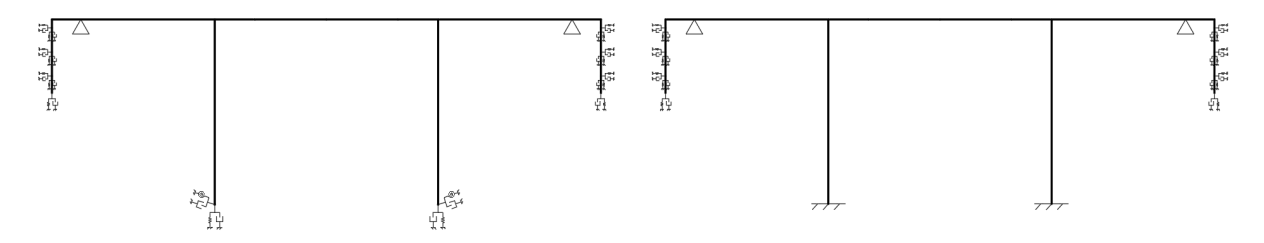


Figure 55. Simplified 2D Model with fixed supports (left) and with both supports and columns fixed (right).

## 4.3.1 Hinnsjöbäcken

The Hinnsjöbäcken bridge has a central span of 20 m and two symmetric side spans of 16 m, with a cantilever extension of 1 m on each side. The deck features a constant cross section in the internal spans, which linearly increase in proximity of the columns, and in correspondence of the abutments. Both the abutments and the columns are supported by shallow foundations placed on compacted crushed rock material.

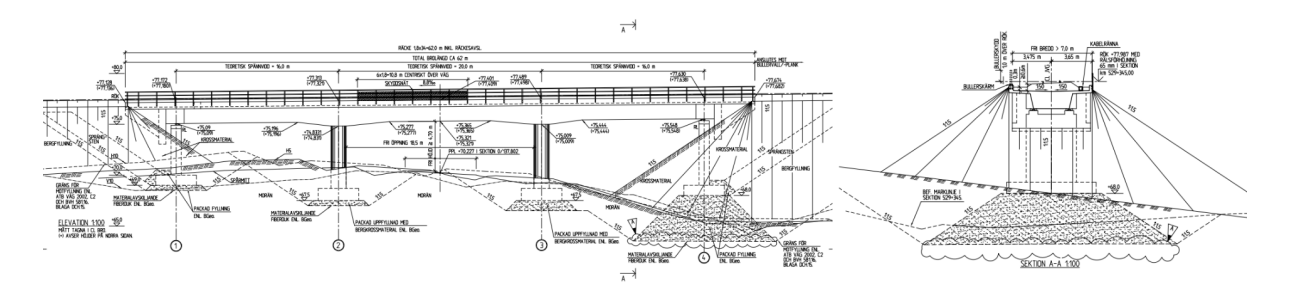


Figure 56. Technical drawings of Hinnsjöbäcken bridge.

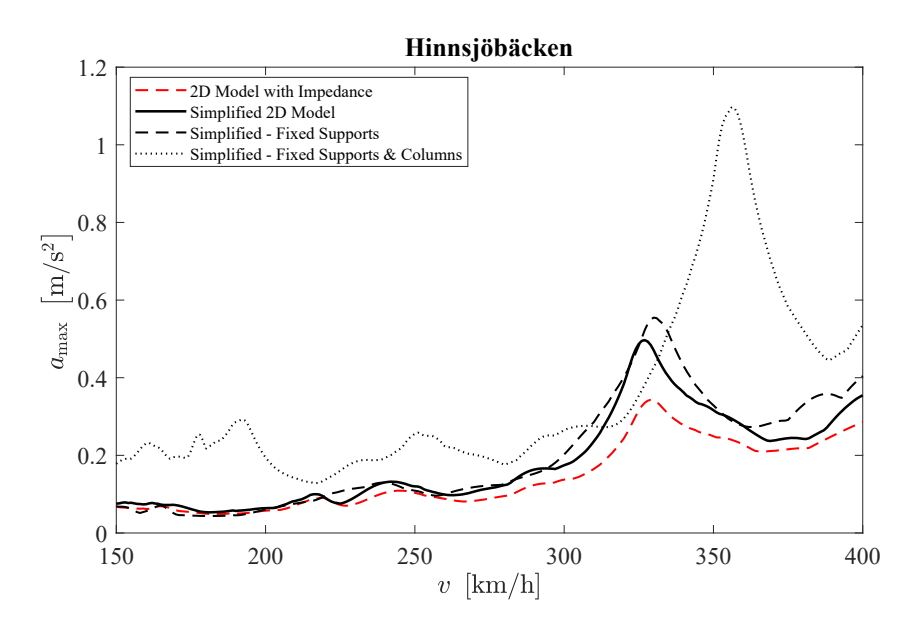


Figure 57. Maximum bridge acceleration during HSLM-A4 train passage: comparison between the 2D model with impedance and three simplified 2D models with varying boundary conditions.

The model comparison in Figure 57 shows no shift in critical speed between the two models, indicating that the overall stiffness is not affected. However, the peak acceleration of the simplified model is higher than that of the model with impedance, indicating that this simplification remains on the conservative side. Replacing the spring-dashpot systems at the support results in a slight increase in acceleration, while the effect is more pronounced when the spring-dashpots

at the columns are fixed. This indicates that the flexibility of the column foundations has a grater influence on the dynamic response of the bridge.

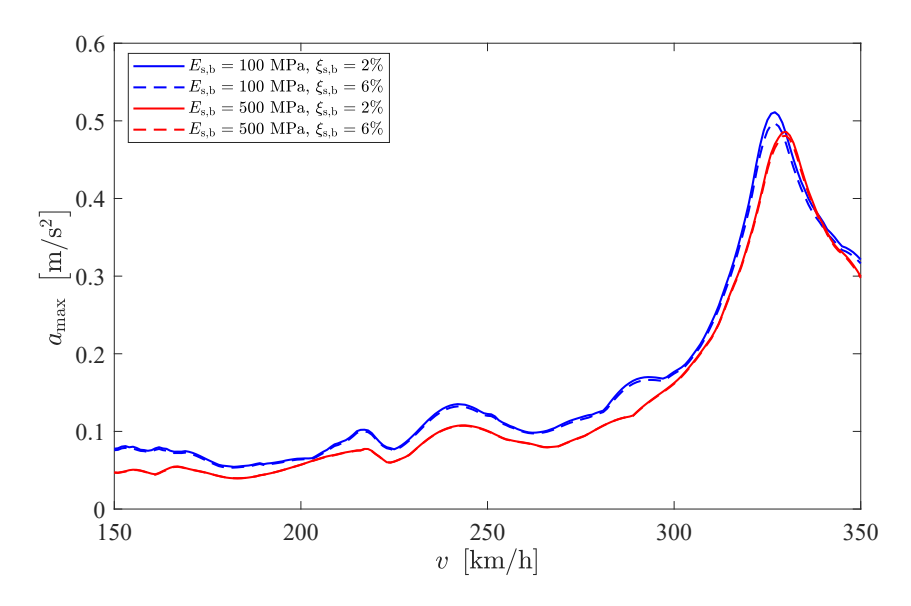


Figure 58. Bridge response for different properties of the backfill soil:  $E_{s,b} = 100 \,\text{MPa}$ ,  $\xi_{s,b} = 6\%$ ;  $E_{s,b} = 100 \,\text{MPa}$ ,  $\xi_{s,b} = 2\%$ ;  $E_{s,b} = 500 \,\text{MPa}$ ,  $\xi_{s,b} = 6\%$ ; and  $E_{s,b} = 500 \,\text{MPa}$ ,  $\xi_{s,b} = 2\%$ .

Table 24. Damping ratio of the first mode for the four scenarios in Figure 58.

Model with:	$\xi_1$ (%)
$E_{\mathrm{s,b}} = 100  \mathrm{MPa}  \mathrm{and}  \xi_{\mathrm{s,b}} = 2\%$	2.05
$E_{\rm s,b} = 100$ MPa and $\xi_{\rm s,b} = 6\%$	2.11
$E_{\mathrm{s,b}} = 500 \mathrm{\ MPa}$ and $\xi_{\mathrm{s,b}} = 2\%$	1.97
$E_{s,b} = 500$ MPa and $\xi_{s,b} = 6\%$	2.00

The sensitivity analysis of the backfill soil in Figure 58 shows no difference between the four scenarios, indicating that the properties of the backfill soil do not significantly affect the bridge's response. However, completely removing the SSI contribution would result in an impact effect at the end-shield during train passage, leading to higher accelerations.

Table 23. First natural frequency and damping ratio of the models in Figure 57.

	$f_1$ (Hz)	$\xi_1$ (%)
2D Model with Impedance	8.76	2.22
Simplified 2D Model	8.62	2.11
Simplified – Fixed Supports	8.74	2.03
Simplified – Fixed Supports and Columns	9.41	1.19

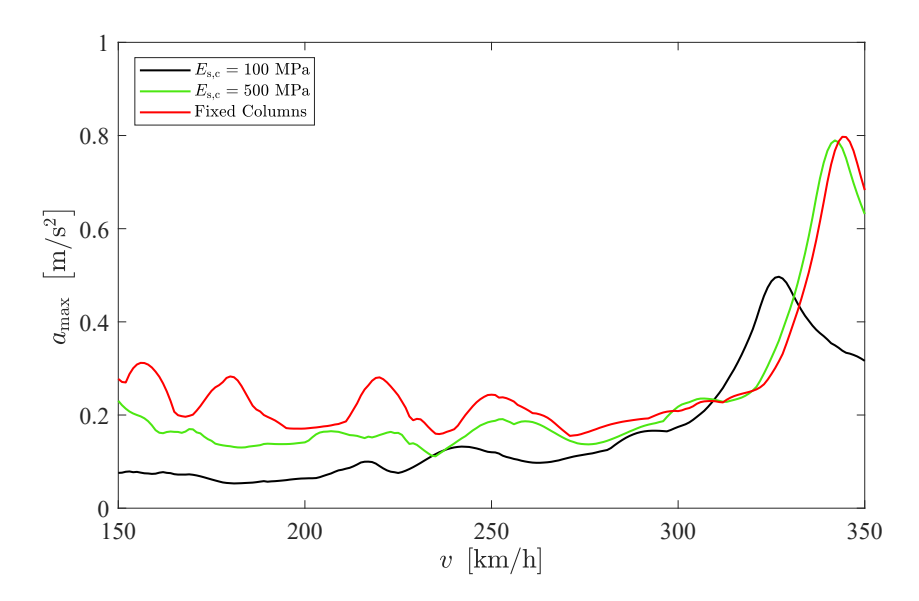


Figure 59. Bridge response for different values of the elastic modulus of the soil beneath the column foundations:  $E_{s,c} = 100 \,\text{MPa}$ ;  $E_{s,c} = 500 \,\text{MPa}$ ; and Fixed, where the springs and dashpots are replaced with fixed constraints.

On the other side, the sensitivity analysis of the column foundations reveals noticeable differences between the cases. Specifically, increasing the elastic modulus from 100 MPa to 500 MPa results in a clear increase in both peak acceleration and natural frequency. However, no difference is observed between the response with stiff soil and with fully fixed column conditions. This suggests that, for very stiff soil, the spring and dashpot behave similarly to a fixed support and may be neglected in the model without significantly affecting accuracy.

## 4.3.2 Husån

The Husån bridge has a central span of 35 m and unsymmetrical side spans of 21 m and 26 m, with a cantilever extension of 0.8 m on each side. The deck features a constant cross section for all its length, except for the part above the abutments. Both the abutments and the columns are supported by shallow foundations placed on compacted crushed rock material.

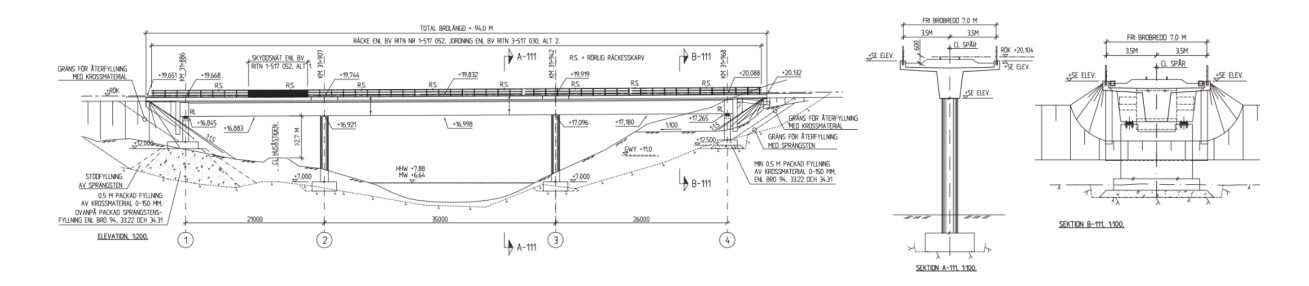


Figure 60. Technical drawings of Husån bridge.

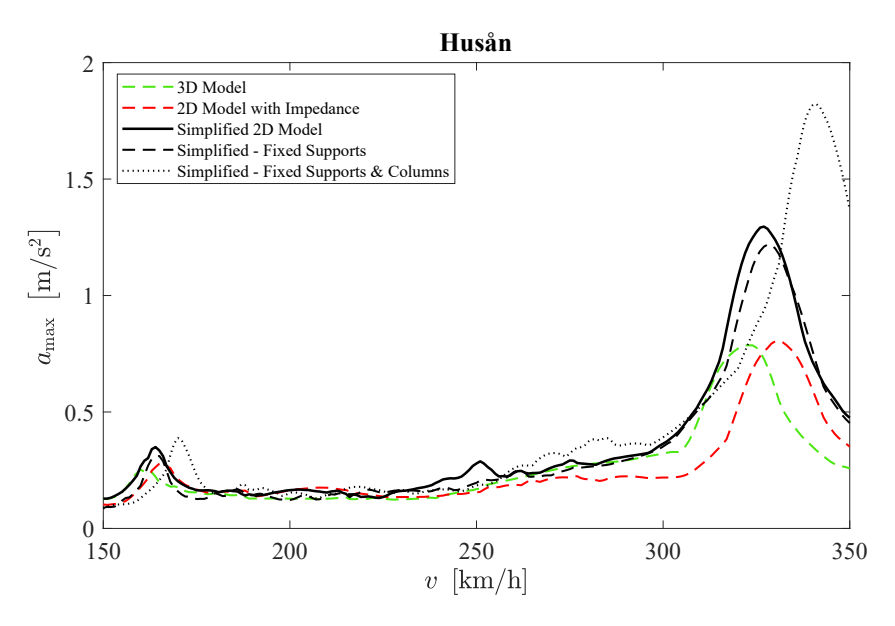


Figure 61. Maximum bridge acceleration during HSLM-A4 train passage: comparison between the 3D model, the 2D model with impedance and three simplified 2D models with varying boundary conditions.

Table 25. First natural frequency and damping ratio of the models in Figure 61.

	$f_1$ (Hz)	<i>ξ</i> <sub>1</sub> (%)
3D Model	4.25	1.30
2D Model with Impedance	4.37	1.27
Simplified 2D Model	4.32	1.22
Simplified – Fixed Supports	4.35	1.22
Simplified – Fixed Supports and Columns	4.52	1.07

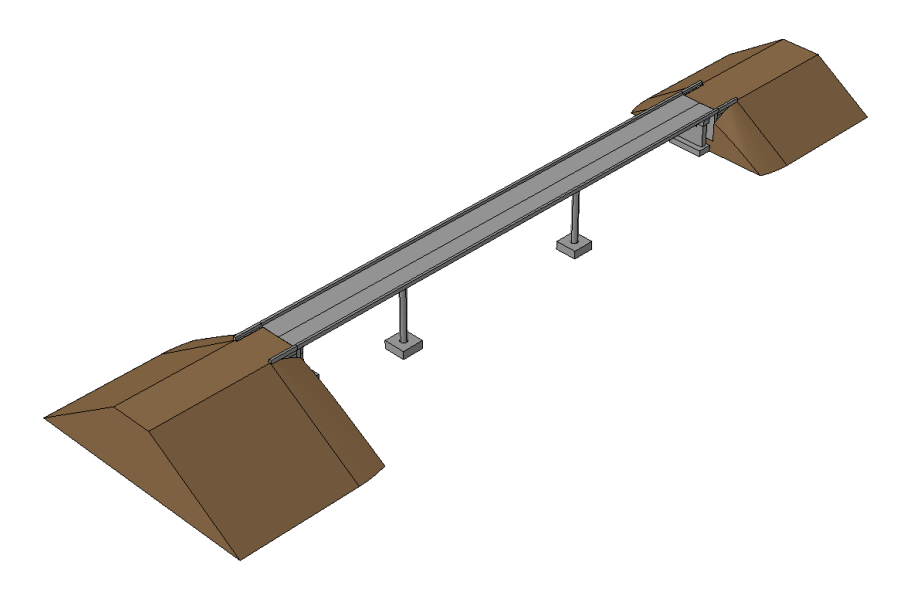


Figure 62. 3D model of Husån bridge created with Abaqus.

Similar to the Brustjärnsbäcken and Leån bridges, this bridge features a deep deck cross-section. Therefore, a 3D model was developed (Figure 62), and the response to high-speed train loading was compared with that of the other models. As shown in Figure 61, the response of the 3D model aligns well with the 2D model with impedance functions at the end-shield. In contrast, the simplified 2D model yields higher accelerations, providing a conservative estimation of the dynamic response. In this case as well, fixing the column supports results in a substantial increase in both maximum acceleration and critical speed, indicating that the flexibility of the column foundation plays an important role in three-span bridges. Conversely, due to the pinned connection between the deck and the abutments, the dynamic response is not significantly affected by fixing the end supports.

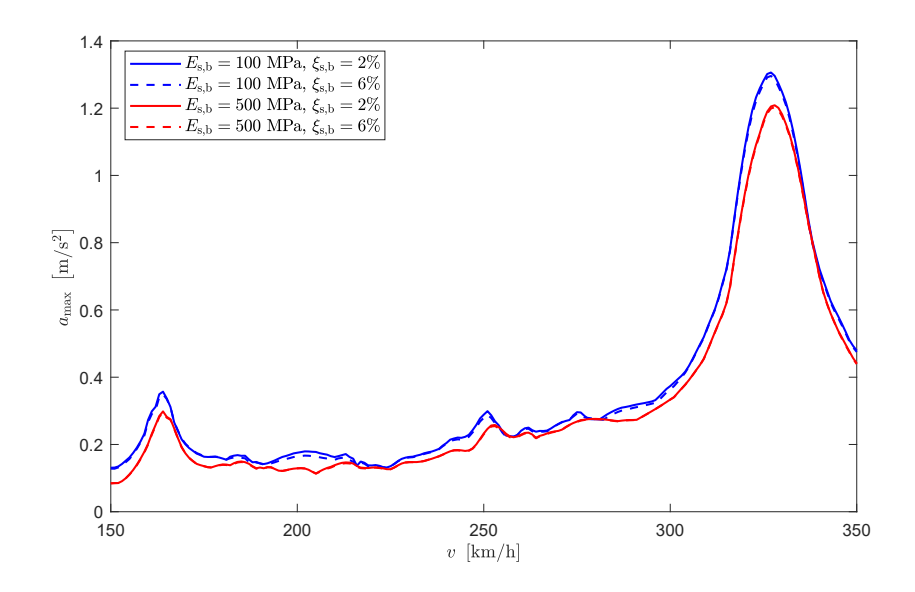


Figure 63. Bridge response for different properties of the backfill soil:  $E_{s,b} = 100 \,\text{MPa}$ ,  $\xi_{s,b} = 6\%$ ;  $E_{s,b} = 100 \,\text{MPa}$ ,  $\xi_{s,b} = 2\%$ ;  $E_{s,b} = 500 \,\text{MPa}$ ,  $\xi_{s,b} = 500 \,\text{MPa}$ ,  $\xi_{s,b} = 500 \,\text{MPa}$ ,  $\xi_{s,b} = 2\%$ .

Table 26. Damping ratio of the first mode for the four scenarios in Figure 63.

Model with:	ξ <sub>1</sub> (%)
$E_{\mathrm{s,b}} = 100 \mathrm{\ MPa}$ and $\xi_{\mathrm{s,b}} = 2\%$	1.05
$E_{\mathrm{s,b}} = 100 \mathrm{MPa}$ and $\xi_{\mathrm{s,b}} = 6\%$	1.08
$E_{\mathrm{s,b}} = 500 \mathrm{\ MPa}$ and $\xi_{\mathrm{s,b}} = 2\%$	1.01
$E_{\mathrm{s,b}} = 500$ MPa and $\xi_{\mathrm{s,b}} = 6\%$	1.03

While the sensitivity analysis on the backfill soil shows minimal differences between the two limit scenarios, the analysis of the properties of the soil below the foundations reveals a significant variation in the bridge response between models with 100 MPa and 500 MPa soil stiffness. In contrast, only a small difference is observed between the 500 MPa case and the fixed column condition. This confirms the substantial influence of soft soil at the column foundations, with a difference in maximum acceleration reaching approximately 0.5 m/s  $^2$ .

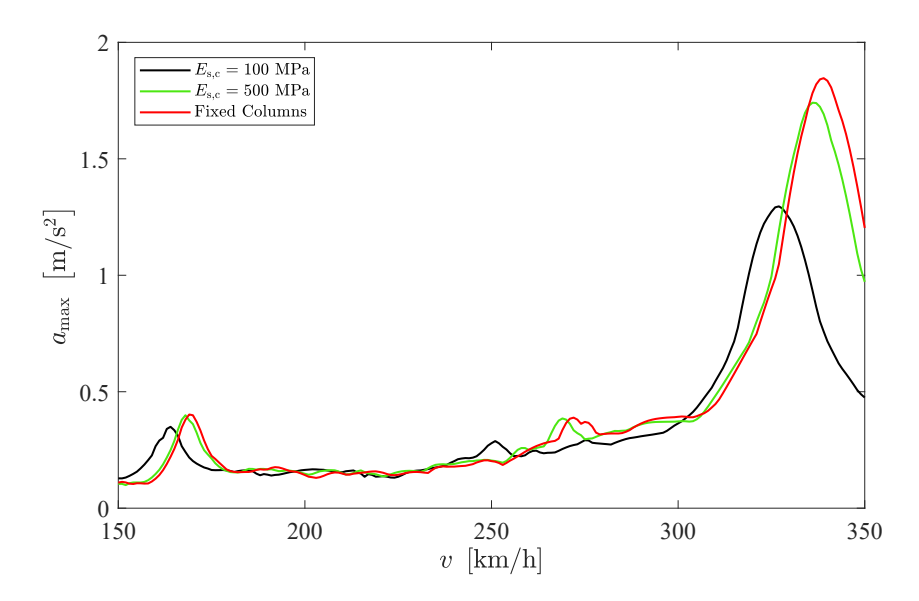


Figure 64. Bridge response for different values of the elastic modulus of the soil beneath the column foundations:  $E_{s,c} = 100 \,\mathrm{MPa}$ ;  $E_{s,c} = 500 \,\mathrm{MPa}$ ; and Fixed, where the springs and dashpots are replaced with fixed constraints.

# 4.3.3 Nordmaling

The Nordmaling bridge has a central span of 14 m and two symmetric side spans of 11 m, with a cantilever extension of 1 m on each side. The deck features a constant cross section throughout its length. Both the abutments and the columns are supported by shallow foundations placed on compacted crushed rock material.

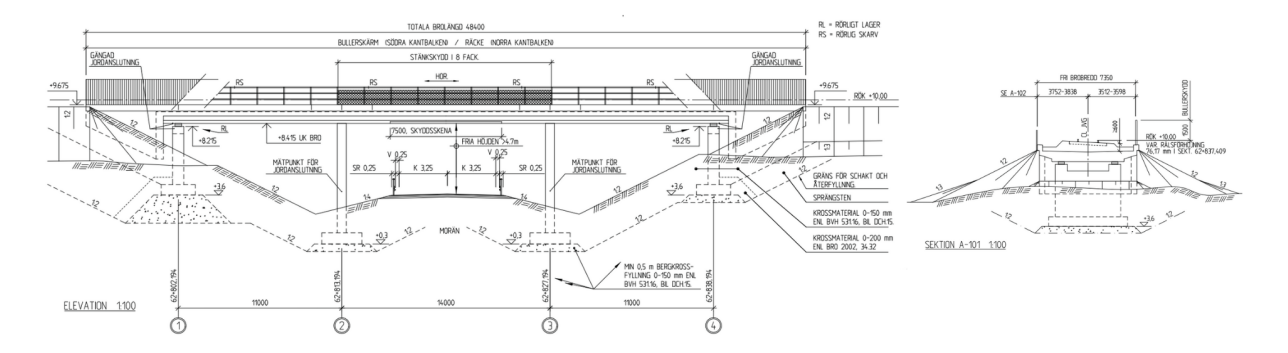


Figure 65. Technical drawings of Nordmaling bridge.

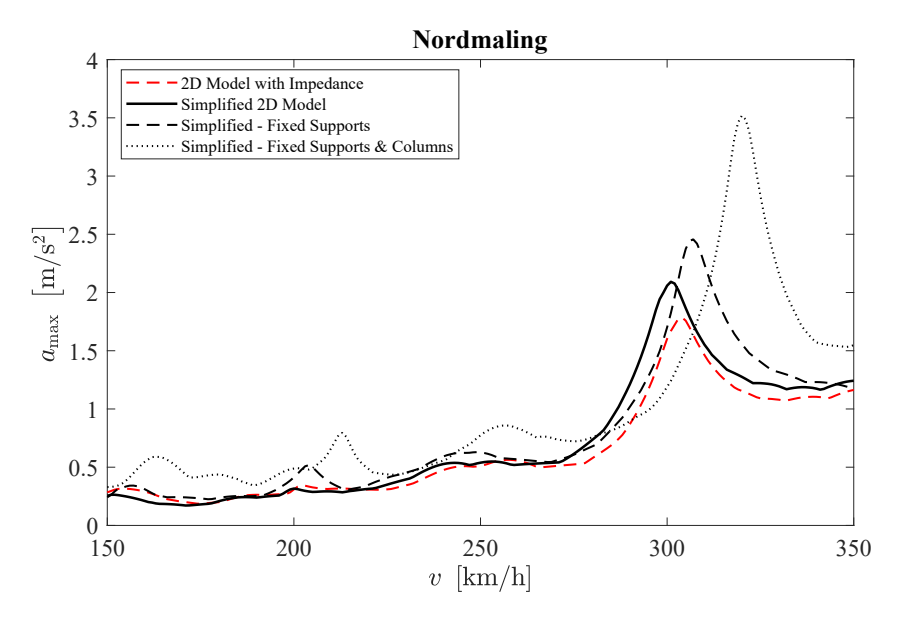


Figure 66. Maximum bridge acceleration during HSLM-A1 train passage: comparison between the 2D model with impedance and three simplified 2D models with varying boundary conditions.

Table 27. First natural frequency and damping ratio of the models in Figure 66.

	$f_1$ (Hz)	<i>ξ</i> <sub>1</sub> (%)
2D Model with Impedance	9.33	1.68
Simplified 2D Model	9.26	1.71
Simplified – Fixed Supports	9.44	1.79
Simplified – Fixed Supports and Columns	9.87	1.54

The model comparison in Figure 66 shows no shift in peak velocity between the two models, indicating that the overall stiffness is preserved. However, the peak acceleration of the simplified model is higher than that of the model with impedance, indicating that this simplification remains on the conservative side. Fixing both the support and the columns results in an increase in both acceleration and stiffness, indicating that the flexibility of the foundations has a big impact on the response of the bridge.

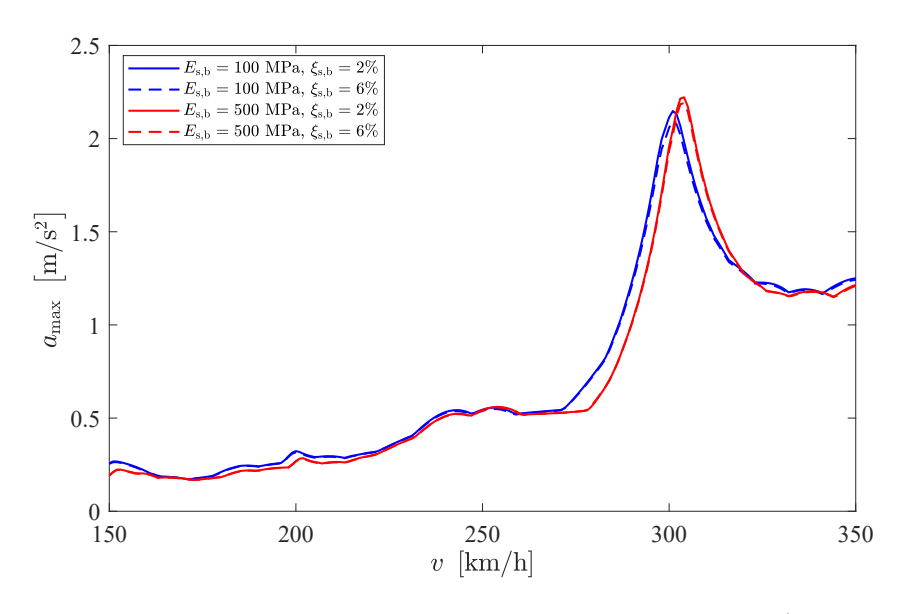


Figure 67. Bridge response for different properties of the backfill soil:  $E_{s,b} = 100 \,\text{MPa}$ ,  $\xi_{s,b} = 6\%$ ;  $E_{s,b} = 100 \,\text{MPa}$ ,  $\xi_{s,b} = 500 \,\text{MPa}$ ,  $\xi_{s,b} = 2\%$ .

Table 28. Damping ratio of the first mode for the four scenarios in Figure 67.

Model with:	ξ <sub>1</sub> (%)
$E_{\mathrm{s,b}} = 100 \mathrm{MPa}$ and $\xi_{\mathrm{s,b}} = 2\%$	1.65
$E_{s,b} = 100$ MPa and $\xi_{s,b} = 6\%$	1.71
$E_{s,b} = 500$ MPa and $\xi_{s,b} = 2\%$	1.48
$E_{\mathrm{s,b}} = 500 \mathrm{MPa}$ and $\xi_{\mathrm{s,b}} = 6\%$	1.50

As for the other three span bridges, the sensitivity analysis on the backfill soil shows minimal differences between the two limit scenarios, while the analysis of the properties of the soil below the foundations (Figure 68) reveals a significant variation in the bridge response between models with 100 MPa and 500 MPa soil stiffness. In contrast, no difference is observed between the 500 MPa case and the fixed column condition. This confirms the influence of the foundation flexibility on the response of the bridge.

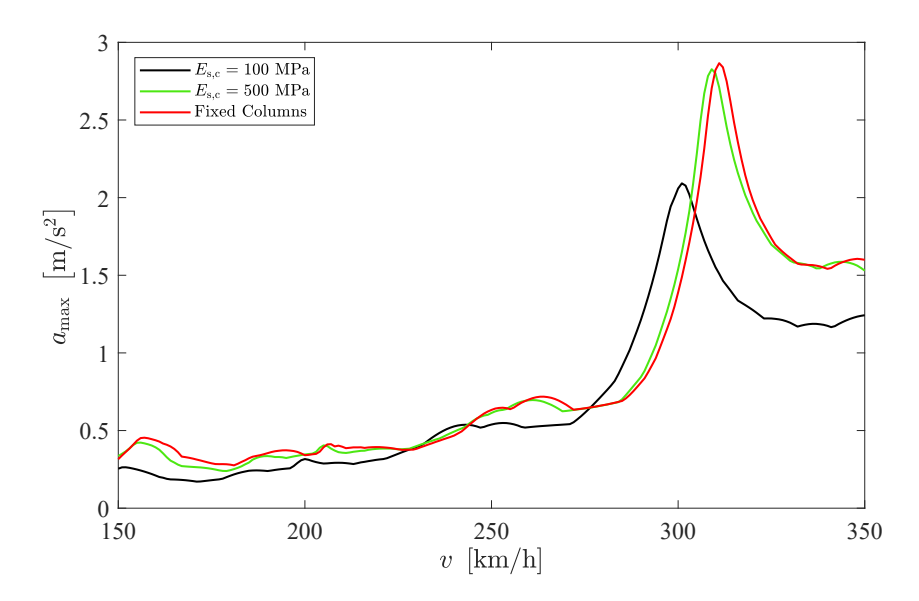


Figure 68. Bridge response for different values of the elastic modulus of the soil beneath the column foundations:  $E_{s,c} = 100 \,\mathrm{MPa}$ ;  $E_{s,c} = 500 \,\mathrm{MPa}$ ; and Fixed, where the springs and dashpots are replaced with fixed constraints.

# 4.3.4 Sidensjövägen

The Sidensjövägen bridge has a central span of 17 m and two symmetric side spans of 13 m, with a cantilever extension of 1 m on each side. The deck features a constant cross section in the internal spans, which increases linearly in proximity of the columns. Both the abutments and the columns are supported by shallow foundations placed on crushed rock material.

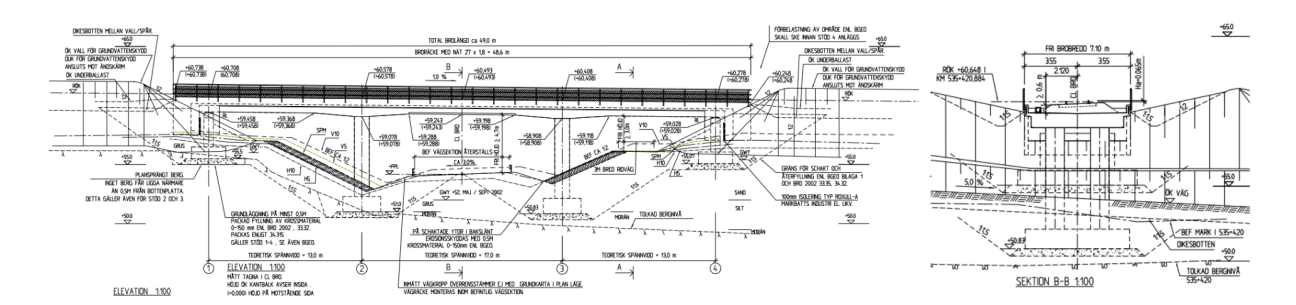


Figure 69. Technical drawings of Sidensjövägen bridge.

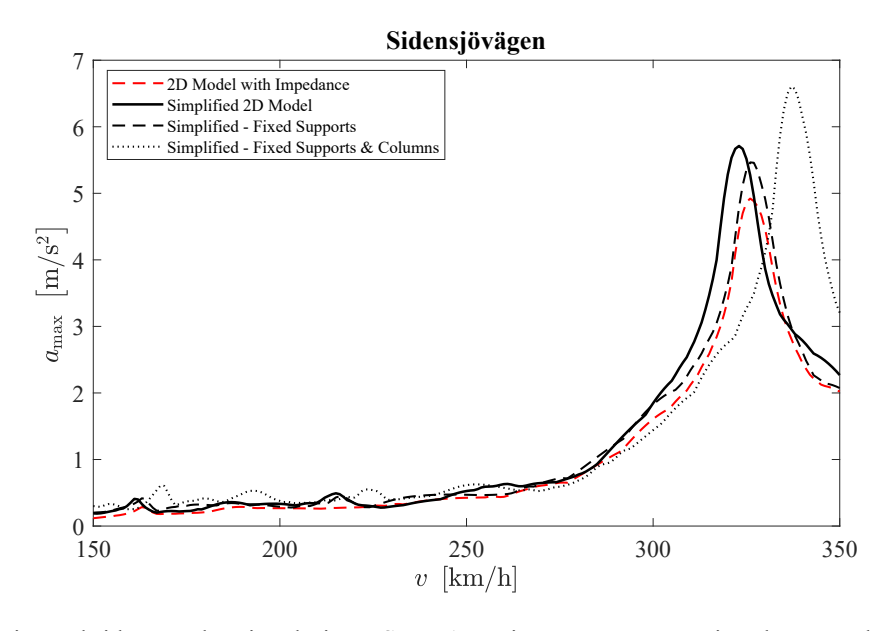


Figure 70. Maximum bridge acceleration during HSLM-A5 train passage: comparison between the 2D model with impedance and three simplified 2D models with varying boundary conditions.

Table 29. First natural frequency and damping ratio of the models in Figure 70.

	$f_1$ (Hz)	<i>ξ</i> <sub>1</sub> (%)
2D Model with Impedance	8.25	0.92
Simplified 2D Model	8.15	0.90
Simplified – Fixed Supports	8.25	0.90
Simplified – Fixed Supports and Columns	8.54	0.79

The model comparison in Figure 70 shows no shift in peak velocity between the two models, indicating that the overall stiffness is preserved. However, the peak acceleration of the simplified model is higher than that of the model with impedance, indicating that this simplification remains on the conservative side. Replacement of the springs and dashpots at the support produces a slight reduction in acceleration; this effect is governed by the change in mode shape produced by the pinned supports. Fixing both the support and the columns results in an increase in both acceleration and stiffness, indicating that the flexibility of the foundations has a big impact on the response of the bridge.

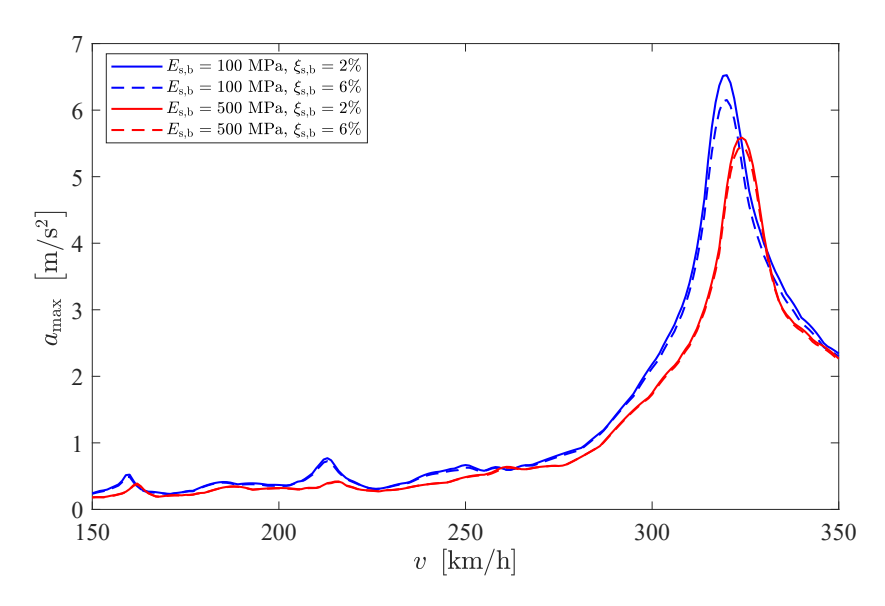


Figure 71. Bridge response for different properties of the backfill soil:  $E_{s,b} = 100 \,\text{MPa}$ ,  $\xi_{s,b} = 6\%$ ;  $E_{s,b} = 100 \,\text{MPa}$ ,  $\xi_{s,b} = 2\%$ ;  $E_{s,b} = 500 \,\text{MPa}$ ,  $\xi_{s,b} = 6\%$ ; and  $E_{s,b} = 500 \,\text{MPa}$ ,  $\xi_{s,b} = 2\%$ .

Table 30. Damping ratio of the first mode for the four scenarios in Figure 71.

Model with:	<i>ξ</i> <sub>1</sub> (%)
$E_{\mathrm{s,b}} = 100 \mathrm{MPa}$ and $\xi_{\mathrm{s,b}} = 2\%$	0.88
$E_{s,b} = 100$ MPa and $\xi_{s,b} = 6\%$	0.99
$E_{s,b} = 500$ MPa and $\xi_{s,b} = 2\%$	0.88
$E_{\mathrm{s,b}} = 500 \mathrm{MPa}$ and $\xi_{\mathrm{s,b}} = 6\%$	0.92

The sensitivity analysis of the backfill soil shows a reduction in peak acceleration when the elastic modulus is increased to 500 MPa. This occurs because the frequency parameter  $\phi$  remains below 1 for both soil stiffness values—0.84 for 100 MPa and 0.38 for 500 MPa, meaning that radiation damping is not activated in either case.

For the column foundations (Figure 72), the difference in response is more pronounced between the soft and stiff soil conditions than between the stiff soil and

the fully fixed configuration. This suggests that beyond a certain stiffness, the soil behaves similarly to a fixed support.

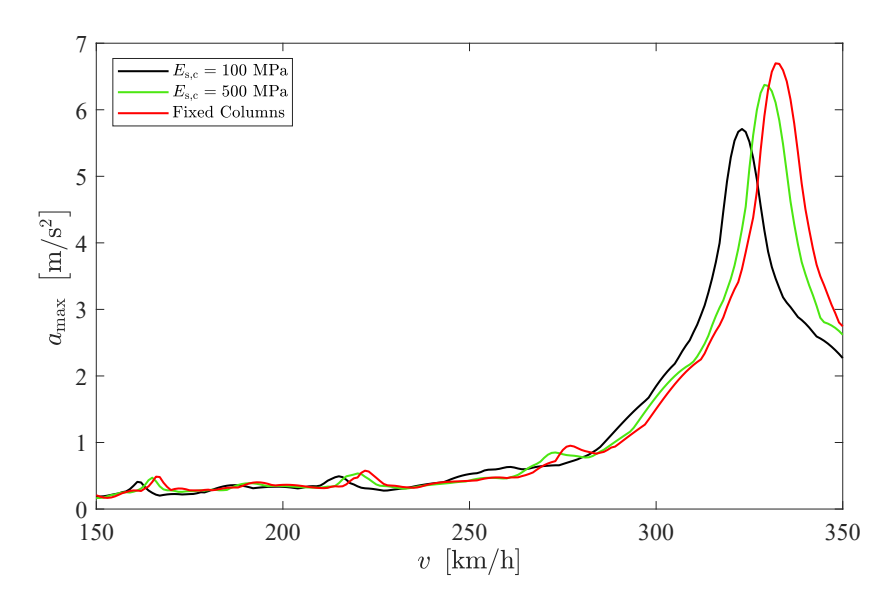


Figure 72. Bridge response for different values of the elastic modulus of the soil beneath the column foundations:  $E_{s,c} = 100 \,\text{MPa}$ ;  $E_{s,c} = 500 \,\text{MPa}$ ; and Fixed, where the springs and dashpots are replaced with fixed constraints.

#### 4.3.5 Styrnäs

The Styrnäs bridge has a central span of 17 m and two symmetric side spans of 13 m, with a cantilever extension of 1 m on each side. The deck features a constant cross section throughout its length. Both the abutments and the columns are supported by shallow foundations placed on compacted crushed rock material.

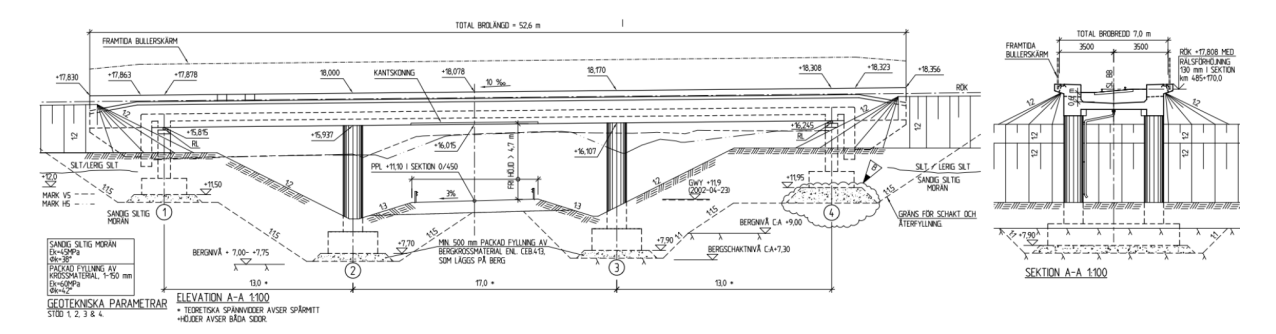


Figure 73. Technical drawings of Styrnäs bridge.

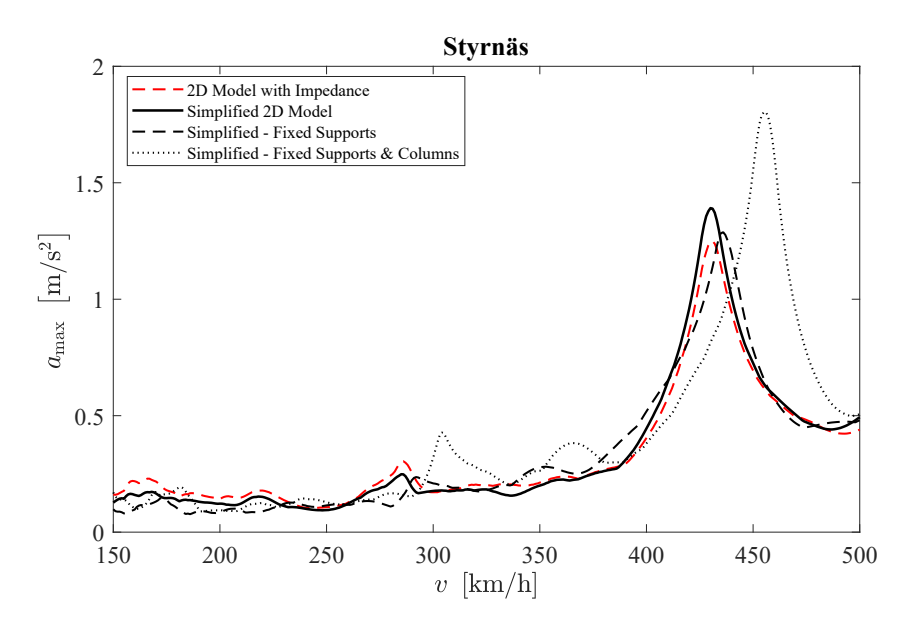


Figure 74. Maximum bridge acceleration during HSLM-A1 train passage: comparison between the 2D model with impedance and three simplified 2D models with varying boundary conditions.

Table 31. First natural frequency and damping ratio of the models in Figure 74.

	$f_1$ (Hz)	<i>ξ</i> <sub>1</sub> (%)
2D Model with Impedance	13.27	1.76
Simplified 2D Model	13.36	1.44
Simplified – Fixed Supports	13.46	1.61
Simplified – Fixed Supports and Columns	14.06	1.29

The model comparison in Figure 74 shows no shift in peak velocity between

the two models, indicating that the overall stiffness is preserved. However, the peak acceleration of the simplified model is higher than that of the model with impedance, indicating that this simplification remains on the conservative side. Replacement of the springs and dashpots at the support produces a slight reduction in acceleration; this effect is governed by the change in mode shape produced by the pinned supports. Fixing both the support and the columns results in an increase in both acceleration and stiffness, indicating that the flexibility of the foundations has a big impact on the response of the bridge.

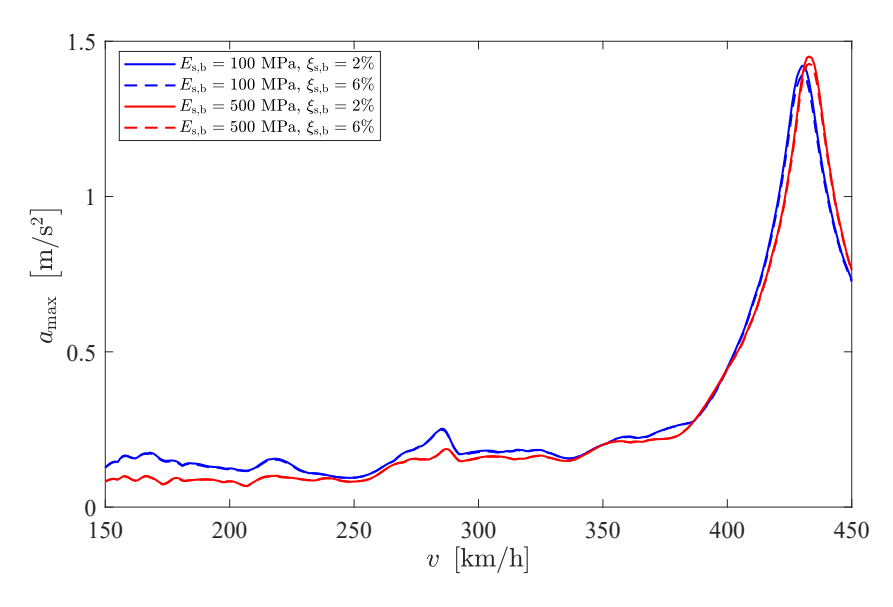


Figure 75. Bridge response for different properties of the backfill soil:  $E_{s,b} = 100 \,\text{MPa}$ ,  $\xi_{s,b} = 6\%$ ;  $E_{s,b} = 100 \,\text{MPa}$ ,  $\xi_{s,b} = 2\%$ ;  $E_{s,b} = 500 \,\text{MPa}$ ,  $\xi_{s,b} = 500 \,\text{MPa}$ ,  $\xi_{s,b} = 2\%$ .

Table 32. Damping ratio of the first mode for the four scenarios in Figure 75.

Model with:	<i>ξ</i> <sub>1</sub> (%)
$E_{\mathrm{s,b}} = 100 \mathrm{MPa}$ and $\xi_{\mathrm{s,b}} = 2\%$	1.59
$E_{s,b} = 100 \text{ MPa}$ and $\xi_{s,b} = 6\%$	1.63
$E_{s,b} = 500$ MPa and $\xi_{s,b} = 2\%$	1.44
$E_{s,b} = 500$ MPa and $\xi_{s,b} = 6\%$	1.47

As for the other three span bridges, the sensitivity analysis on the backfill soil shows minimal differences between the two limit scenarios, while the analysis of the properties of the soil below the foundations (Figure 76) reveals a significant variation in the bridge response between models with 100 MPa and 500 MPa soil stiffness. In contrast, no difference is observed between the 500 MPa case and the fixed column condition. This confirms the influence of the foundation flexibility on the response of the bridge.

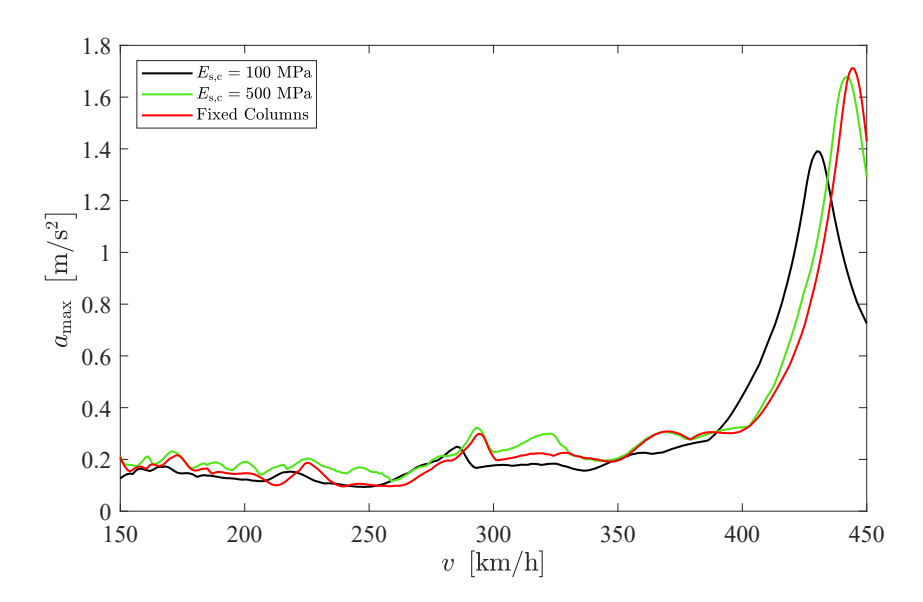


Figure 76. Bridge response for different values of the elastic modulus of the soil beneath the column foundations:  $E_{s,c} = 100 \,\mathrm{MPa}$ ;  $E_{s,c} = 500 \,\mathrm{MPa}$ ; and Fixed, where the springs and dashpots are replaced with fixed constraints.

### 4.3.6 Sörmjöleån

The Sörmjöleån bridge has a central span of 21 m and two symmetric side spans of 15 m, with a cantilever extension of 0.8 m on each side. The deck features a constant cross section for all its length, except for the part above the abutments. Both the abutments and the columns are supported by pile foundations, with depths of 11 m and 12 m for the abutments and the columns, respectively. Unlike the other bridges, the columns are not rigidly connected to the deck; they present, instead, a pinned joint.

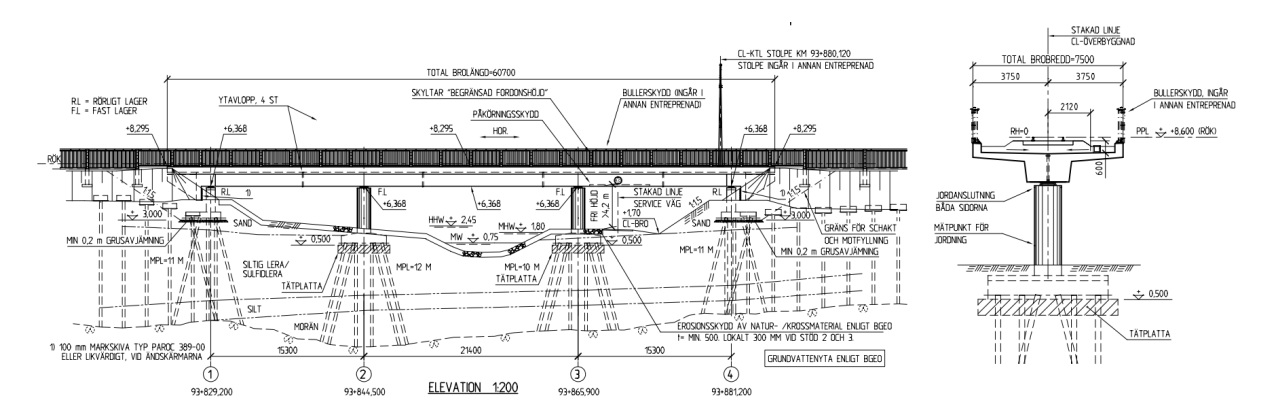


Figure 77. Technical drawings of Sörmjöleån bridge.

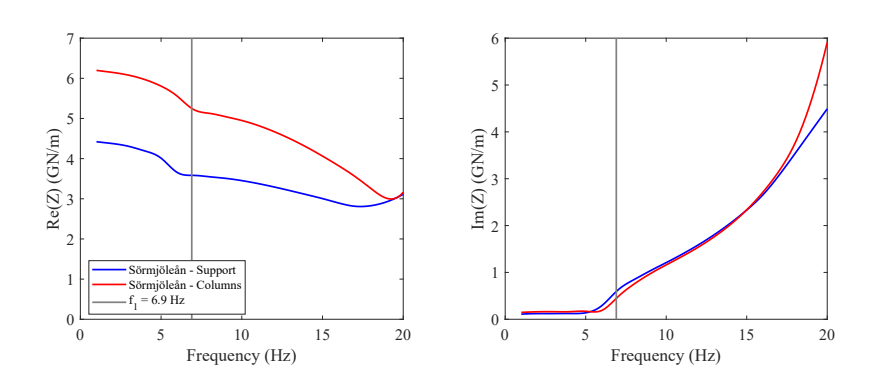


Figure 78. Vertical impedance function of the pile group for the Sörmjöleån bridge: real part (left) and imaginary part (right). Each plot shows two curves corresponding to the response at the supports and at the columns.

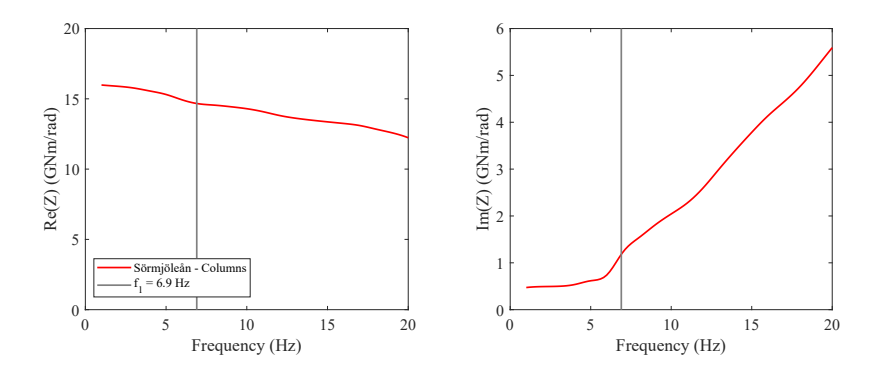


Figure 79. Rotational impedance function of the pile group for the Sörmjöleån bridge: real part (left) and imaginary part (right), corresponding to the response at the columns

Figure 78 presents the vertical impedance functions for both the supports and the columns. Although the two foundations have a similar depth, the stiffness component (real part) differs significantly, primarily due to variations in the number of piles and their configuration. In contrast, the damping component (imaginary part) shows no substantial variation near the frequency range of interest, suggesting that it is more closely related to the foundation depth than to the pile configuration.

For the columns, the rotational impedance was also evaluated. Since the columns are pinned to the deck, their rotational stiffness does not influence the global dynamic response of the bridge. Nevertheless, the rotational impedance was included in the analysis for the sake of completeness.

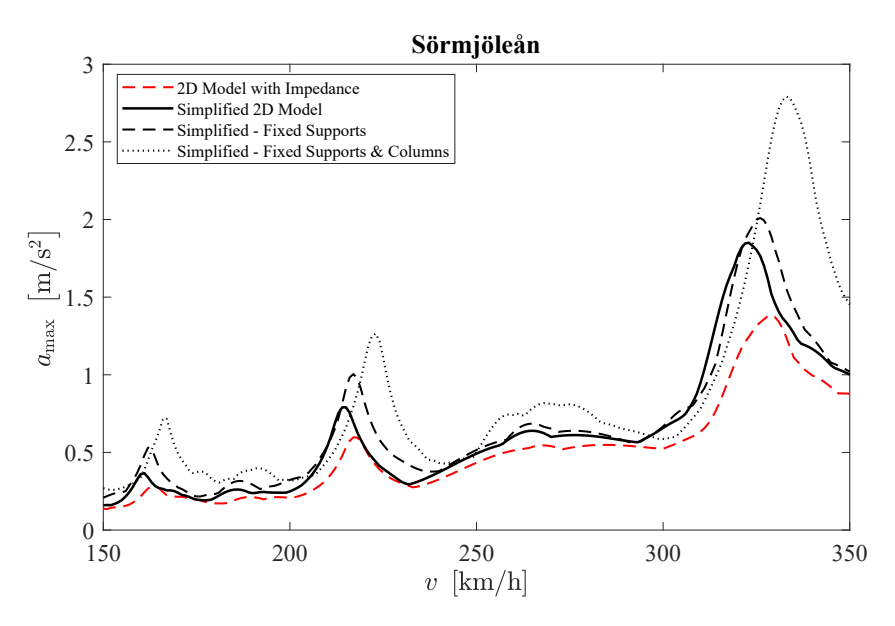


Figure 80. Maximum bridge acceleration during HSLM-A9 train passage: comparison between the 2D model with impedance and three simplified 2D models with varying boundary conditions.

Table 33. First natural frequency and damping ratio of the models in Figure 80.

	$f_1$ (Hz)	<i>ξ</i> <sub>1</sub> (%)
2D Model with Impedance	6.96	1.40
Simplified 2D Model	6.86	1.30
Simplified – Fixed Supports	6.94	1.28
Simplified – Fixed Supports and Columns	7.13	1.12

As shown in Figure 80, the comparison between models reveals no significant shift in natural frequency. The bridge features a deep cross-section, and similarly to the previously analysed bridges of this type, there is a difference of approximately 0.5 m/s<sup>2</sup> in peak acceleration between the 2D model with impedance functions and the simplified 2D model. Fixing both the supports

and the columns results in a notable increase in maximum acceleration, providing a conservative estimate of the bridge's dynamic response.

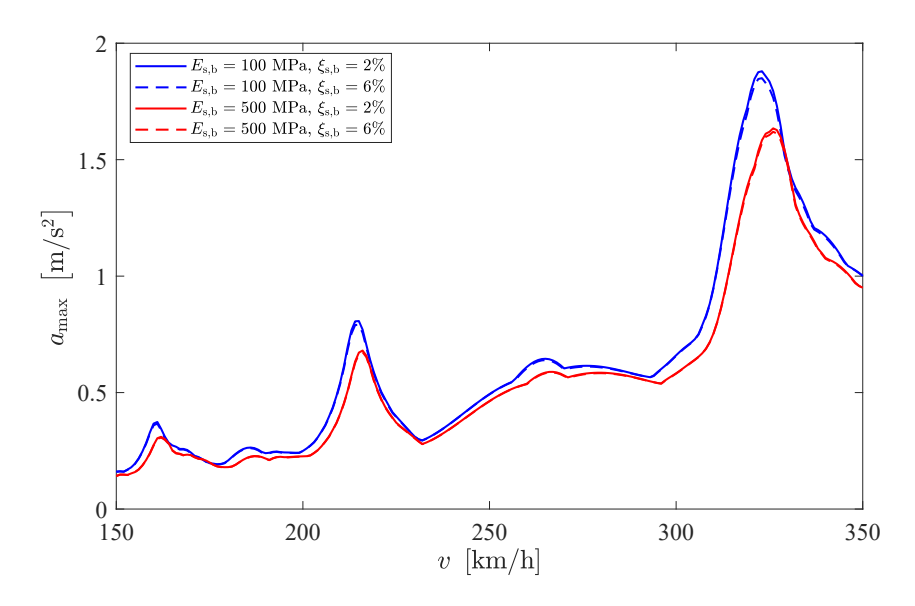


Figure 81. Bridge response for different properties of the backfill soil:  $E_{s,b} = 100 \,\text{MPa}$ ,  $\xi_{s,b} = 6\%$ ;  $E_{s,b} = 100 \,\text{MPa}$ ,  $\xi_{s,b} = 2\%$ ;  $E_{s,b} = 500 \,\text{MPa}$ ,  $\xi_{s,b} = 500 \,\text{MPa}$ ,  $\xi_{s,b} = 500 \,\text{MPa}$ ,  $\xi_{s,b} = 2\%$ .

Table 34. Damping ratio of the first mode for the four scenarios in Figure 81.

Model with:	<i>ξ</i> <sub>1</sub> (%)
$E_{\rm s,b} = 100$ MPa and $\xi_{\rm s,b} = 2\%$	1.27
$E_{s,b} = 100$ MPa and $\xi_{s,b} = 6\%$	1.30
$E_{s,b} = 500$ MPa and $\xi_{s,b} = 2\%$	1.29
$E_{\rm s,b} = 500$ MPa and $\xi_{\rm s,b} = 6\%$	1.31

The sensitivity analysis of the backfill soil (Figure 81) shows a reduction in maximum acceleration when the elastic modulus is increased to 500 MPa. This occurs because, in this case, the frequency parameter  $\phi$  is below 1 for both soil stiffness values: 0.72 for 100 MPa and 0.32 for 500 MPa. As  $\phi < 1$  in all cases, radiational damping is not activated and only material (hysteretic) damping is used. Since material damping is lower than radiational damping, increase in soil stiffness is predominant in this case and the model with  $E_{\rm s,b} = 500$  MPa exhibits higher damping and consequently lower peak accelerations.

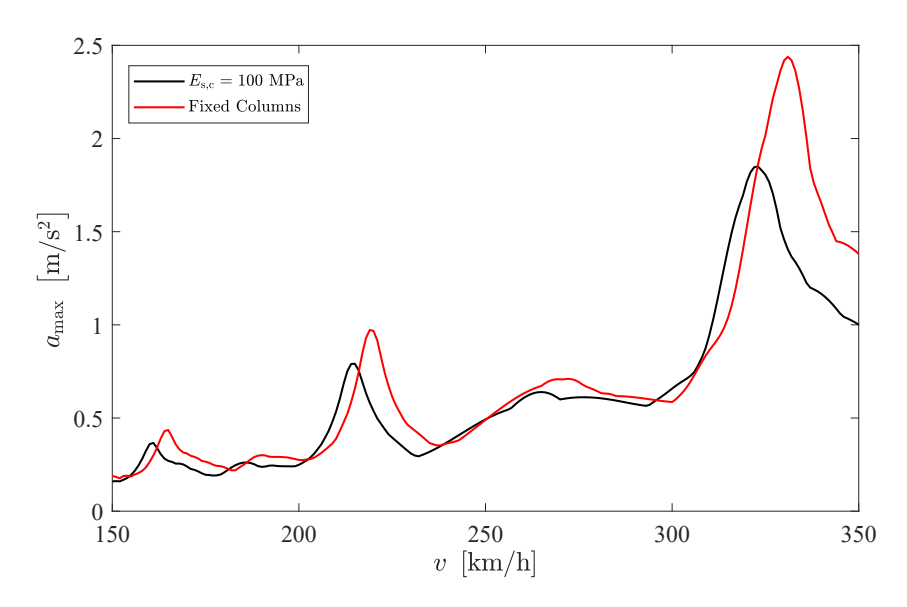


Figure 82. Bridge response for different conditions of the column foundations:  $E_{s,c} = 100 \text{ MPa}$  and Fixed, where the springs and dashpots are replaced with fixed constraints.

Figure 82 illustrates the influence of column foundation flexibility on the dynamic response of the bridge. As previously observed, fixing the columns leads to a significant increase in peak acceleration, despite the fact that the connection between the deck and the columns is not rigid. In general, when the dynamic characterization of the pile foundation is not available, applying fixed boundary conditions offers a conservative approximation of the bridge's dynamic behavior.

### 4.3.7 Vasavägen

The Vasavägen bridge has a central span of 12.5 m and two symmetric side spans of 8.6 m, with a cantilever extension of 1 m on each side. The deck features a constant cross section throughout its length. Both the abutments and the columns are supported by shallow foundations placed on compacted crushed rock material.

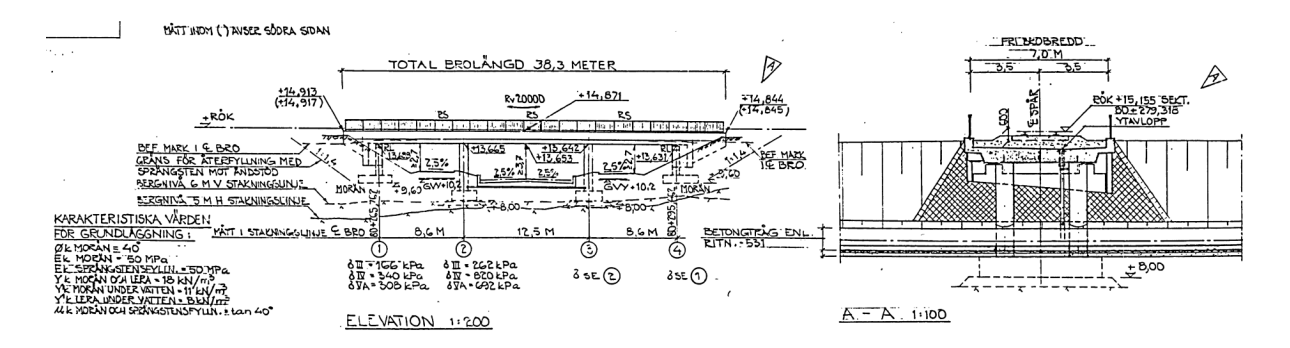


Figure 83. Technical drawings of Vasavägen bridge.

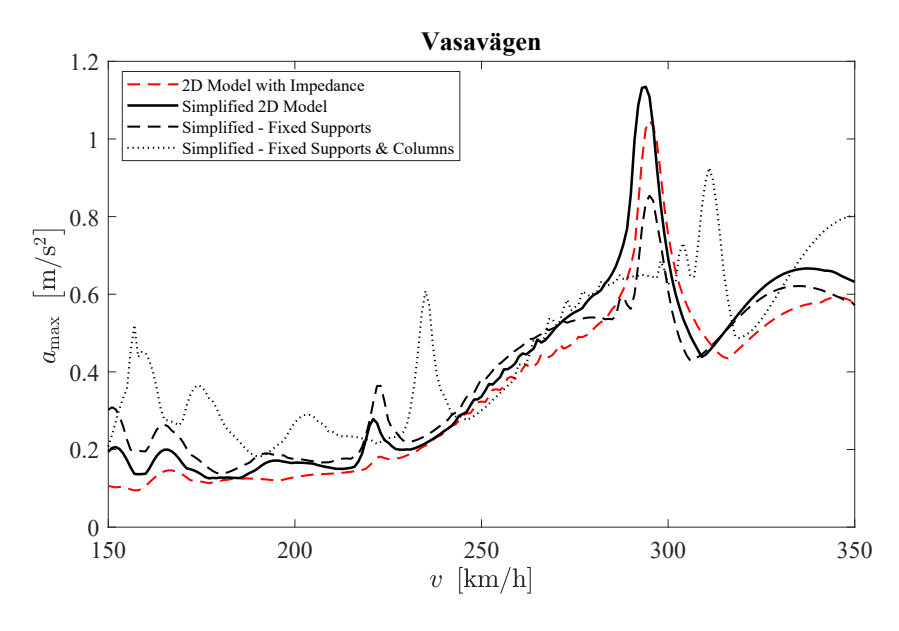


Figure 84. Maximum bridge acceleration during HSLM-A3 train passage: comparison between the 2D model with impedance and three simplified 2D models with varying boundary conditions.

As shown in Figure 84 and Table 35, there is no shift in natural frequency between the 2D model with impedance functions and the simplified model, indicating comparable global stiffness. Fixing the supports leads to a notable reduction in peak acceleration, primarily due to changes in the mode shape. Interestingly, the model with both supports and columns fixed yields a slightly lower acceleration than the model with springs and dashpots. Although this result is influenced by the specific configuration of the bridge, the difference is small and would not significantly affect the overall dynamic response.

Table 35. First natural frequency and damping ratio of the models in Figure 84.

	$f_1$ (Hz)	<i>ξ</i> <sub>1</sub> (%)
2D Model with Impedance	12.30	0.76
Simplified 2D Model	12.25	0.75
Simplified – Fixed Supports	12.35	0.75
Simplified – Fixed Supports and Columns	13.05	0.60

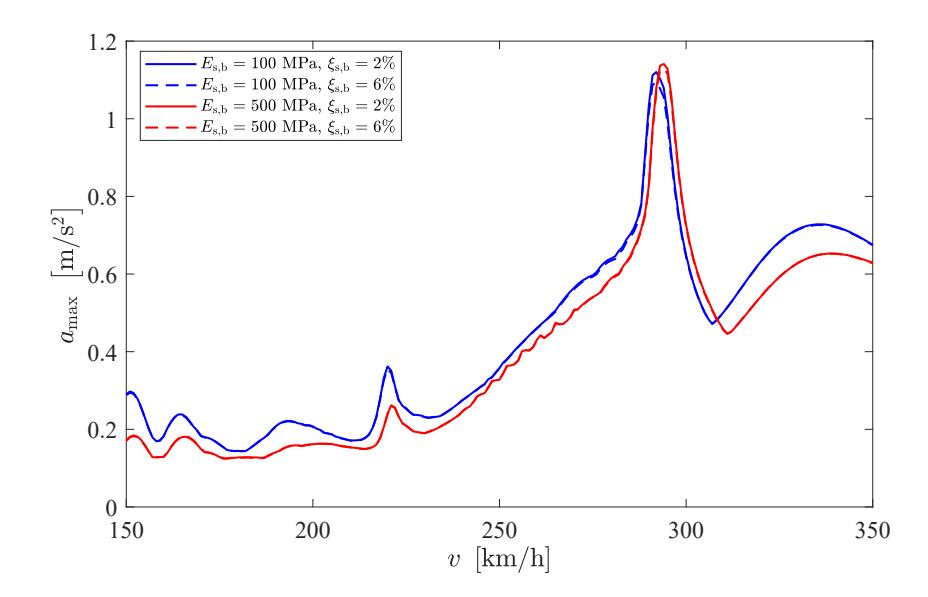


Figure 85. Bridge response for different properties of the backfill soil:  $E_{s,b} = 100 \,\text{MPa}$ ,  $\xi_{s,b} = 6\%$ ;  $E_{s,b} = 100 \,\text{MPa}$ ,  $\xi_{s,b} = 2\%$ ;  $E_{s,b} = 500 \,\text{MPa}$ ,  $\xi_{s,b} = 500 \,\text{MPa}$ ,  $\xi_{s,b} = 500 \,\text{MPa}$ ,  $\xi_{s,b} = 2\%$ .

Table 36. Damping ratio of the first mode for the four scenarios in Figure 85.

Model with:	ξ <sub>1</sub> (%)
$E_{\rm s,b} = 100$ MPa and $\xi_{\rm s,b} = 2\%$	0.85
$E_{s,b} = 100$ MPa and $\xi_{s,b} = 6\%$	0.88
$E_{\mathrm{s,b}} = 500 \mathrm{\ MPa}$ and $\xi_{\mathrm{s,b}} = 2\%$	0.75
$E_{\mathrm{s,b}} = 500 \mathrm{MPa}$ and $\xi_{\mathrm{s,b}} = 6\%$	0.76

As for the other three span bridges, the sensitivity analysis on the backfill soil shows minimal differences between the two limit scenarios, while the analysis of the properties of the soil below the foundations (Figure 86) reveals a significant variation in the bridge response between models with 100 MPa and 500 MPa soil stiffness. In contrast, small difference is observed between the 500 MPa case and the fixed column condition. This confirms the influence of the foundation flexibility on the response of the bridge.

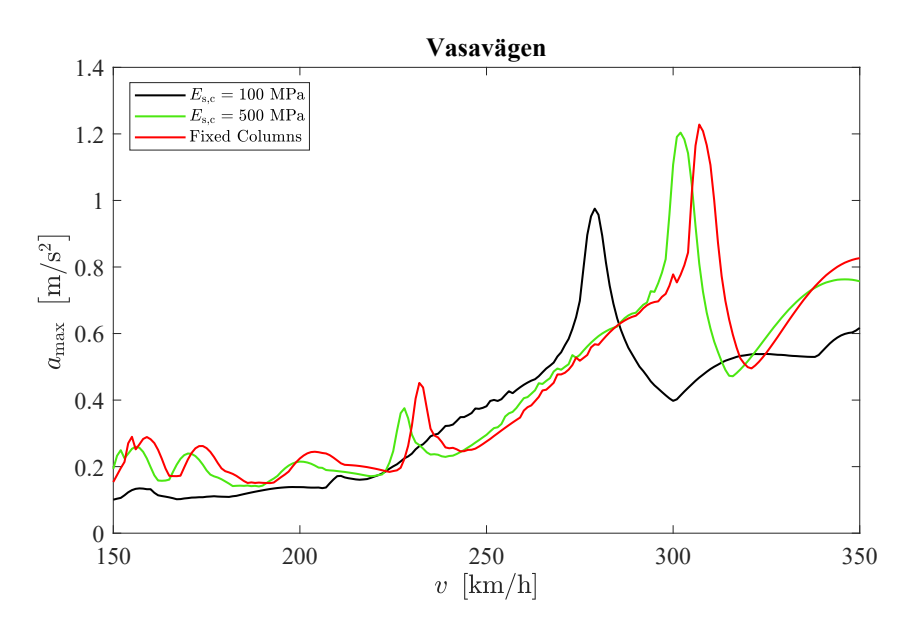


Figure 86. Bridge response for different values of the elastic modulus of the soil beneath the column foundations:  $E_{s,c} = 100 \,\mathrm{MPa}$ ;  $E_{s,c} = 500 \,\mathrm{MPa}$ ; and Fixed, where the springs and dashpots are replaced with fixed constraints.

# 4.3.8 Åhedaån

The Åhedaån bridge has a central span of 35 m and two symmetric side spans of 21 m, with a cantilever extension of 1 m on each side. The deck features a constant cross section for all its length, except for the part above the abutments. The two columns and the abutment on the left (Figure 87) are supported by pile foundations, while the abutment on the right is supported by a shallow foundation placed on compacted crushed material.

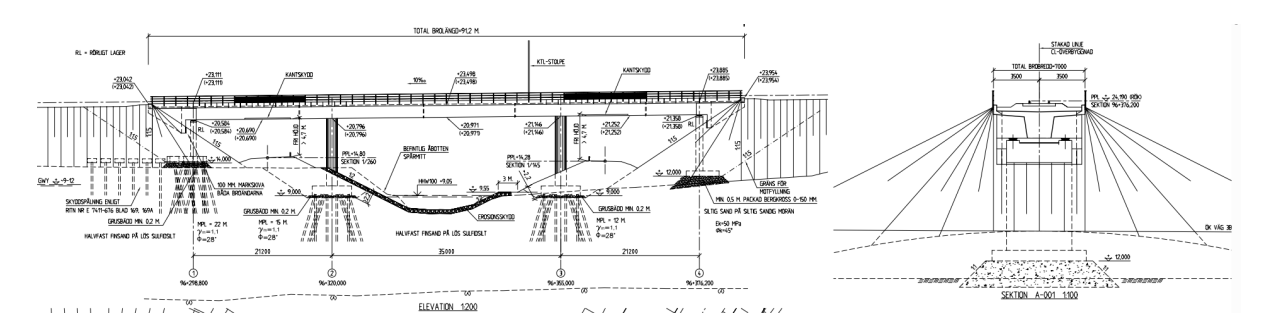


Figure 87. Technical drawings of Åhedaån bridge.

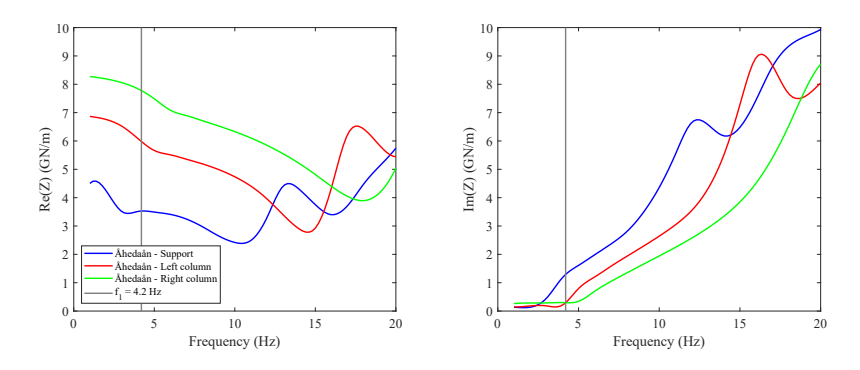


Figure 88. Vertical impedance function of the pile group for the Åhedaån bridge: real part (left) and imaginary part (right). Each plot shows three curves corresponding to the response at the supports, left column, and right column.

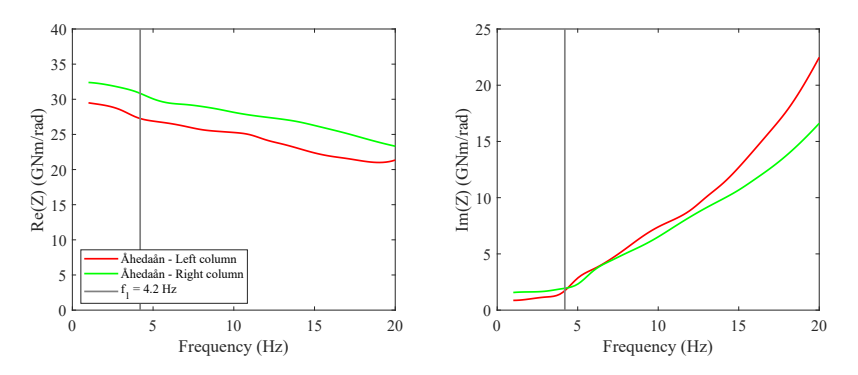


Figure 89. Rotational impedance function of the pile group for the Åhedaån bridge: real part (left) and imaginary part (right). Each plot shows two curves corresponding to the response at the left column and at the right column.

Figure 88 presents the vertical impedance functions for the supports and for the left and right columns, which have different foundation depths. The results clearly show that foundation depth has a significant influence on dynamic stiffness, particularly for the two columns, which share the same pile configuration but differ in depth (15 m and 12 m, respectively). The damping component (imaginary part) is also affected by this variation, primarily due to differences in the natural frequency of the respective models.

Conversely, the rotational impedance functions shown in Figure 89 are not significantly influenced by the depth of the pile group, with only minor differences observed between the two curves.

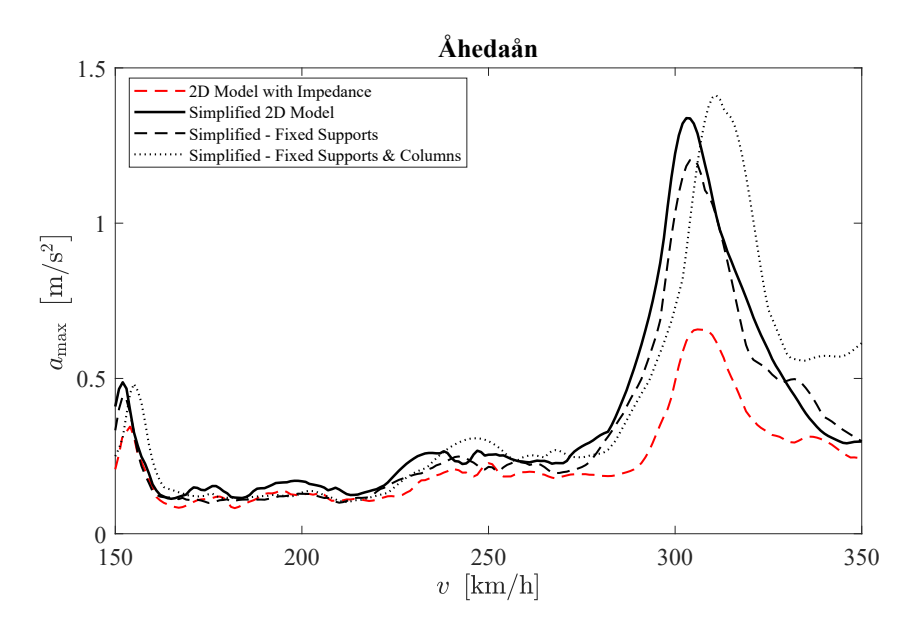


Figure 90. Maximum bridge acceleration during HSLM-A3 train passage: comparison between the 2D model with impedance and three simplified 2D models with varying boundary conditions.

Table 37. First natural frequency and damping ratio of the models in Figure 90.

	$f_1$ (Hz)	<i>ξ</i> <sub>1</sub> (%)
2D Model with Impedance	4.27	1.09
Simplified 2D Model	4.22	1.06
Simplified – Fixed Supports	4.25	1.08
Simplified – Fixed Supports and Columns	4.33	1.06

As shown in Figure 90, the comparison between models reveals no significant shift in natural frequency. The bridge features a deep cross-section, and similarly to the previously analyzed bridges of this type, there is a difference of approximately 0.5 m/s<sup>2</sup> in peak acceleration between the 2D model with impedance functions and the simplified 2D model. Fixing the supports, and subsequently both the supports and the columns, results in only minor variations in the bridge's response. This behavior can be attributed to the considerable length of the bridge, where the influence of the surrounding soil is relatively

small compared to the structural stiffness of the concrete. This is further supported by the constant modal damping ratios reported in Table 37.

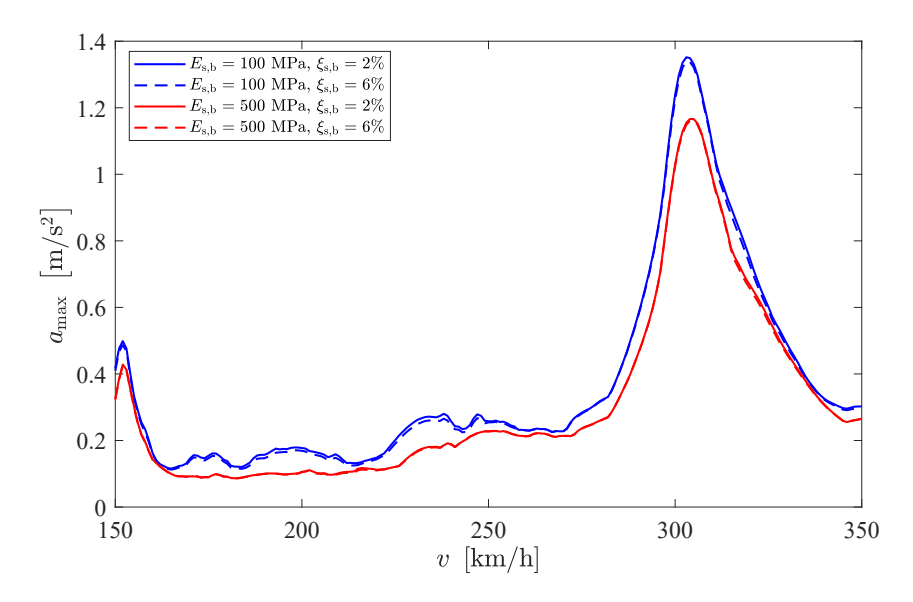


Figure 91. Bridge response for different properties of the backfill soil:  $E_{s,b} = 100 \,\text{MPa}$ ,  $\xi_{s,b} = 6\%$ ;  $E_{s,b} = 100 \,\text{MPa}$ ,  $\xi_{s,b} = 2\%$ ;  $E_{s,b} = 500 \,\text{MPa}$ ,  $\xi_{s,b} = 500 \,\text{MPa}$ ,  $\xi_{s,b} = 500 \,\text{MPa}$ ,  $\xi_{s,b} = 2\%$ .

Table 38. Damping ratio of the first mode for the four scenarios in Figure 91.

Model with:	<i>ξ</i> <sub>1</sub> (%)
$E_{\rm s,b} = 100$ MPa and $\xi_{\rm s,b} = 2\%$	1.04
$E_{s,b} = 100$ MPa and $\xi_{s,b} = 6\%$	1.06
$E_{s,b} = 500$ MPa and $\xi_{s,b} = 2\%$	1.03
$E_{\rm s,b} = 500$ MPa and $\xi_{\rm s,b} = 6\%$	1.04

The sensitivity analysis of the backfill soil (Figure 91) shows a reduction in maximum acceleration when the elastic modulus is increased to 500 MPa. This occurs because, in this case, the frequency parameter  $\phi$  is below 1 for both soil stiffness values: 0.85 for 100 MPa and 0.38 for 500 MPa. As  $\phi < 1$  in all cases, radiational damping is not activated and only material (hysteretic) damping is used. Since material damping is lower than radiational damping, increase in soil stiffness is predominant in this case and the model with  $E_{\rm s,b} = 500$  MPa exhibits lower peak accelerations.

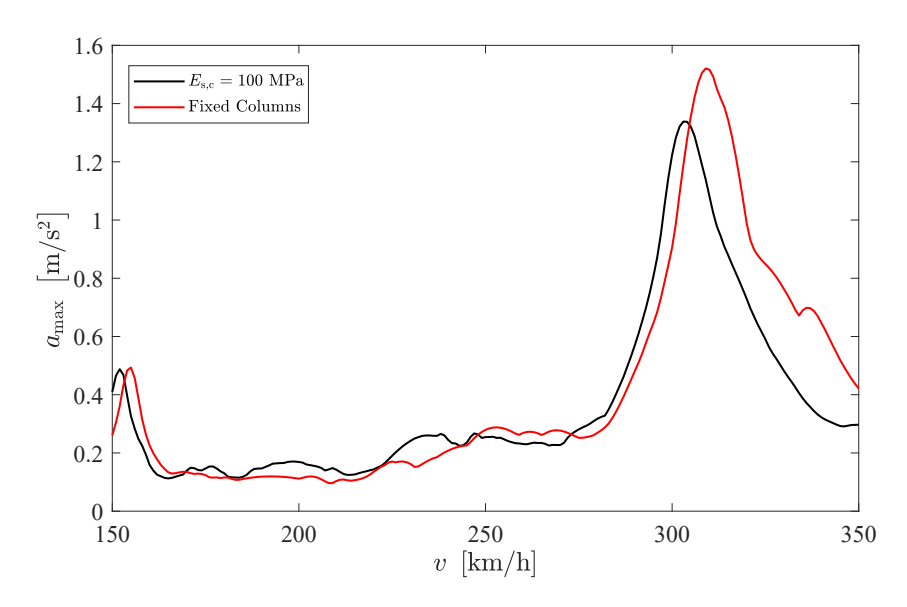


Figure 92. Bridge response for different conditions of the column foundations:  $E_{s,c} = 100 \text{ MPa}$  and Fixed, where the springs and dashpots are replaced with fixed constraints.

Figure 92 illustrates the influence of column foundation flexibility on the dynamic response of the bridge. As previously observed, fixing the columns does not significantly affect the maximum acceleration or the critical speed. The influence of column foundation flexibility is minimal in this case, and neglecting the SSI at the foundations provides a conservative and sufficiently accurate approximation of the bridge's dynamic response.

The results of the analyses highlight both the effectiveness and limitations of the proposed simplified 2D modeling approach for assessing the dynamic response of end-shield bridges under high-speed train loading.

Across the 18 analyzed bridges, the deck accelerations during critical train passages remain below the prescribed limits in all but two cases. This indicates that, in general, end-shield bridges do not exhibit significant dynamic issues when subjected to high-speed train loads.

The simplified model consistently produced slightly higher accelerations and lower natural frequencies compared to the reference models with impedance functions or full 3D finite element models. This behavior confirms its conservative nature and supports its use in preliminary design or assessment stages, particularly when detailed soil data is unavailable.

The influence of boundary conditions varied depending on the bridge typology:

Single-span bridges with shallow foundations showed minimal sensitivity to support conditions. Fixing the supports had negligible impact on the dynamic response, and the simplified model provided safe, conservative estimates.

In single-span bridges with pile foundations, especially those with high natural frequencies, the soil's dynamic stiffness and damping played a more significant role. While neglecting SSI still resulted in conservative outcomes, these bridges showed greater sensitivity to foundation modeling.

For two-span bridges, the influence of the backfill soil and the column–soil interaction was similar to the single-span cases. The column foundations contributed little to the global response, and fixing them had a limited effect on acceleration or frequency.

In three-span bridges, however, the flexibility of column foundations proved to be a critical factor. Fixing the columns led to notable increases in both natural frequency and maximum acceleration. This highlights the importance of accurately modeling column—soil interaction for multi-span structures. In contrast, the effect of end-shield—soil interaction was found to be minor in this bridge category, with little influence on the fundamental frequency, regardless of the modeling approach. However, completely neglecting the SSI at the end-shields can lead to an impact effect, causing a substantial increase in maximum acceleration.

The sensitivity analysis on the backfill soil further emphasized the role of the

frequency parameter  $\phi$ . Depending on the bridge's natural frequency and the geometry of the backfill, the maximum acceleration occurred with either stiff or soft soil. This variation is attributed to the presence or absence of radiational damping, which dominates when  $\phi$  exceeds 1. As a result, a preliminary estimation of  $\phi$  is essential to guide the choice of appropriate soil stiffness during modeling.

Overall, these results underscore the suitability of the simplified model for preliminary assessments of an end-shield bridge's dynamic response. The simplified model consistently provides conservative results, making it a reliable tool for early-stage evaluation. When the predicted maximum acceleration is well below the 3.5 m/s<sup>2</sup> limit, the results can be considered acceptable without further refinement. However, if the acceleration values are close to or exceed the threshold, additional investigation of material properties and the development of more detailed 3D models may be necessary to obtain more accurate and project-specific predictions.

- [1] M. Sandberg, P. Jensen, I. Ramic, and P. Simonsson, "Knowledge-based bridge design", *IABSE Congress: Challenges in Design and Construction of an Innovative and Sustainable Built Environment*, 2016. [Online]. Available: https://www.researchgate.net/publication/349136590\_Knowledge-based\_bridge\_design.
- [2] E. C. for Standardization, "Eurocode: Basis of structural design", European Union, Tech. Rep. EN 1990, 2002. [Online]. Available: https://www.cen.eu.
- [3] S. A. H. Tehrani, "Dynamic analysis of end-shield bridges considering soil-structure interaction", Ph.D. dissertation, KTH Royal Institute of Technology, 2024. [Online]. Available: https://kth.diva-portal.org/smash/record.jsf?pid=diva2:1900358.
- [4] M. Ülker-Kaustell, R. Karoumi, and C. Pacoste, "Simplified analysis of the dynamic soil—structure interaction of a portal frame railway bridge", *Engineering Structures*, vol. 32, no. 11, pp. 3692–3698, 2010, ISSN: 0141-0296. DOI: https://doi.org/10.1016/j.engstruct.2010.08.013. [Online]. Available: https://www.sciencedirect.com/science/article/pii/S0141029610003020.
- [5] A. Zangeneh, C. Svedholm, A. Andersson, C. Pacoste, and R. Karoumi, "Dynamic stiffness identification of portal frame bridge—soil system using controlled dynamic testing", *Procedia Engineering*, vol. 199, pp. 1062–1067, 2017, X International Conference on Structural Dynamics, EURODYN 2017, ISSN: 1877-7058. DOI: https://doi.org/10.1016/j.proeng.2017.09.293. [Online]. Available: https://www.sciencedirect.com/science/article/pii/S1877705817337748.
- [6] A. Zangeneh, C. Svedholm, A. Andersson, C. Pacoste, and R. Karoumi, "Identification of soil-structure interaction effect in a portal frame railway bridge through full-scale dynamic testing", *Engineering Structures*, vol. 159, pp. 299–309, 2018, ISSN: 0141-0296. DOI: https://doi.org/10.1016/j.engstruct.2018.01.014. [Online]. Available: https://www.sciencedirect.com/science/article/pii/S0141029617332790.
- [7] S. A. H. Tehrani, A. Andersson, A. Zangeneh, and J.-M. Battini, "Dynamic soil-structure interaction of a continuous railway bridge", *Journal of Physics: Conference Series*, vol. 2647, no. 10, p. 102 007, Jun. 2024. DOI: 10.1088/1742-6596/2647/10/102007. [Online]. Available: https://dx.doi.org/10.1088/1742-6596/2647/10/102007.
- [8] S. A. H. Tehrani, A. Andersson, A. Zanganeh, and J.-M. Battini, "Dynamic soil–structure interaction of a three-span railway bridge subject to high-speed train passage", *Engineering Structures*, vol. 301, p. 117 296, 2024, ISSN: 0141-0296. DOI: https://doi.org/10.1016/j.engstruct.2023.117296. [Online]. Available: https://www.sciencedirect.com/science/article/pii/S014102962301711X.
- [9] S. A. H. Tehrani, A. Zanganeh, A. Andersson, and J.-M. Battini, "Simplified soil–structure interaction modeling techniques for the dynamic assessment of end shield bridges", *Engineering Structures*, vol. 319, p. 118 803, 2024, ISSN: 0141-0296. DOI: https://doi.org/10.1016/j.engstruct.2024.118803. [Online]. Available: https://www.sciencedirect.com/science/article/pii/S0141029624013658.
- [10] E. C. for Standardization, "Eurocode 1: Actions on structures part 2: Traffic loads on bridges", European Union, Tech. Rep. EN 1991-2, 2003. [Online]. Available: https://www.cen.eu.

